National Library of Canada

Acquisitions and Bibliographic Services Branch

395 Wellington Street
Ottawa, Ontario
K1A 0N4

Bibliothèque nationale du Canada

Direction des acquisitions et des services bibliographiques

395, rue Wellington
Ottawa (Ontario)
K1A 0N4

Your file Votre référence

Our file Notre référence

NOTICE

The quality of this microform is heavily dependent upon the quality of the original thesis submitted for microfilming. Every effort has been made to ensure the highest quality of reproduction possible.

If pages are missing, contact the university which granted the degree.

Some pages may have indistinct print especially if the original pages were typed with a poor typewriter ribbon or if the university sent us an inferior photocopy.

Reproduction in full or in part of this microform is governed by the Canadian Copyright Act, R.S.C. 1970, c. C-30, and subsequent amendments.

AVIS

La qualité de cette microforme dépend grandement de la qualité de la thèse soumise au microfilmage. Nous avons tout fait pour assurer une qualité supérieure de reproduction.

S'il manque des pages, veuillez communiquer avec l'université qui a conféré le grade.

La qualité d'impression de certaines pages peut laisser à désirer, surtout si les pages originales ont été dactylographiées à l'aide d'un ruban usé ou si l'université nous a fait parvenir une photocopie de qualité inférieure.

La reproduction, même partielle, de cette microforme est soumise à la Loi canadienne sur le droit d'auteur, SRC 1970, c. C-30, et ses amendements subséquents.

Canada

UNIVERSITY OF ALBERTA

ORTHODONTIC FORCE SYSTEMS AND TOOTH MOVEMENT

by

JEFFREY ANTHONY LEONCE KEMPS

©

A thesis submitted to the Faculty of Graduate Studies and Research in partial fulfillment of the requirements for the degree of Master of Science.

Department of Mechanical Engineering

Edmonton, Alberta

Fall 1993

National Library of Canada

Acquisitions and Bibliographic Services Branch

395 Wellington Street
Ottawa, Ontario
K1A 0N4

Bibliothèque nationale du Canada

Direction des acquisitions et des services bibliographiques

395, rue Wellington
Ottawa (Ontario)
K1A 0N4

Your file Votre référence

Our file Notre référence

The author has granted an irrevocable non-exclusive licence allowing the National Library of Canada to reproduce, loan, distribute or sell copies of his/her thesis by any means and in any form or format, making this thesis available to interested persons.

L'auteur a accordé une licence irrévocable et non exclusive permettant à la Bibliothèque nationale du Canada de reproduire, prêter, distribuer ou vendre des copies de sa thèse de quelque manière et sous quelque forme que ce soit pour mettre des exemplaires de cette thèse à la disposition des personnes intéressées.

The author retains ownership of the copyright in his/her thesis. Neither the thesis nor substantial extracts from it may be printed or otherwise reproduced without his/her permission.

L'auteur conserve la propriété du droit d'auteur qui protège sa thèse. Ni la thèse ni des extraits substantiels de celle-ci ne doivent être imprimés ou autrement reproduits sans son autorisation.

ISBN 0-315-88366-9

Canada

UNIVERSITY OF ALBERTA

RELEASE FORM

Name of Author:	**Jeffrey Anthony Leonce Kemps**
Title of Thesis:	**Orthodontic Force Systems and Tooth Movement**
Degree:	Master of Science
Year this degree granted:	Fall 1993

Permission is hereby granted to the **University of Alberta Library** to reproduce single copies of this thesis and to lend or sell such copies for private, scholarly or scientific research purposes only.

The author reserves all other publication and other rights in association with the copyright in the thesis, and except as hereinbefore provided neither the thesis nor any substantial portion thereof may be printed or otherwise reproduced in any material form without the author's written consent.

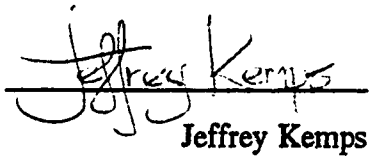

Jeffrey Kemps

6303 - 148 Avenue

Edmonton, Alberta

T5A 1V2

Date: OCTOBER 8, 1993

UNIVERSITY OF ALBERTA

FACULTY OF GRADUATE STUDIES AND RESEARCH

The undersigned certify that they have read, and recommend to the Faculty of Graduate Studies and Research for acceptance, a thesis entitled **Orthodontic Force Systems and Tooth Movement** submitted by **Jeffrey Anthony Leonce Kemps** in partial fulfillment of the requirements for the degree of **Master of Science.**

Dr. M.G. Faulkner (Supervisor)

Dr. A.W. Lipsett (Co-Supervisor)

Dr. D.R. Budney

Dr. P.W. Major

Date: OCTOBER 8, 1993

To my parents...

Abstract

For several decades, the relationship between the force systems applied to teeth by orthodontic appliances and the resultant movements of teeth has been investigated in various clinical scenarios, using data collected *in vivo* and/or from *in vitro* models of the human intraoral environment. However, difficulties in predictably controlling how the teeth are moved, wide variations in dentofacial anatomy between patients, and the limitations to measuring the forces applied and the displacements of teeth with sufficient confidence have hampered efforts to comprehend the phenomena of tooth movement in all patients.

In this study, the anterior segment retraction approach to the segmented arch technique of space closure was used for the orthodontic treatment of the maxillary dental arch of five patients for periods of six to eleven months. Force systems and tooth displacements were determined from geometric relationships using data that was collected *in vivo* without interrupting treatment. The force systems produced by the orthodontic spring and applied to the anterior teeth were calculated using the material properties of the spring, the spring's initial geometry, and its geometric boundary conditions at each clinical visit. Tooth displacements on each side of the arch were determined from changes in the positions of two points representing the canine tooth axis (and therefore the anterior segment of teeth) with respect to the "anchored" posterior segment.

Despite the lack of strong linear relationships between averages in distal force and rate of space closure, intrusive force and rate of intrusion, and M/F ratio and rate of rotation, some statements could be made about the results of this study. For the majority

of the patients, distal forces of 4 to 4.5 N appeared to produce movements of the anterior segment at rates of up to 1 mm/30 days, as much as 0.5 mm/30 days faster than with forces less than 4 N. Intrusive forces of about 1 N generally caused some intrusive displacement of the anterior segment. The M/F ratio required for translation of the segment ranged from 5 to 8 mm between patients in this study, but this variation could be attributed to the need for a more effective standard of determining the center of resistance of the anterior segment.

Acknowledgements

I am grateful to Dr. M.G. Faulkner and Dr. A.W. Lipsett for their guidance and support throughout the course of this work and for helping put the research into the proper perspective. In addition to his role in collecting the clinical data for this study, the time, experience, and valuable advice given by Dr. D. Haberstock was of great service to this research. The efforts of Ian Buttar, by assisting in the operation of the Micro-Val apparatus, and John Foy, with his expertise in photography, are greatly appreciated as well.

I would also like to take this opportunity to thank several other individuals who, in a variety of ways, helped in the composition of this thesis: Donald Raboud, Gail Thornton, Vincent Pisio, Victor del Valle, Bruce Larson, Victor Tam, and Raymond Mah. I apologize for failing to mention any others who also contributed to the completion of this research.

Table of Contents

	page #
Chapter 1: INTRODUCTION	1
1.1 BACKGROUND IN ORTHODONTICS	1
1.1.1 Introduction to Orthodontic Techniques	1
1.1.2 The Segmented Arch Technique to Space Closure	2
1.1.3 Force Systems and Tooth Movements	5
1.2 LITERATURE REVIEW	10
1.3 THESIS OUTLINE	17
Chapter 2: MATERIALS AND METHODS	19
2.1 GENERAL CHARACTERISTICS OF THE STUDY	19
2.2 CLINICAL PROCEDURE	22
2.3 TOOTH DISPLACEMENT DETERMINATION	27
2.3.1 Global Coordinate System	27
2.3.2 Location of Canine Tooth Axis	29
2.3.3 Angular Orientation of Anterior Segment	33
2.3.4 Location of Point of Force Application to Anterior Segment	34
2.3.5 Translational and Rotational Displacements	36
2.3.6 General Error Analysis	37
2.4 FORCE SYSTEM DETERMINATION	42
2.4.1 Installation and Activation of the Orthodontic Appliance	43
2.4.2 Representation of Spring Geometry	45
2.4.3 Sensitivity Analysis	48

page #

Chapter 3: RESULTS AND DISCUSSION 52

3.1 SIGN CONVENTIONS 52

3.2 RESULTS 55

3.2.1 Movement of the Anterior Segment of Teeth 56

3.2.2 Axial Force and X Displacement 63

3.2.3 Shear Force and Y Displacement 71

3.2.4 M/F Ratio and Rotational Displacement 79

3.3 DISCUSSION OF RESULTS 86

3.3.1 Axial Force and Rate of Space Closure 87

3.3.2 Shear Force and Rate of Intrusion 90

3.3.3 M/F Ratio and Rate of Rotation 92

Chapter 4: CONCLUSIONS 98

4.1 SUMMARY 98

4.2 RECOMMENDATIONS FOR FURTHER STUDY 100

References 103

Appendix A: ERROR ANALYSIS 106

A.1 Error Analysis of Translational Displacements 106

A.2 Error Analysis of Rotational Displacements 109

page #

A.3 Error Analysis of Last Node Vertical Offset 111

A.4 Sample Numerical Calculation of Displacements 113

Appendix B: SENSITIVITY ANALYSIS 115

Appendix C: CLINICAL DATA 118

List of Tables

		page #
Table 2.1:	*General demographic characteristics of the patients*	22
Table 2.2:	*Total uncertainties in measurements with intraoral micrometer*	40
Table 2.3:	*Estimated overall errors in force systems components and M/F ratio*	51
Table 3.1:	*Averages of axial force and rate of space closure*	70
Table 3.2:	*Averages of shear force and rate of intrusion*	78
Table 3.3:	*Averages of M/F ratio and rate of rotation*	85
Table 3.4:	*Estimated M/F ratios required for translation*	94
Table A.1:	*Sample measurements of inter-tooth distances*	113
Table A.2:	*Positions, orientations, and last node vertical offsets calculated from sample measurements*	114
Table A.3:	*Translational and rotational displacement calculated from sample measurements*	114
Table B.1:	*Errors in force systems from measurement errors in spring geometry*	116
Table B.2:	*Errors in force systems from measurement errors in bracket geometry*	117
Table B.3:	*Errors in force systems from error in accepted modulus of elasticity*	117
Table C.1:	*Inter-tooth distances measured in vivo in patient RD*	118

Table C.2: *Inter-tooth distances measured in vivo in patient DK* 119

Table C.3: *Inter-tooth distances measured in vivo in patient NM* 119

Table C.4: *Inter-tooth distances measured in vivo in patient TT* 120

Table C.5: *Inter-tooth distances measured in vivo in patient RZ* 120

Table C.6: *Measurements of spring/brackets geometry taken from impressions of patient RD* 121

Table C.7: *Measurements of spring/brackets geometry taken from impressions of patient DK* 122

Table C.8: *Measurements of spring/brackets geometry taken from impressions of patient NM* 122

Table C.9: *Measurements of spring/brackets geometry taken from impressions of patient TT* 123

Table C.10: *Measurements of spring/brackets geometry taken from impressions of patient RZ* 123

Table C.11: *Geometries of springs for both sides of patient RD* 125

Table C.12: *Geometries of springs for both sides of patient DK* 126

Table C.13: *Geometry of replacement spring for right side of patient DK* 127

Table C.14: *Geometries of springs for both sides of patient NM* 128

Table C.15: *Geometries of springs for both sides of patient TT* 129

Table C.16: *Geometries of springs for both sides of patient RZ* 130

List of Figures

		page #
Figure 1.1:	*Segmented arch technique (anterior retraction)*	4
Figure 1.2:	*Position of center of resistance*	6
Figure 1.3:	*Schematic of tooth movements for different M/F values*	8
Figure 1.4:	*Orthodontic retraction springs*	9
Figure 2.1:	*Pre-activated T-spring*	21
Figure 2.2:	*Schematic of installed T-spring (right side)*	23
Figure 2.3:	*Intraoral micrometer*	24
Figure 2.4:	*Aluminum measurement blocks*	24
Figure 2.5:	*Measurement of inter-tooth distances*	26
Figure 2.6:	*Geometric representation of inter-tooth distances*	28
Figure 2.7:	*An arbitrary triangle*	30
Figure 2.8:	*Angular orientation of anterior segment*	33
Figure 2.9:	*Positive displacement of anterior segment*	37
Figure 2.10:	*Impression of spring and brackets combined*	42
Figure 2.11:	*Initial and deformed geometries of a typical T-spring*	44
Figure 2.12:	*Pre-activated T-loop spring sectioning*	46
Figure 2.13:	*Geometric properties of T-spring changing with time*	47
Figure 3.1:	*Positive directions for force system components and tooth displacements for the patient's left side*	53

Figure 3.2: *Positive directions for force system components and tooth displacements for the patient's right side* 54

Figure 3.3: *Movement of anterior segment for RD (left)* 57

Figure 3.4: *Movement of anterior segment for RD (right)* 57

Figure 3.5: *Movement of anterior segment for DK (left)* 58

Figure 3.6: *Movement of anterior segment for DK (right)* 58

Figure 3.7: *Movement of anterior segment for NM (left)* 59

Figure 3.8: *Movement of anterior segment for NM (right)* 59

Figure 3.9: *Movement of anterior segment for TT (left)* 60

Figure 3.10: *Movement of anterior segment for TT (right)* 60

Figure 3.11: *Movement of anterior segment for RZ (left)* 61

Figure 3.12: *Movement of anterior segment for RZ (right)* 61

Figure 3.13: *Axial force and x displacement of point P over time for RD (left)* 64

Figure 3.14: *Axial force and x displacement of point P over time for RD (right)* 64

Figure 3.15: *Axial force and x displacement of point P over time for DK (left)* 65

Figure 3.16: *Axial force and x displacement of point P over time for DK (right)* 65

Figure 3.17: *Axial force and x displacement of point P over time for NM (left)* 66

Figure 3.18: *Axial force and x displacement of point P over time for NM (right)* 66

Figure 3.19: *Axial force and x displacement of point P over time for TT (left)* 67

Figure 3.20: *Axial force and x displacement of point P over time for TT (right)* 67

Figure 3.21: *Axial force and x displacement of point P over time for RZ (left)* 68

Figure 3.22: *Axial force and x displacement of point P over time for RZ (right)* 68

Figure 3.23: *Shear force and y displacement of point P over time for RD (left)* 73

Figure 3.24: *Shear force and y displacement of point P over time for RD (right)* 73

Figure 3.25: *Shear force and y displacement of point P over time for DK (left)* 74

Figure 3.26: *Shear force and y displacement of point P over time for DK (right)* 74

Figure 3.27: *Shear force and y displacement of point P over time for NM (left)* 75

Figure 3.28: *Shear force and y displacement of point P over time for NM (right)* 75

Figure 3.29: *Shear force and y displacement of point P over time for TT (left)* 76

Figure 3.30: *Shear force and y displacement of point P over time for TT (right)* 76

Figure 3.31: *Shear force and y displacement of point P over time for RZ (left)* 77

Figure 3.32: *Shear force and y displacement of point P over time for RZ (right)* 77

Figure 3.33: *M/F ratio and angle of anterior segment over time for RD (left)* 80

Figure 3.34: *M/F ratio and angle of anterior segment over time for RD (right)* 80

Figure 3.35: *M/F ratio and angle of anterior segment over time for DK (left)* 81

Figure 3.36: *M/F ratio and angle of anterior segment over time for DK (right)* 81

Figure 3.37: *M/F ratio and angle of anterior segment over time for NM (left)* 82

Figure 3.38: *M/F ratio and angle of anterior segment over time for NM (right)* 82

Figure 3.39: *M/F ratio and angle of anterior segment over time for TT (left)* 83

Figure 3.40: *M/F ratio and angle of anterior segment over time for TT (right)* 83

Figure 3.41: *M/F ratio and angle of anterior segment over time for RZ (left)* 84

Figure 3.42: *M/F ratio and angle of anterior segment over time for RZ (right)* 84

Figure 3.43: *Axial force over time for both sides of all patients* 87

Figure 3.44: *Average axial force versus average rate of space closure* 88

Figure 3.45: *Average shear force versus average rate of intrusion* 92

Figure 3.46: *Average M/F ratio versus average rate of rotation* 93

Glossary

alveolar bone *(n.)* - the bone which surrounds and supports the roots of the teeth.

alveolar crest *(n.)* - the tissue layer which includes the border between the tooth cementum and the gum.

anterior *(adj.)* - toward the front of the body.

apex *(n.)* - the tip of the tooth root (*(adj.)* apical).

buccal *(adj.)* - next to or toward the cheek.

crown *(n.)* - that portion of a tooth which is normally visible in the oral cavity.

dental arch *(n.)* - the curve formed by the grouping of a normal set of teeth.

distal *(adj.)* - away from the midline of the dental arch.

gingival *(adj.)* - next to or in the periodontium.

labial *(adj.)* - next to or toward the lips.

lingual *(adj.)* - next to or toward the tongue.

mandibular *(adj.)* - pertaining to the lower jaw.

maxillary *(adj.)* - pertaining to the upper jaw.

mesial *(adj.)* - toward the midline of the dental arch.

occlusal *(adj.)* - toward the biting surface of a posterior tooth.

periodontium *(n.)* - the surrounding supportive structures around a tooth, including the the alveolar bone and gum.

posterior *(adj.)* - toward the back of the body.

sagittal *(adj.)* - referring to a plane which divides the body into two halves.

transpalatal *(adj.)* - across the palate, the partition which seperates the nasal and oral cavities in the roof of the mouth.

Chapter 1

INTRODUCTION

1.1 BACKGROUND IN ORTHODONTICS

1.1.1 Introduction to Orthodontic Techniques

Whether it is due to overcrowding, an overjet (projected upper front teeth) or a crossbite, many people have an abnormal relationship between their maxillary (upper) and mandibular (lower) teeth. This is called a malocclusion. For reasons concerning aesthetics, functionality, or both, the malocclusion calls for orthodontic treatment to correct it. This orthodontic treatment generally involves force systems being mechanically applied to the teeth to change their positions within the dental arches. Malocclusions are typically treated by removing certain teeth and taking advantage of the extra space to properly align the remaining teeth. This is called space closure.

A number of techniques can be employed to achieve space closure following alignment, and these are classified as using either sliding mechanics or wire loop mechanics. In sliding mechanics, an archwire is used to guide the repositioning of the teeth, using elastomers or wire springs for force application to induce movement. However because of frictional resistance between the archwire and the brackets mounted to the teeth, the actual force system applied to the teeth is indeterminate and the resulting movement is somewhat unpredictable. Wire loop mechanics uses an activated loop of wire between individual teeth or groups of teeth to generate the necessary forces to

stimulate movement.

Techniques using wire loop mechanics can be sub-categorized as either continuous arch or segmented arch types. For the continuous arch approach, the wire loop spring is incorporated into the archwire which is attached to the brackets on the teeth. Activation of this loop spring provides the forces, but there are limitations to the force systems that can be generated due to space restrictions between the teeth requiring repositioning. On the other hand, the segmented arch approach involves the repositioning of groups, or segments, of teeth using specific appliances (springs) to pull these segments together. Each segment of teeth is held together by an archwire, and this segmentation of the archwires lends more flexibility to the design of the springs that provide the force systems. In addition, the actual force systems applied are easier to solve for than those with sliding mechanics techniques.

1.1.2 The Segmented Arch Technique to Space Closure

Once spaces have been created by the removal of certain teeth, the segmented arch technique calls for the segments of teeth to be aligned using local archwires. These segments of teeth can then be repositioned relative to each other. There are three approaches to "en masse" space closure with the segmented arch technique, and the choice of approach depends on which teeth are removed and which segment of teeth is prescribed to undergo the most movement into the space provided. First there is anterior retraction, in which the 1st premolars are extracted and the anterior segment moves posteriorly while the posterior segment remains "anchored", or essentially fixed. The

second approach is posterior protraction, in which the second premolars are extracted and the posterior segment moves anteriorly while the anterior segment remains "anchored". The last approach is a combination of the first two approaches, with both the anterior and posterior segments moving into the extraction sites, regardless of which set of premolars has been removed. Overjets or overcrowding of the anterior teeth are some of the typical reasons for seeking orthodontic therapy, and these malocclusions can be effectively treated by moving the anterior segment of teeth posteriorly into the space created. All of the patients used in this study had excessive overjets (see Section 2.1), so for orthodontic treatment, **anterior retraction** was the approach to space closure used in the clinical part of this study.

In the early stages of treatment with anterior retraction, spaces are created by the extraction of the 1st premolars, as shown in Figure 1.1. With the 1st premolars removed, the dental arch (whether it be the maxillary or mandibular) is split into three groups of teeth: the left and right buccal (posterior) segments, each comprised of the molars and 2nd premolar; and the anterior segment, which is comprised of the four incisors and the two canines. Once alignment within the buccal segments has been achieved, the teeth in each buccal segment are joined by a buccal stabilizing archwire [1]. The functions of this stabilizing archwire are to combine all the posterior teeth on one side of the dental arch into one unit and to help maintain the alignment of the unit. The 1st molars of the buccal segments are then stabilized with a lingual (for the mandibular arch) or transpalatal (for the maxillary arch) archwire, thereby consolidating the left and right buccal segments into one group of teeth called the posterior anchorage unit [1]. After

the anterior segment has undergone alignment, a stabilizing archwire is placed through the brackets creating a single dental segment.

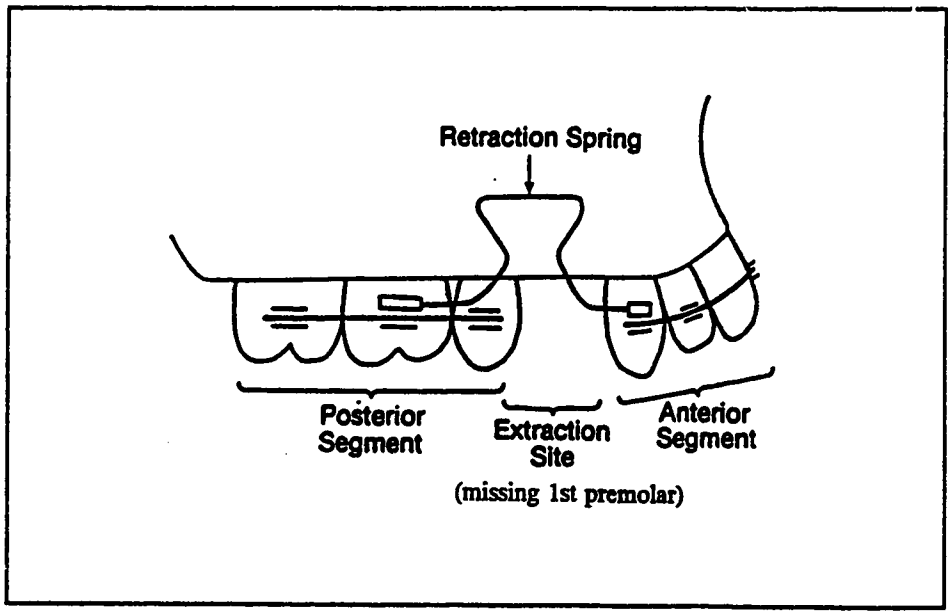

Figure 1.1: *Segmented arch technique (anterior retraction)*

With anterior retraction, it is expected that the posterior anchorage unit moves considerably less than the anterior segment in the mesial/distal direction, with the extraction sites used mostly for retraction of the anterior segment. This is a reasonable expectation because the teeth in the posterior anchorage unit have a greater total root surface area over which stresses in the periodontium can be distributed than the teeth in the anterior segment. Therefore during space closure, in essence, two large multi-rooted segments of teeth are being pulled together to form a new dental arch [1]. This simplifies the application of force systems to the teeth to accomplish space closure, since a force acting anywhere on a segment should cause all the teeth in the segment to move together. Many orthodontic appliances can be used to achieve space closure through

anterior retraction. One retraction system employs a vertical, metallic loop or spring as the only connection between tooth segments, and its main advantage is that it can apply both forces and moments to the teeth [2]. The importance of applying both forces and moments to teeth are discussed below.

1.1.3 Force Systems and Tooth Movements

With the segmented arch technique, the orthodontic appliance can be directly manipulated by the orthodontist to deliver the necessary force systems to move the teeth [3]. The orthodontic appliance used to perform the anterior retraction will have various effects on tooth movement, depending on the force system it applies. The tooth or tooth segment can rotate and translate as it is repositioned. Relative rates of translation and rotation can be described using the center of rotation along the tooth's axis [4]. This will be discussed later.

The center of resistance is defined as a singular point in a body (tooth or tooth segment) through which the line of action of a force must pass to produce translation of that body in the direction of the force. The resistance of the supportive tissues (ie. periodontal ligament, gingiva, etc.) of a tooth or tooth segment to its displacement influences its center of resistance. Figure 1.2 is a schematic representation of the axial forces and moments applied to teeth, a molar and an incisor in this case, by an orthodontic appliance [5]. Figure 1.2a shows that the center of resistance (CR) of the maxillary incisor is above the alveolar crest (C) or "gumline", typically located approximately one-third of the distance from the alveolar crest and the apex of the root

(A) for a single rooted tooth [6]. As the free body diagram of the incisor of Figure 1.2b demonstrates, the principle of equilibrium requires a reactive axial force and moment (F_r and M_r respectively) at the center of resistance in response to the axial force and moment applied to the tooth (F and M respectively). Since it is impractical to apply force directly to a point in the root of the tooth, a force applied at any point on the exposed tooth surface will tend to rotate, as well as translate, a tooth or tooth segment. In order for the tooth to translate, there must be no reactive moment occurring at the tooth's center of resistance, that is $M_r = 0$ for translation. According to the equations of equilibrium with Figure 1.2b, the applied M/F ratio needed for translation should equal the distance between the center of resistance and the point at which the force system is applied to the tooth (called ℓ in Figures 1.2a and 1.2b).

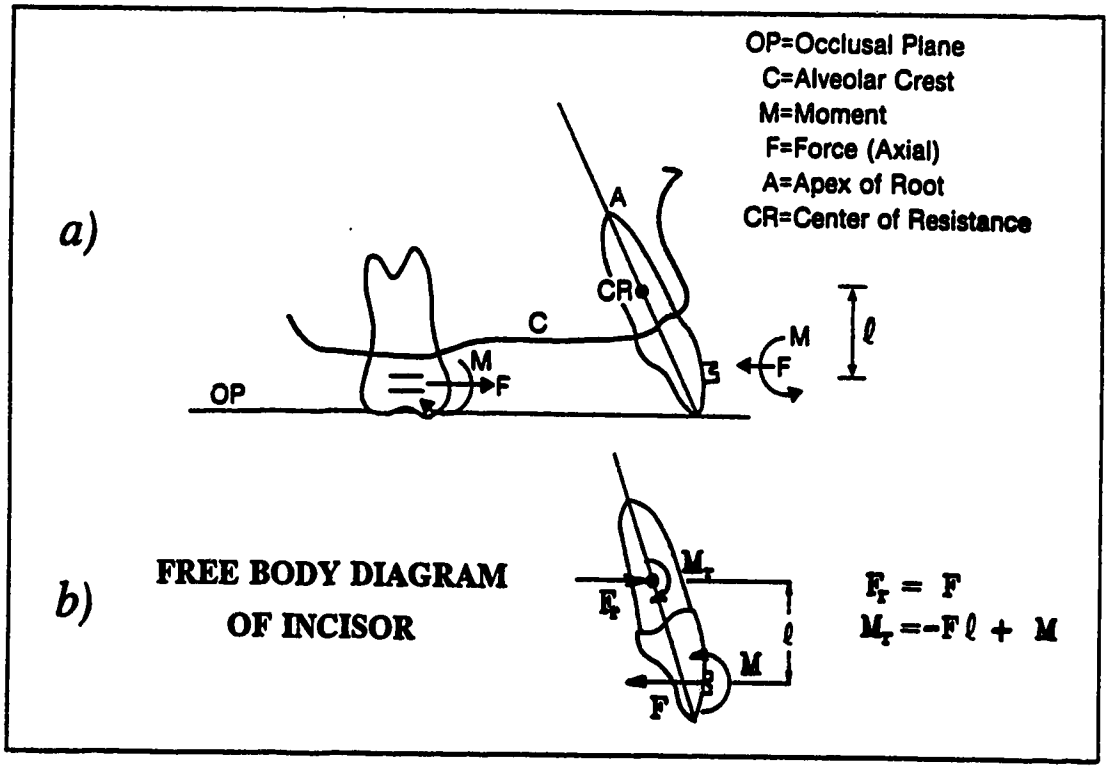

Figure 1.2: *Position of center of resistance*

As a consequence, it is necessary to provide both a force and a moment if translation of a tooth or tooth segment is desired. If only a pure moment is applied anywhere on a tooth or tooth segment, the resulting movement would be pure rotation with the center of resistance as the center of rotation. A force system which produces a combination of force and moment can generate a variety of tooth movements. For example in Figure 1.3, a simple force (ie. M/F = 0: Figure 1.3a) causes **uncontrolled tipping** of the incisor, with the center of rotation located somewhere between the center of resistance and the root apex. Adding some moment (Figure 1.3b) shifts the center of rotation to the root apex, and this allows for **controlled tipping** of the tooth about the apex. For a ratio of moment-to-force equal to the distance between the center of resistance and the point of force application as in Figure 1.3c, **translation** occurs. The center of rotation is then located at infinity. Increasing the magnitude of the moment further (Figure 1.3d) places the center of rotation at the incisal tip, causing **root movement.** As mentioned before, removing the force completely and imparting any significant magnitude of pure moment (Figure 1.3e) results in rotation of the incisor about its center of resistance.

From a clinical perspective, two questions for repositioning teeth must be considered. What type of force system produces a given center of rotation (and therefore, a given type of tooth movement)? What force systems lead to optimal tooth movement [3] ? Both of these questions are directly tied to the mechanical nature of the orthodontic appliance employed to accomplish space closure, as well as the force systems themselves generated by the appliance. The appliance must experience an acceptable range of

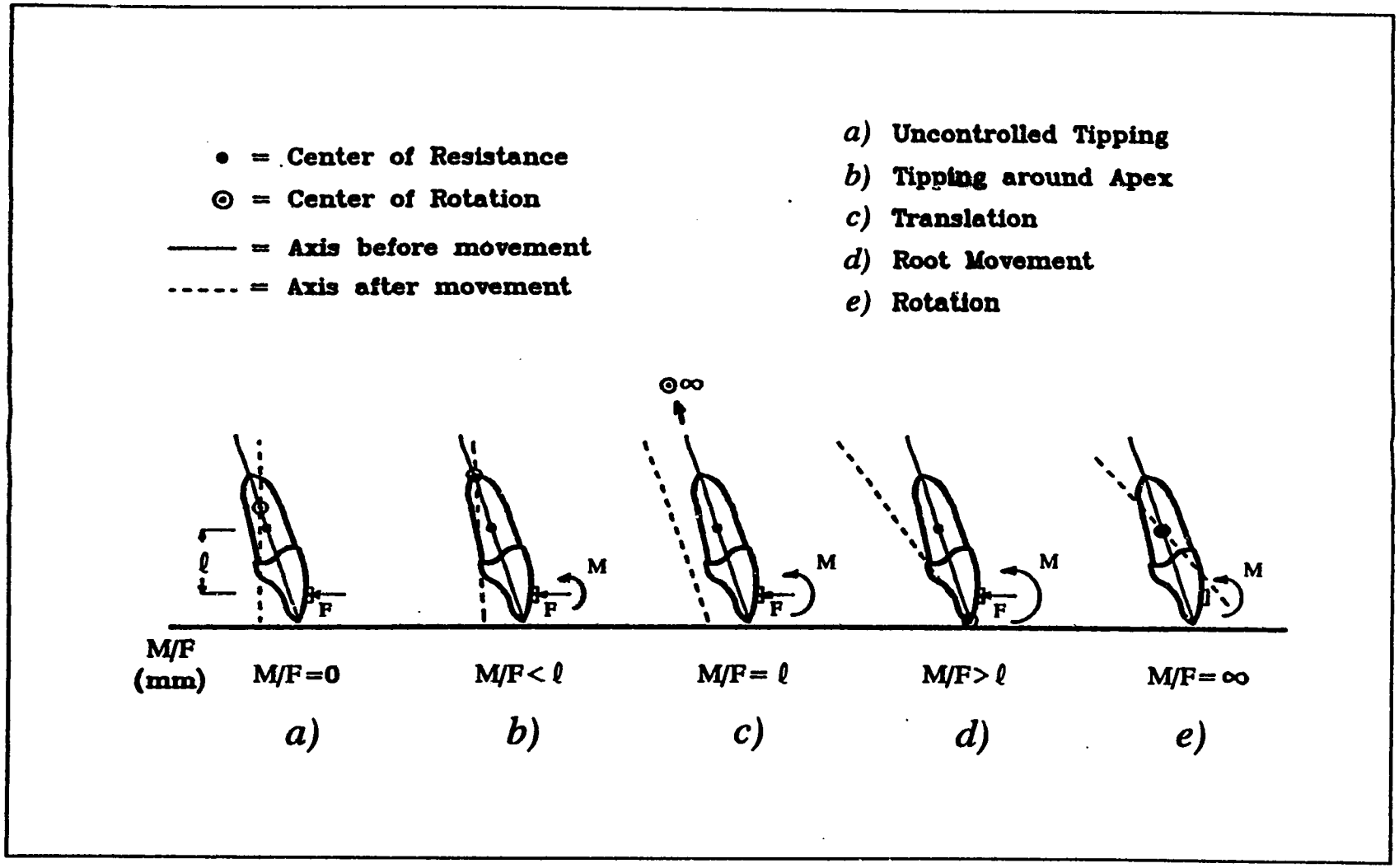

Figure 1.3: *Schematic of tooth movements for different M/F values*

activation/deactivation so that it delivers reasonably constant forces and moments. In addition, the appliance must be accommodated by the limited space in the intraoral environment [2].

Figure 1.4 shows three different configurations for retraction springs: the straight vertical loop, the T-loop, and the pre-activated T-loop. These loops can be fabricated as independent devices, with their ends attached to the brackets of two segments of teeth. The mechanical characteristics of these loops depend on their dimensions, such as the height of the loop and the radius of curvature of each of its bends, as well as the spring's anterioposterior placement between the segments of teeth. The results of the study by Faulkner et al. [2] show that an ordinary vertical loop, like the first loop shown in Figure 1.4, is incapable of producing M/F ratios necessary to cause translation or even controlled tipping. The magnitude of the force and moment are extremely sensitive to small changes in the spring's activation, and this severely impairs the orthodontist's control over the force system.

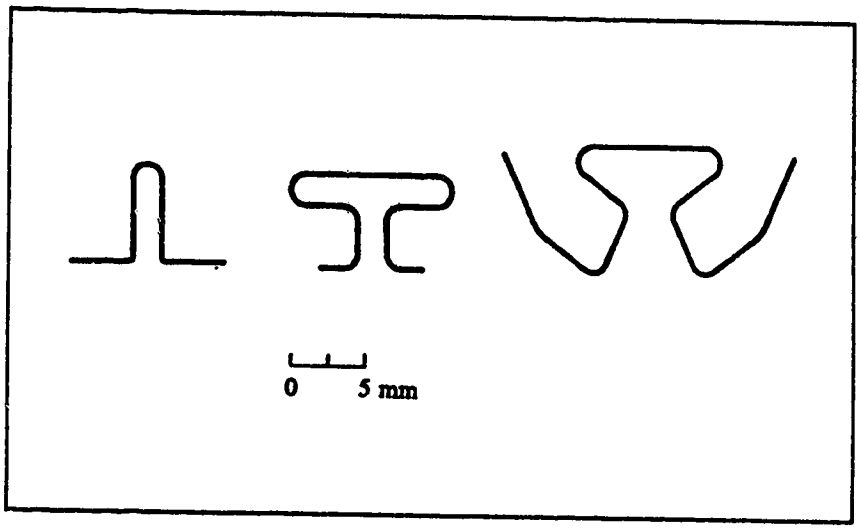

Figure 1.4: *Orthodontic retraction springs*

To overcome this deficiency, the loop design may use preactivation. Preactivation involves gabling the legs of the spring, which means pre-bending the legs to some angle to the direction of activation. This creates larger moments since the spring's legs must first be brought parallel to each other before its installation and subsequent activation. For the segmented arch procedures, the T-loop design, the second design shown in Figure 1.4, is commonly employed to deliver the proper M/F ratio necessary for the desired tooth movement [5]. Preactivated bends provide larger ranges of activation and more appropriate M/F ratios so that translation of the teeth is possible. These pre-activated T-loop springs "produce force/deflection, moment/deflection, and M/F characteristics that make them less sensitive to minor manufacturing and placement errors than the standard vertical loop" [2].

1.2 LITERATURE REVIEW

Strategies in orthodontic therapy have been largely based on "clinical empiricism", and though it has its merits this approach also has serious limitations. As noted by Quinn and Yoshikawa [7], there are "a limited number of observations made with inadequate measurement techniques, complicated by observer bias and unduly influenced by extreme cases", all of which can lead to incorrect conclusions. Nonetheless, Burstone [8] commented that despite great variations in the dentofacial complex between individuals, it is commonly perceived that "perhaps some cephalometric average could be a guide for treatment".

There have been many investigations into the relationships between force systems

applied and resultant tooth movements. One of the pioneering studies in the examination of orthodontic force systems and tooth movements was by Smith and Storey [9]. In this investigation, 8 patients were treated by mandibular (except for one patient, for which it was maxillary) cuspid retraction and studied for 4 to 10 weeks with weekly visits for observation. Initially, light continuous forces of about 1.7 to 2.9 N (or 175 to 300 g, with 300 g × 9.81 m/s^2 = 2.943 N ≈ 2.9 N) were applied to one side of the dental arch while higher, less continuous forces of 3.9 to 5.9 N were applied to the other side. From their results, Smith and Storey concluded that the optimal force range extended from approximately 1.5 to 2.5 N, with virtually no movement above this range and very little below it. One of the main problems with this study was that the retraction mechanism delivered only a simple force through the canine bracket, so the canine tipped into the extraction sites. Another question is the method by which tooth displacement was measured. The positions of the cuspid tooth and the anchor unit were determined with reference to a fixed point in the mandibular arch when the mandible was closed into its centric position (at rest with maximum contact between the maxillary and mandibular dental arches). But whether or not that centric position was consistently returned to for each clinical visit cannot be confidently known, suggesting possible errors to the measurements of the tooth displacements. Furthermore, the study was of short duration, with only 4 weeks of observation for some patients.

In the study by Andreasen and Johnson [10], eccentric Kloehn-type headgears were used to achieve distal movement of the maxillary 1st permanent molars. A force of 3.9 N was applied to the molar on one side of the arch while a force of 2.0 N was

applied to the molar on the opposite side of the arch. Forces were measured through *in vitro* simulations on a "force board" using Correx force gauges, and tooth movement was measured *in vivo* with a spring bow divider. It was concluded that the teeth receiving the 3.9 N force moved approximately 1 mm/month, about 2.5 times faster and farther than the teeth receiving 2.0 N force. However, the forces applied to the teeth may not have been held constant, as the *in vitro* simulations on the "force board" could have introduced errors in attempting to reproduce the headgear's configuration *in vivo*. The 16 female (a demographic bias) patients in this study were of ages 8 to 10, and at these ages there is considerable growth taking place in the dentofacial anatomy of the patients. Even for a 12 week period of observation such as with this study, the varying rates of growth could have contributed to the large variations in tooth movement between patients.

Two studies by Hixon et al. [11,12] examined the effects of a wide range of forces on the maxillary and mandibular canines when they were distally retracted. A force of 3.0 N was applied to the right side and a range of forces from 0.5 to 14.7 N was applied to the left in each patient. In one of the studies [11], despite the use of an *in vitro* model of the dental arch to calibrate the retraction spring so as to ensure bodily movement, there still was some tipping. Radiographs and fixed landmarks on tantalum implants placed on each side of the maxilla and the mandible were used to measure tooth movements in this study. Hixon concluded that translatory movement was slower than tipping, which explained the rapid tooth movement from "light" forces. Hixon also admitted that even though a heavier force moved teeth at a greater rate (up to 3.0

mm/month), variation in the biological response of each patient overshadowed any differences in force magnitude [12]. Inconsistencies in the protocol of these studies were evident as well, in which for the left side of three patients in one of the studies [11] the initial activation force was allowed to decay. These two experiments were conducted for only 8 weeks.

Boester and Johnston [13] observed from the results of their study that above some magnitude of applied force, the average rate of tooth movement remained constant. With forces ranging from 1.4 to 3.0 N, space closure proceeded at essentially the same rate of about 3.6 mm/month, while lower forces like 0.5 N produced considerably less movement, averaging only 2.0 mm/month. With rates of tooth movement from 2.0 to 3.6 mm/month, it seems most likely the type of movement that occurred in this study was tipping. Quinn and Yoshikawa [7] pointed out that the large mean square residuals in Boester and Johnston's data indicate the presence of large measurement errors. There was also the assumption that the maxillary and mandibular arches behave identically, but Hixon et al. [12] noted that maxillary canines move as much as 1.2 mm/month faster than mandibular ones.

Andreasen and Zwanziger [14] used an apparatus similar to the earlier study by Andreasen and Johnson [10] to determine the forces applied by an edgewise bracket to both anterior and posterior teeth. The intent of this study was to test the hypothesis that at low forces of 1.0 to 1.5 N, the canine tooth will move but not the anchor unit, while at high forces of 3.9 to 4.9 N, the anchor unit will experience more movement than the canine. It was concluded on the basis of the clinical data collected from 14 patients in

this investigation that the hypothesis is not necessarily true. However, there were some problems with the measurement and data analysis protocols in this study. With the incisor teeth used as a "stable" reference point from which to measure the movement of the molar and the canine, a systematic error may have been introduced to the results. Andreasen and Zwanziger also neglected to apply statistical analysis to their data. Without knowledge of the uncertainty in the movement of the teeth, the actual amounts of movement experienced by the teeth remain unknown.

In 1985, Quinn and Yoshikawa [7] conducted a reassessment of the six studies on force magnitudes and tooth movement previously discussed, all of which have been frequently cited in orthodontic literature. It was identified in this review that three major problems complicate clinical studies of force systems and tooth movement: the lack of control over the type of tooth movement (tipping or translation); measurements of tooth displacement that are not coordinated with the activations of the orthodontic appliance; and large measurement errors. With the clinical data from the six studies and a hypothesis that the rate of tooth movement reaches a plateau at a certain force level, Quinn and Yoshikawa estimated that the optimal canine retraction force is between 1.0 and 2.0 N. Aside from limitations of the individual studies, the clinical data from which Quinn and Yoshikawa drew their conclusions was based on the repositioning of a single tooth, namely a canine. Therefore, one can expect that the optimal force necessary for retracting the multi-toothed anterior segment would be considerably higher than 1.0 to 2.0 N.

Due to the limited number of quantitative studies at the time, Nikolai [15]

investigated the force distribution in the periodontium around the tooth generated by force application to the exposed part of the tooth, as well as the types of tooth movement resulting from various force systems. Employing a mathematical model of a maxillary canine, Nikolai determined that the center of rotation is located 0.3 to 0.4 times the distance from the root apex to the alveolar crest and the center of resistance is approximately mid-root for a single-rooted tooth. In addition to this, it was also concluded that the product of the optimum force magnitude and the sum of the reactive periodontal stress values at the alveolar crest and the root apex was the same for the four cases examined in the study. The stress values were presumed to be from projected areas (though it was not explicitly stated by Nikolai) since the model of the tooth was two-dimensional. For example, if a distal force of 0.6 N was sufficient to cause tipping of a maxillary canine in a particular patient, then a distal force of about 2.1 N would have produced bodily movement (translation). To produce root movement in the same patient, a moment of 26 N mm combined with a "distal crown-holding force" of 1.6 N would have been required. Unfortunately, the results derived from a mathematical model are only as accurate as the assumptions that the model is based on, such as the material properties of the periodontium and the average size and geometry of the tooth. As with experiments using *in vitro* models, the conclusions reached from mathematical models of biological systems are not readily accepted for clinical practice.

More recently, Cohen [16] explored the phenomena of tooth movement under the application of orthodontic force systems. With average forces of 1.5 to 2.0 N applied, the average rates of distal tooth movement varied from approximately 0.5 to 1.0

mm/month. This study examined occlusal/gingival (extrusive/intrusive) movements as well as space closure, and Cohen observed an alternation between up and down movement, which she attributed to tipping and uprighting of the tooth. The most severe limitation to Cohen's study was the very small sample population used. At the start of the research, the movements of 7 maxillary cuspids from 4 patients were studied. However data from 3 of these cuspids were not used for drawing conclusions, due to problems with the anatomy of the patient's teeth or to a lack of movement during the treatment. Similar to the study by Smith and Storey [9], the orthodontic appliances were tested *in vitro* to determine the force systems produced at certain activations. The actual change in tooth position was also measured *in vitro* from plaster casts of the patient's dental arch at each visit. The reliability of results from *in vivo* measurements is always greater than for *in vitro* ones. Though the frequency of the measurements was high (3 times a week), the duration of this study was only 6 to 8 weeks, which is short compared to most of the studies that have been discussed in this section.

There has been considerable research conducted on the relationship between the moment-to-axial force ratio (M/F) and the rotational displacement of teeth. As remarked in Section 1.1, the M/F ratio can potentially determine the type of movement that will be experienced by the anterior segment. Most of the studies of this subject have dealt with a single tooth, such as in Figure 1.3, rather than groups of teeth like the anterior segment. For instance, Tanne et al. [17] located the center of resistance of an upper right central incisor at 0.24 times the root length measured apically from the alveolar crest, employing a three-dimensional FEM (Finite Element Model) based on average tooth

dimensions. In another example, using a two-dimensional model with a parabolic root, Nägerl et al. [6] located the center of resistance of a maxillary (upper) canine at an average of one-third the distance from the alveolar crest to the apex. There was also one investigation by Vanden Bulcke et al. [18] using a laser reflection technique to locate the center of resistance of units of teeth in the anterior maxillary dentition. Units composed of two incisors, four incisors, and six anterior teeth were studied, with the conclusion that the center of resistance shifted apically (toward the apex of the root) as more teeth were included in the anterior segment. However, the measurements performed in this study were *in vitro* not *in vivo* and the sample population was extremely small (2 skulls), and therefore diminishes the reliability of this study.

1.3 THESIS OUTLINE

The objective of the research presented in this thesis was to determine the forces and moments generated by an orthodontic appliance and the resultant movements of the teeth. This was to assist in the determination of an optimal force system, if one exists, for tooth repositioning. The methods used for determining the force systems and tooth movements are presented in Chapter 2, describing the clinical procedures for collecting data during treatment as well as the approaches to processing the data. Furthermore, analyses of the uncertainties in the components of the force systems and in the tooth displacements are presented in this chapter. Chapter 3 presents the sign conventions established for the force systems and the tooth displacements, and discusses how the components of the force systems, the moment-to-force ratio (M/F) and the displacements

changed over time. A quantitative analysis of the tooth movements is also included in this chapter, showing how the anterior segment of teeth moved with respect to the posterior segment. The relevance of the data gathered in this study to clinical procedure is then discussed. Chapter 4 summarizes the conclusions of the study.

Chapter 2

MATERIALS AND METHODS

In Chapter 2, the general characteristics of this study are listed, followed by a description of the clinical procedure used for monitoring tooth movement and the geometry of the orthodontic appliance during treatment. Several approaches to converting the clinical data into standardized translational and rotational displacements are explained. The theory behind determining the uncertainty in those displacements and how this theory was used to choose one of the approaches is discussed. This is followed by a description of the protocol for determining the force systems produced by the appliance and their accessory uncertainties.

2.1 GENERAL CHARACTERISTICS OF THE STUDY

As evidenced by previous studies discussed in Chapter 1 (specifically Section 1.2), there are many approaches to determining displacements of teeth and the forces that cause those displacements. In this study, the forces, as well as the displacements, are determined entirely on the basis of geometric relationships. The force systems generated by the orthodontic appliance are implied through analysis of the appliance's shape. All preliminary (clinical) data, which is listed in Appendix C, was acquired *in vivo* so as to avoid interrupting treatment and adding inconsistencies to the observations.

There were five patients in this study, referred to as RD, DK, NM, TT, and RZ. Though the focus is on the maxillary arch in this study, all of the patients needed to undergo orthodontic treatment for their maxillary and mandibular arches. All of the patients had extractions in the maxillary arch, but only patients NM and TT had extractions in their mandibular arch. Alignment of the mandibular arch was done for all five patients.

Generally one week before the fixed appliances were attached to the teeth, both maxillary 1st premolars were extracted. For each patient, the size of the main bracket slots on the four central incisors was 0.018″ × 0.025″ (0.457 mm × 0.635 mm), and for the canines, 2nd premolars, and molars, it was 0.022″ × 0.028″ (0.559 mm × 0.711 mm). The brackets had built-in torque, but the archwire did not introduce additional forces and moments at the beginning of treatment. A stainless steel 0.018″ × 0.025″ (0.457 mm × 0.635 mm) main stabilizing archwire was attached to the main slots of the brackets. This main archwire initially was attached to the brackets of all remaining teeth in the maxillary arch, then was segmented on the day the T-spring was placed. The buccal (posterior) segments were connected with a 0.036″ (0.914 mm) diameter transpalatal archwire, with its ends pre-bent, ligated, soldered, and trimmed before being snugly fitted into 0.072″ × 0.036″ (1.82 mm) lingual sheaths on the 1st molars. The transpalatal archwire was installed when the banding of the teeth was done.

The anterior retraction technique of space closure described in Chapter 1 was employed for all five patients. On both sides of the patient, anterior retraction was accomplished using pre-activated 0.017″ × 0.025″ (0.432 mm × 0.635 mm) TMA

(Titanium Molybdenum Alloy) T-springs, one of which is displayed in Figure 2.1. These T-springs were attached to 0.018" × 0.025" horizontal auxiliary tubes on the canine and 1st molar brackets on each side. All of the patients were under observation for six to eleven months, with clinical visits at intervals of approximately one month.

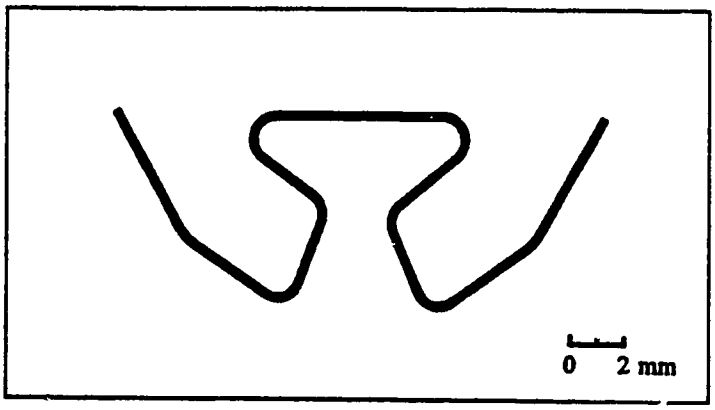

Figure 2.1: *Pre-activated T-spring*

Table 2.1 shows the general demographic characteristics of the five patients in this study. These characteristics include age, gender, molar relation classification, skeletal classification, and the extent of overbite/overjet. In addition, the length of time between extraction and the beginning of retraction for each patient is shown in this table. Since some of the patients were under observation for nearly a year, the age of each patient at the beginning of their period of treatment is indicated in the table below. Despite the wide age variation, all patients had their 2nd molars for anchorage. For skeletal classifications, class I denotes a straight hard tissue profile, class II indicates a convex hard tissue profile.

Table 2.1: *General demographic characteristics of the patients*

patient	RD	DK	NM	TT	RZ
age (years)	12	18	15	20	16
gender	female	male	female	female	male
molar relation	class II	class II	class II	class II	class II
skeletal class	class II	class II	class II	class II	class I
overbite/overjet	excessive	excessive	excessive	excessive	excessive
time from extraction to retraction	6 months	4 months	2 months	3 months	5 months

2.2 CLINICAL PROCEDURE

For each side of the maxillary dental arch of each patient in this study, a general clinical procedure was performed, spanning from the initial installation of the orthodontic appliance to the patient's last visit.

Once the orthodontist has bent the TMA wire into the pre-activated T-loop configuration of Figure 2.1, this orthodontic appliance was photocopied. The photocopy was enlarged to four times its original size so that the spring's geometry could be determined, as will be explained in sub-section 2.4.2. The spring was then installed between the two segments of teeth. Figure 2.2 shows how the ends of the spring were passed through the auxiliary tubes of the brackets mounted on the buccal surface of the 1st molar and the labial surface of the canine. After sufficient length of each end of the spring was pulled through its respective tube and crimped to hold the spring in place, an

impression, formed in "impression compound" produced by the Kerr® company, was made of the geometry of the spring and both brackets combined. This impression, combined with the unloaded shape (eg. Figure 2.1), enabled the determination of the force system generated by the retraction spring. This will also be explained in sub-section 2.4.2.

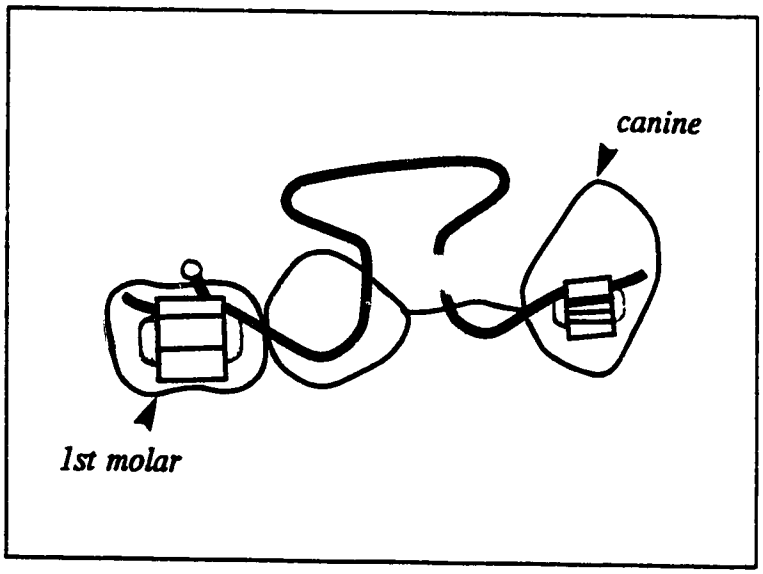

Figure 2.2: *Schematic of installed T-spring (right side)*

The **inter-tooth distances** were then measured for the first time. These distances are measured between four points located below the maxillary occlusal plane using the custom-built intraoral micrometer of Figure 2.3. For the view of a model of a patient's left side in Figure 2.4, the pair of points on the right (ie. UP, upper posterior, and LP, lower posterior) represents the tooth axis of the 1st molar (and therefore, the posterior segment) and the other pair on the left (ie. UA, upper anterior, and LA, lower anterior)

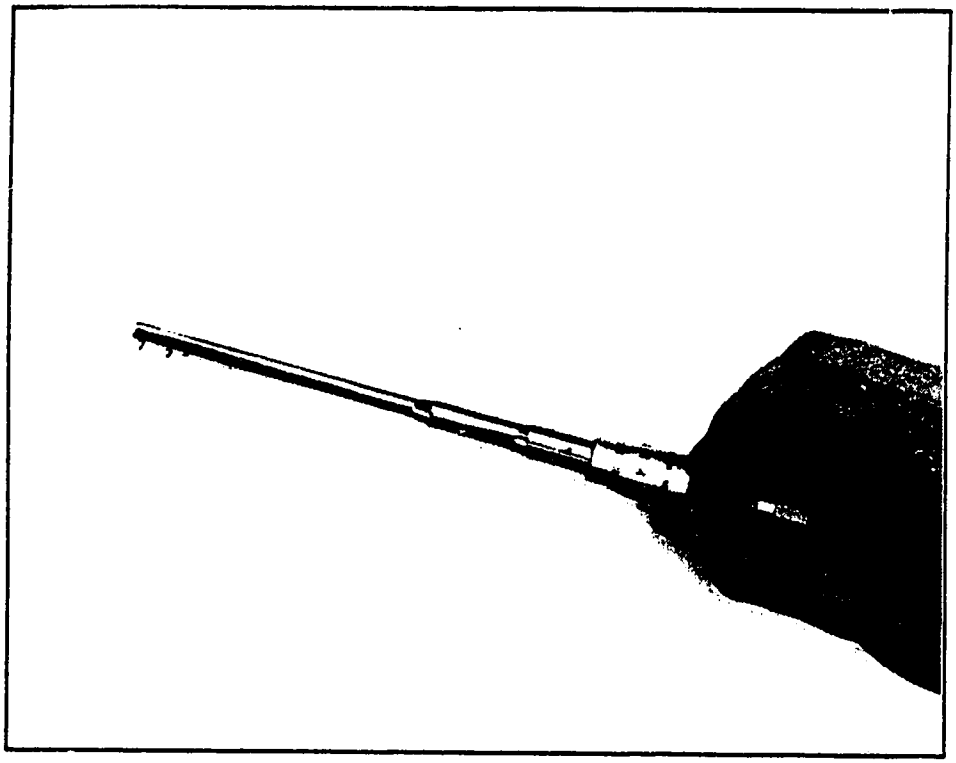

Figure 2.3: *Intraoral micrometer*

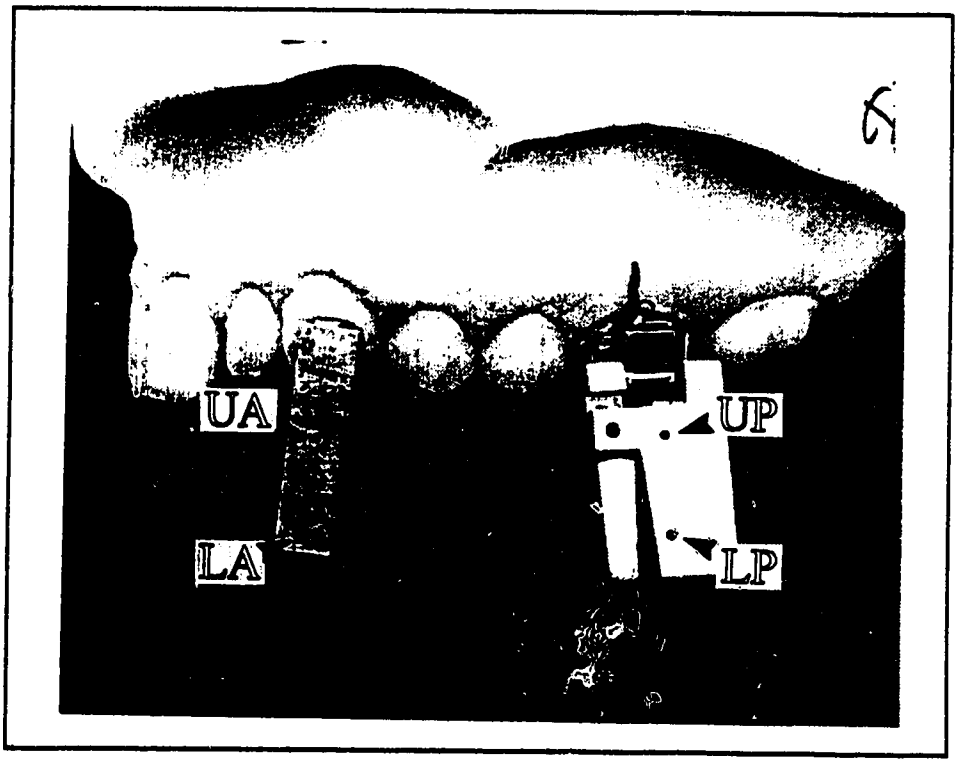

Figure 2.4: *Aluminum measurement blocks*

represents the tooth axis of the canine (and therefore, the anterior segment). Each pair of points is set on an aluminum block which was either clamped (as with the posterior block) or snugly-fitted (as with its anterior counterpart) onto its corresponding bracket.

There were four inter-tooth distances measured using the intraoral micrometer, pictorially depicted in Figure 2.5: *a)* UA to UP; *b)* LA to LP; *c)* LA to UP; and *d)* UA to LP. Aside from the inter-tooth distances, one other measurement was made which is called the **inter-bracket distance (I.B.D.)**. This measurement, performed with calipers, is the distance between the points at which the ends of the spring first enter the tubes of the brackets.

At each appointment of the patient (approximately monthly), a new impression of the combined spring-and-bracket geometry was made and the inter-tooth distances were measured again. At each "reactivation" of the spring (approximately every two months), its ends were shortened by pulling one end of the spring further through the tube of the bracket. This reactivation was done to increase the force levels which decreased as the space between the teeth closed.

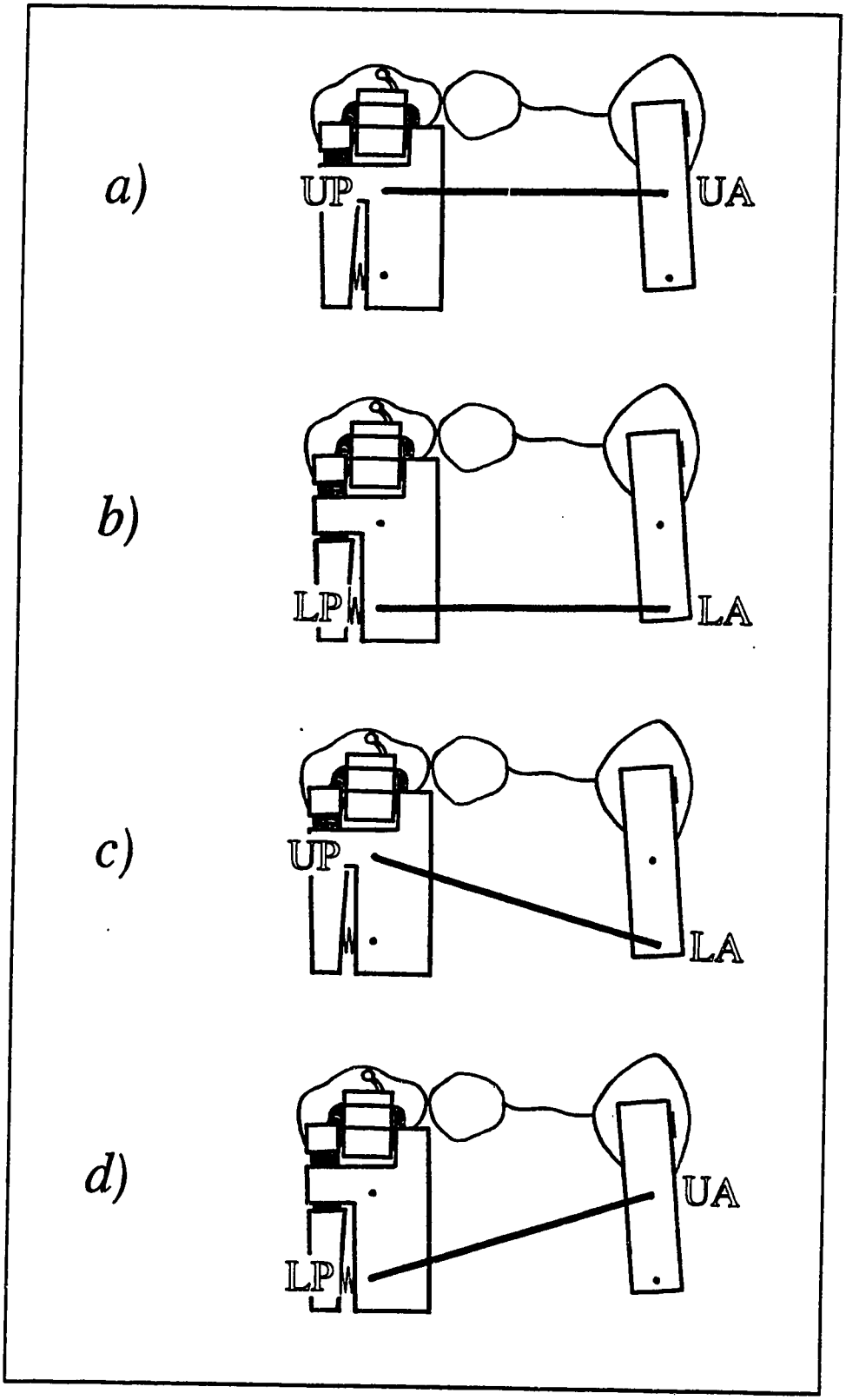

Figure 2.5: *Measurement of inter-tooth distances*

2.3 TOOTH DISPLACEMENT DETERMINATION

The translational and rotational displacements of the anterior segment of teeth (relative to the posterior segment) are determined by the "monthly" measurements of the **inter-tooth distances.** However, with these inter-tooth distances, there are several approaches to ascertaining the actual tooth displacements. It is necessary to find which approach is optimal, and the primary criterion for this is the minimization of the uncertainty in the displacements. Therefore, an extensive error analysis was performed on each approach.

2.3.1 Global Coordinate System

The first step for measuring displacements under any circumstances is the establishment of a global coordinate system. In this case, the global coordinate system is two-dimensional, since labio-palatal, or "out-of-the-measurement-plane", movements of the anterior segment of teeth are ignored. Exclusion of the out-of-plane movements is justified since the force systems generated by the orthodontic appliance act, for the most part, in the measurement plane only. Movements of the anterior segment are to be determined with respect to the posterior segment, since the amount of movement of the posterior segment is assumed to be much less than that of the anterior segment (especially in the mesial/distal direction). Therefore, it is logical to place the origin of the coordinate system at one of the two points on the posterior measurement block (ie. UP or LP). The lower posterior point (ie. LP) is chosen as the origin as indicated in Figure 2.6.

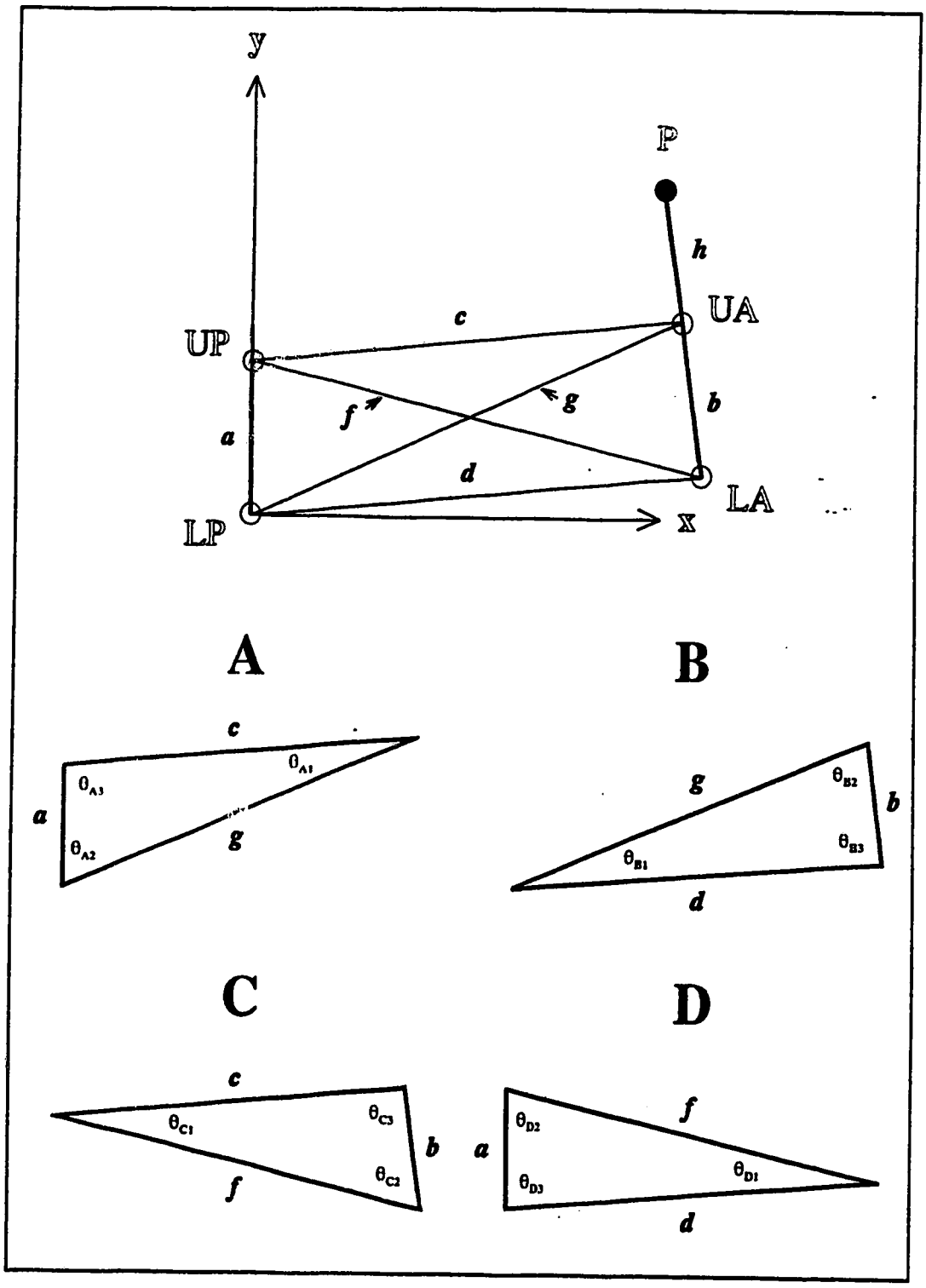

Figure 2.6: *Geometric representation of inter-tooth distances*

2.3.2 Location of Canine Tooth Axis

To monitor the movements of the anterior segment of teeth, it is unnecessarily complicated to observe the motion of all six teeth of the segment individually. The technique of space closure in this study was **anterior segment retraction.** Since the anterior segment is connected with a rigid full-sized rectangular archwire, translation and rotation of the entire anterior segment in the sagittal plane is characterized by the long axis of the canine. The line formed by the two points on the anterior measurement block (UA and LA) is assumed to represent the canine tooth axis, and therefore, the anterior segment. This line is perpendicular to the tube of the canine bracket through which one end of the orthodontic spring passes. A similar assumption concerning the tooth axis also pertains to the 1st molar and the posterior segment.

To determine the position and orientation of the canine tooth axis with respect to the 1st molar tooth axis every "month", the cartesian (ie. x and y) coordinates of points UA and LA must be calculated using the inter-tooth distances measured with each clinical visit. The inter-tooth distances form four individual triangles labelled **A, B, C,** and **D,** as shown schematically in Figure 2.6 for a patient's right side. With the given global coordinate system, triangle **A** can only determine the coordinates of the upper anterior segment point (UA), while triangle **D** can only determine the coordinates of the lower anterior segment point (LA). Triangles **B** and **C** cannot independently determine the coordinates of either anterior segment point since both triangles do not form an angle with the y axis. Simultaneous determination of the coordinates of UA and LA can only be accomplished using the following combinations of the four triangles:

{A & B}, {A & D} and {C & D}

Of all the angles in triangles A, B, C, and D shown in Figure 2.6, only six of them are necessary for calculating the positions of UA and LA: θ_{A2}, θ_{A3}, θ_{B1}, θ_{C1}, θ_{D2}, and θ_{D3}. Since none of the angles in the four triangles are known, these six angles must be calculated using the inter-tooth distances and the distances between the points on the measurement blocks (ie. *a*, *b*, *c*, *d*, *f*, & *g*). This is accomplished using the cosine law. In the example of Figure 2.7, the lengths of all three sides of a triangle are known. To determine the angle opposite to side L_3, θ, the cosine law gives

$$(L_3)^2 = (L_1)^2 + (L_2)^2 - 2\,L_1\,L_2\cos\theta\,, \tag{2.1}$$

which can be solved for the angle θ as

$$\theta = \cos^{-1}\left(\frac{(L_1)^2 + (L_2)^2 - (L_3)^2}{2\,L_1\,L_2}\right). \tag{2.2}$$

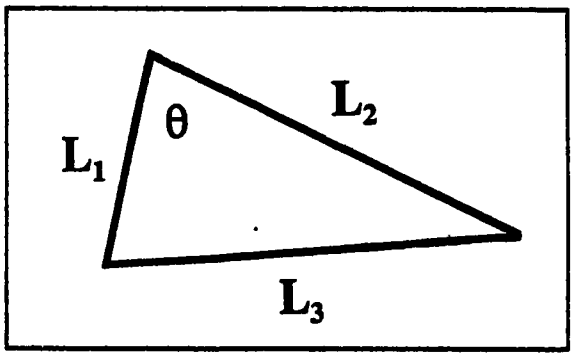

Figure 2.7: *An arbitrary triangle*

Using this expression the six angles previously mentioned become,

$$\theta_{A2} = \cos^{-1}\left(\frac{a^2+g^2-c^2}{2ag}\right) = \cos^{-1} p; \qquad p = \mathcal{F}(a,c,g), \tag{2.3}$$

$$\theta_{A3} = \cos^{-1}\left(\frac{a^2+c^2-g^2}{2ac}\right) = \cos^{-1} r; \qquad r = \mathcal{F}(a,c,g), \tag{2.4}$$

$$\theta_{B1} = \cos^{-1}\left(\frac{d^2+g^2-b^2}{2dg}\right) = \cos^{-1} s; \qquad s = \mathcal{F}(b,d,g), \tag{2.5}$$

$$\theta_{C1} = \cos^{-1}\left(\frac{c^2+f^2-b^2}{2cf}\right) = \cos^{-1} u; \qquad u = \mathcal{F}(b,c,f), \tag{2.6}$$

$$\theta_{D2} = \cos^{-1}\left(\frac{a^2+f^2-d^2}{2af}\right) = \cos^{-1} v; \qquad v = \mathcal{F}(a,d,f), \tag{2.7}$$

$$\theta_{D3} = \cos^{-1}\left(\frac{a^2+d^2-f^2}{2ad}\right) = \cos^{-1} w; \qquad w = \mathcal{F}(a,d,f), \tag{2.8}$$

where the notation $\mathcal{F}(a, c, g)$ means "a function of the lengths a, c, and g".

From the three combinations of triangles, there are three approaches to obtaining the cartesian coordinates of UA (ie. x_{UA}, y_{UA}):

$$\begin{aligned} x_{UA} &= c \sin\theta_{A3} = c\sqrt{1-r^2} \\ y_{UA} &= a - c\cos\theta_{A3} = a - cr \end{aligned} \tag{2.9}$$

$$\begin{aligned} x_{UA} &= g \sin\theta_{A2} = g\sqrt{1-p^2} \\ y_{UA} &= g \cos\theta_{A2} = gp \end{aligned} \tag{2.10}$$

$$\begin{aligned} x_{UA} &= c \sin(\theta_{C1}+\theta_{D2}) = c\left(v\sqrt{1-u^2}+u\sqrt{1-v^2}\right) \\ y_{UA} &= c \cos(\theta_{C1}+\theta_{D2}) = c\left(uv-\sqrt{1-u^2}\sqrt{1-v^2}\right) \end{aligned} \tag{2.11}$$

Similarly, there are also three approaches to obtaining the cartesian coordinates of LA (ie. x_{LA}, y_{LA}):

$$\begin{aligned} x_{LA} &= f \sin\theta_{D2} = f\sqrt{1-v^2} \\ y_{LA} &= a - f\cos\theta_{D2} = a - fv \end{aligned} \tag{2.12}$$

$$\begin{aligned} x_{LA} &= d \sin\theta_{D3} = d\sqrt{1-w^2} \\ y_{LA} &= d \cos\theta_{D3} = dw \end{aligned} \tag{2.13}$$

$$\begin{aligned} x_{LA} &= d \sin(\theta_{A2}+\theta_{B1}) = d\left(s\sqrt{1-p^2}+p\sqrt{1-s^2}\right) \\ y_{LA} &= d \cos(\theta_{A2}+\theta_{B1}) = d\left(ps-\sqrt{1-p^2}\sqrt{1-s^2}\right) \end{aligned} \tag{2.14}$$

It is evident that there are many ways of locating the two points of the canine tooth axis. However, each approach for obtaining the coordinates of UA cannot necessarily be used with any of the approaches to obtaining the coordinates of LA, and vice versa. This restriction will be explained in sub-section 2.3.4. The values of the dimensions on the posterior and anterior measurement blocks, *a* and *b* respectively, are both 6.97 mm.

2.3.3 Angular Orientation of Anterior Segment

Regardless of which set of equations is employed for calculating the positions of UA and LA, a general expression for the angular orientation of the anterior segment with respect to the posterior segment can be formulated. In Figure 2.8, the angular orientation of the anterior segment, α, is shown in its positive sense. The angle α of the anterior segment is calculated from either

$$\sin\alpha = \frac{x_{LA} - x_{UA}}{b} \tag{2.15}$$

$$\cos\alpha = \frac{y_{UA} - y_{LA}}{b}. \tag{2.16}$$

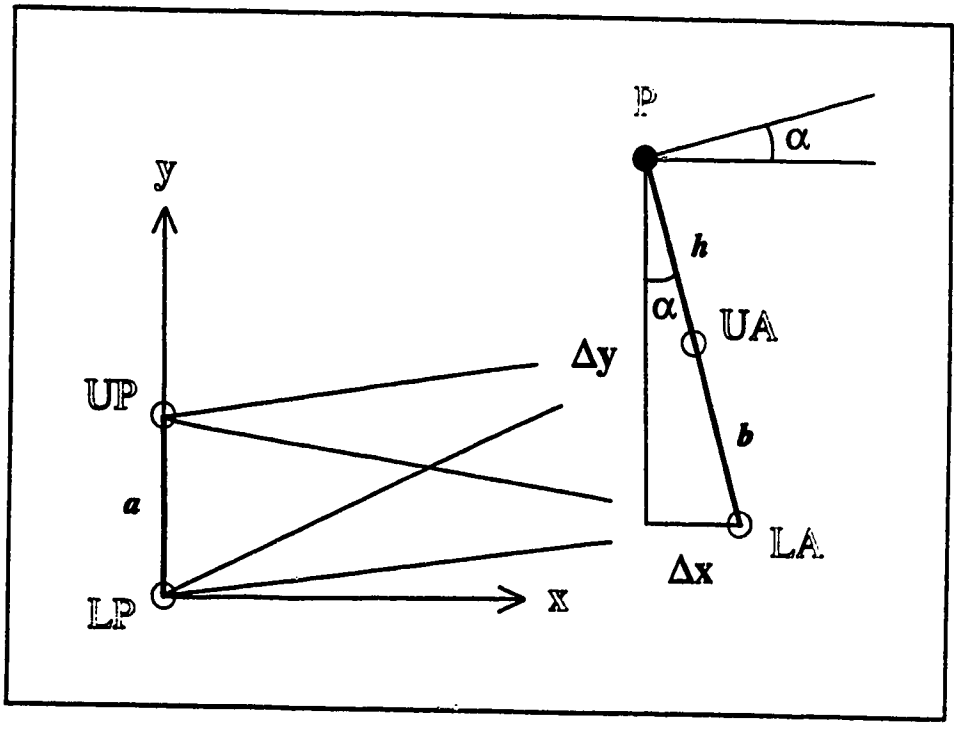

Figure 2.8: *Angular orientation of anterior segment*

2.3.4 Location of Point of Force Application to Anterior Segment

The two points representing the canine tooth axis (UA and LA) are located below the point at which the orthodontic spring applies forces and moments to the anterior segment. The displacement of the anterior segment can be observed from the point at which the forces and moments are applied to it by the orthodontic appliance, and this is located on the bracket of the canine tooth. To locate this point, called P in Figures 2.6 and 2.8, the cartesian coordinates of points UA and LA and the angular orientation of the anterior segment α previously discussed are used.

Referring to Figure 2.8, the differences in the x and y coordinates of LA and P (Δx and Δy, respectively) are calculated using angle α and the distance from LA to P:

$$\Delta x = (b+h)\sin\alpha = (b+h)\frac{x_{LA}-x_{UA}}{b} = (1+\frac{h}{b})(x_{LA}-x_{UA}) \qquad (2.17)$$

$$\Delta y = (b+h)\cos\alpha = (b+h)\frac{y_{UA}-y_{LA}}{b} = (1+\frac{h}{b})(y_{UA}-y_{LA}) \qquad (2.18)$$

where h is the distance between points P and UA and is equal to 7.25 mm. Knowing the coordinates of LA, the coordinates of P become

$$x_P = x_{LA} - \Delta x = x_{LA} - (1+\frac{h}{b})(x_{LA}-x_{UA}) = x_{UA} + \frac{h}{b}(x_{UA}-x_{LA}) \qquad (2.19)$$

$$y_P = y_{LA} + \Delta y = y_{LA} + (1+\frac{h}{b})(y_{UA}-y_{LA}) = y_{UA} + \frac{h}{b}(y_{UA}-x_{LA}). \quad (2.20)$$

As discussed in sub-section 2.3.2, there are several approaches to locating points UA and LA. Only some approaches to locating UA work with each approach to locating LA and this is restricted by the three combinations of the triangles in Figure 2.6 listed that can be used. These combinations are {A & B}, {A & D} and {C & D}. For example, the {A & D} combination uses either equations (2.9) and (2.12) or equations (2.10) and (2.13) to find the positions of UA and LA. For determining the position of P, the combination of triangles which yielded the lowest uncertainties in the positions of UA and LA was deemed most appropriate. These uncertainties were calculated using the general approach that will be described in sub-section 2.3.6. The {A & B} combination of triangles using equations (2.10) and (2.14) (for locating points UA and LA respectively) was chosen on the basis of this criterion.

With a specific approach to determining the positions of UA and LA established, equations (2.19) and (2.20) determine the cartesian coordinates of point P directly from the values of the inter-tooth distances:

$$x_P(a,b,c,d,g,h) = g(1+\frac{h}{b})\sqrt{1-p^2} - \frac{dh}{b}(p\sqrt{1-s^2} + s\sqrt{1-p^2}) \quad (2.21)$$

$$y_p(a,b,c,d,g,h) = g\left(1+\frac{h}{b}\right)p - \frac{dh}{b}\left(ps - \sqrt{1-p^2}\sqrt{1-s^2}\right) \qquad (2.22)$$

where p and s are given by equations (2.3) and (2.5). In addition, the angle of orientation α is determined by taking the inverse sine of both sides of equation (2.15),

$$\alpha = \sin^{-1} q$$
$$\textit{where:}\quad q(a,b,c,d,g) = \frac{1}{b}\left[d\left(p\sqrt{1-s^2} + s\sqrt{1-p^2}\right) - g\sqrt{1-p^2}\right]. \qquad (2.23)$$

2.3.5 Translational and Rotational Displacements

With the position of point P and angle of orientation α of the anterior segment at each clinical visit calculated, determining the translational and rotational displacement of the segment is a simple matter of subtraction. In the general case shown in Figure 2.9, the initial position of P is $(x_p)_1$, $(y_p)_1$ and its final position is $(x_p)_2$, $(y_p)_2$. According to this general case, the translational displacements in the positive sense are

$$\Delta x_p = (x_p)_1 - (x_p)_2 \qquad (2.24)$$

$$\Delta y_p = (y_p)_2 - (y_p)_1 . \qquad (2.25)$$

Positive x or horizontal displacement indicates the anterior segment is moving toward the posterior segment. Positive y or vertical displacement signifies that the anterior segment is moving gingivally, or into the periodontium. For the rotation of the anterior

segment, regardless of its initial and final orientation,

$$\Delta\alpha = \alpha_2 - \alpha_1 . \qquad (2.26)$$

With the general case of Figure 2.9, the rotation of the anterior segment is in the positive sense, which therefore represents a positive rotational displacement.

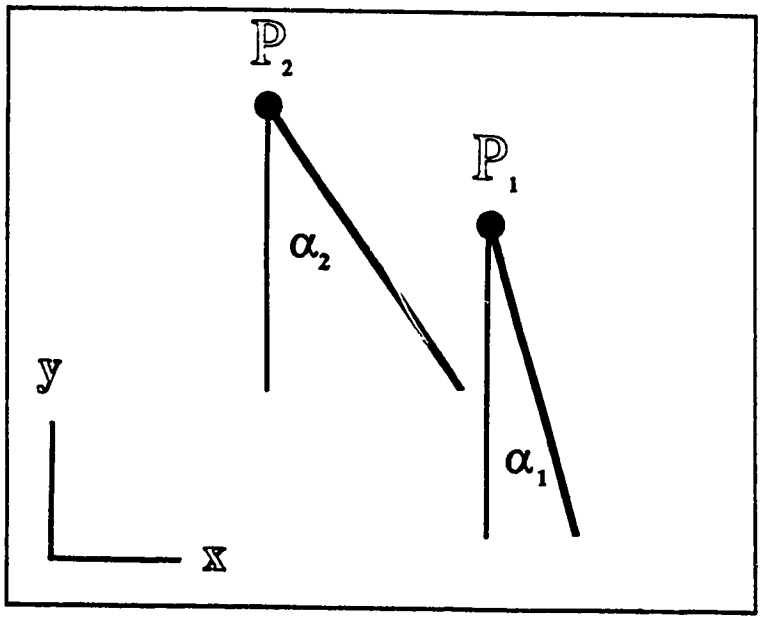

Figure 2.9: *Positive displacement of anterior segment*

2.3.6 General Error Analysis

Any calculated result is only as accurate as the values used to achieve that result. The formulas for calculating the cartesian coordinates of point P and the angular orientation α of the anterior segment -- equations (2.21), (2.22) and (2.23) -- are no exceptions to this. These equations are functions of the inter-tooth distances measured at each clinical visit (ie. *c*, *d* & *g*) and the dimensions of the measurement blocks (ie. *a*,

b & *h*). Uncertainties of these measurements affect the overall uncertainty in the position of P and the angle α at each visit. Subsequently, this affects the uncertainty in the translational and rotational displacements of the anterior segment between visits.

There is a general theory for finding the uncertainty in a function of several variables. Suppose that a set of measurements $x_1, x_2, \ldots x_n$ with respective uncertainties of $\delta x_1, \delta x_2, \ldots \delta x_n$ is made and the measured values are used to compute a function $G(x_1, x_2, \ldots x_n)$. If the uncertainties in $x_1, x_2, \ldots x_n$ are random, independent and expressed with a common level of confidence, then the uncertainty of the function at that level of confidence is [19]

$$\delta G = \sqrt{\left(\frac{\partial G}{\partial x_1}\delta x_1\right)^2 + \left(\frac{\partial G}{\partial x_2}\delta x_2\right)^2 + \ldots\ldots + \left(\frac{\partial G}{\partial x_n}\delta x_n\right)^2}. \qquad (2.27)$$

Before the uncertainty of the function can be found, the uncertainties of the measurements $\delta x_1, \delta x_2, \ldots \delta x_n$ must be determined. Each measurement's uncertainty is comprised of three components: the repeatability of the instrument when making that specific measurement (ie. R_I); the repeatability of the calibrator for the instrument (ie. R_C); and the systematic uncertainty of the calibrator (ie. S_C).

Repeatability, otherwise known as random uncertainty, is the range within which a high percentage of the values would lie if a measurement was repeated an extremely large number of times under identical conditions [20]. For all of the measurements with the intraoral micrometer, the repeatability range is the 95% confidence interval, and this also applies to both the random and systematic uncertainties of the calibrator. The test

for the repeatability of each inter-tooth distance's measurement was performed on one side of one patient, while the tests for the other measurements (ie. *a*, *b* & *h*) were performed without a patient.

It was not practical to repeat the measurements of the inter-tooth distances "an extremely large number of times", primarily for the sake of the patient's comfort. Ten readings were taken for each inter-tooth distance, while twenty readings were made for the remaining measurements. To compensate for the small size of the sample populations, the Student t distribution is used to define the 95% confidence interval around each mean value, so that the repeatability R_I is

$$R_I = t_{\nu,95\%}\,\sigma \tag{2.28}$$

in which $t_{\nu,95\%}$ is the Student t value for $\nu = n - 1$ degrees of freedom (n is the number of readings taken) and σ is the standard deviation of the batch of readings [20]. Using the measurement of *"a"* from Figures 2.6 and 2.8 as an example, the standard deviation is calculated with the formula

$$\sigma_a = \sqrt{\frac{1}{n-1}\sum_{i=1}^{n}(a_i - \bar{a})^2} \tag{2.29}$$

where a_i is the *i*th reading of *"a"* and $\bar{a}$ is the mean of the n readings taken.

To calibrate the intraoral micrometer the Brown & Sharpe Micro-Val™ Coordinate Measuring System [21], with a resolution of 0.001 mm, was used. In a

similar protocol as with the micrometer, the test for the repeatability of the calibrator was performed at an arbitrary reading of the micrometer, with the measurement repeated several times in rapid succession under identical conditions. The calibrator's repeatability (R_C), using the Student t distribution, was determined to be ±0.01 mm. According to its manufacturer's specifications, the systematic uncertainty, or constant bias within each measurement, of the Micro-Val™ (S_C) is a maximum of ±0.02 mm. These calibration errors were assumed to be the same for any measurement made by the micrometer.

All three components of the total uncertainty in any measurement with the micrometer have now been defined. Again using the example of the measurement of *"a"*, the total uncertainty in *"a"* is therefore

$$\delta a = \sqrt{R_{I,a}^2 + R_C^2 + S_C^2} \tag{2.30}$$

Of the three components in the total uncertainty of a measurement, the repeatability of the instrument when making the measurement, R_I, is always the dominant component. The total uncertainties for all of the measurements made with the intraoral micrometer (the dimensions of the measurement blocks as well as the inter-tooth distances, as shown in Figure 2.6) are listed in Table 2.2.

Table 2.2: *Total uncertainties in measurements with intraoral micrometer (in mm)*

δa	δb	δc	δd	δf	δg	δh
±0.04	±0.04	±0.13	±0.30	±0.22	±0.16	±0.25

Using the general formula (2.27) on equations (2.21), (2.22) and (2.23) with the total uncertainties in the measurements displayed in Table 2.2, the uncertainties in the cartesian coordinates of point P and angle α can be calculated. The average uncertainties in the x and y coordinates of point P were determined to be ± 0.40 mm and ± 0.76 mm respectively, while the average uncertainty in angle α was $\pm 2.8°$. Details of the calculations for these uncertainties are in Appendix A. For the uncertainty in any displacement, whether it is translational or rotational, the uncertainties in the initial and final positions or orientations are simply added together. This is because when adding or subtracting any number of quantities, the uncertainties in those quantities always add to compute the maximum overall uncertainty [19].

2.4 FORCE SYSTEM DETERMINATION

Forces and moments produced by any orthodontic appliance cannot be directly measured without interrupting treatment, and even the removal of the appliance from the patient's mouth creates errors in measurements. Without removing the appliance, the forces and moments it generates can be indirectly determined from its shape. This analysis of the appliance is accomplished with a photocopy of the spring in its initial, unstressed geometry (for example, Figure 2.1) and impressions of the installed spring (like the example in Figure 2.10) during each clinical visit.

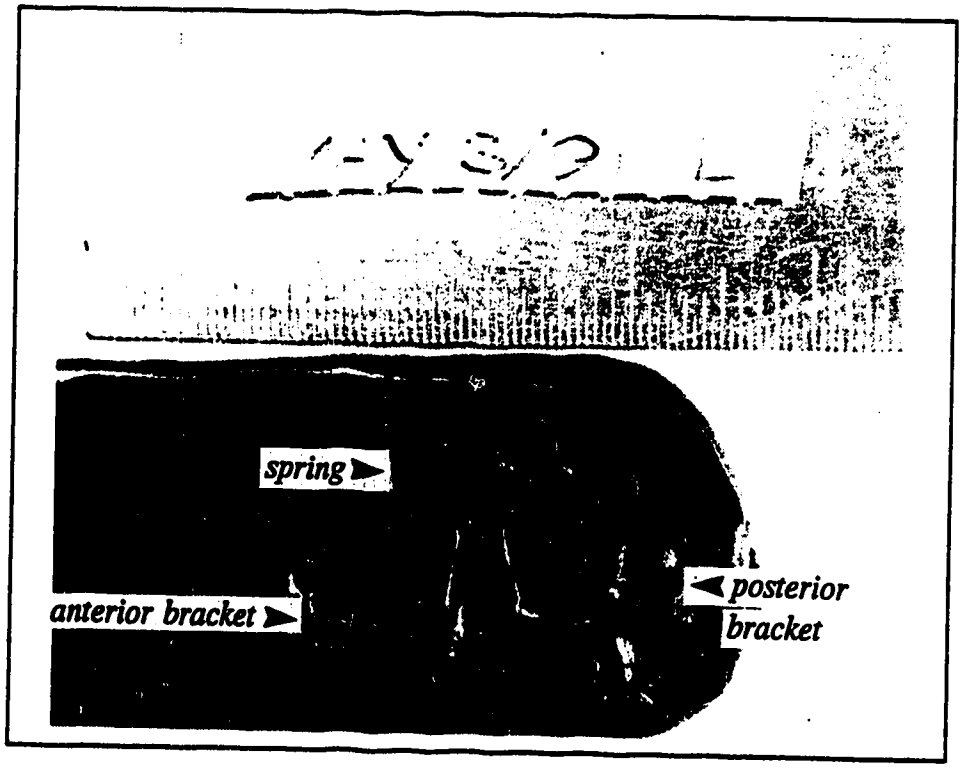

Figure 2.10: *Impression of spring and brackets combined*

2.4.1 Installation and Activation of the Orthodontic Appliance

As previously mentioned in the first two sections of this chapter, space closure in each patient is accomplished through the use of an orthodontic appliance called a pre-activated T-spring. In Section 2.2, the clinical procedure briefly described how the spring is installed and "reactivated" periodically. Figure 2.11a shows a typical T-spring in its unstressed condition before installation between the anterior and posterior segments of the teeth. Figure 2.11b depicts the **neutral position** of the T-spring, in which the ends of the spring are pulled down so that they are collinear. In this position, the spring is ideally generating no axial forces on either side (F_l and $F_r = 0$), so only shear forces (V_l and V_r) and moments (M_l and M_r) are present, where the subscripts l and r denote left and right respectively. The shear forces, which are very small in magnitude, are produced by the spring in its neutral position because an actual spring is not perfectly symmetric, with slight differences in corresponding dimensions between sides causing some shear at the ends. This is also true when the spring is "activated" while its ends remain collinear. Figure 2.11c demonstrates the initial **activation** of the spring, and in this example, the spring has been activated 3 mm. Here the ends of the spring are first inserted and pulled through their respective tubes. The activation (separation of the ends of the spring) is what generates the axial forces. In general, the greater the distance these ends are pulled apart, the higher the axial force levels produced. Approximately once every two months the spring is "reactivated", in which its ends are pulled further through their tubes. This "reactivation" is done in order to increase the force magnitude which had decreased as the segments of teeth (and therefore, the brackets) drew closer together.

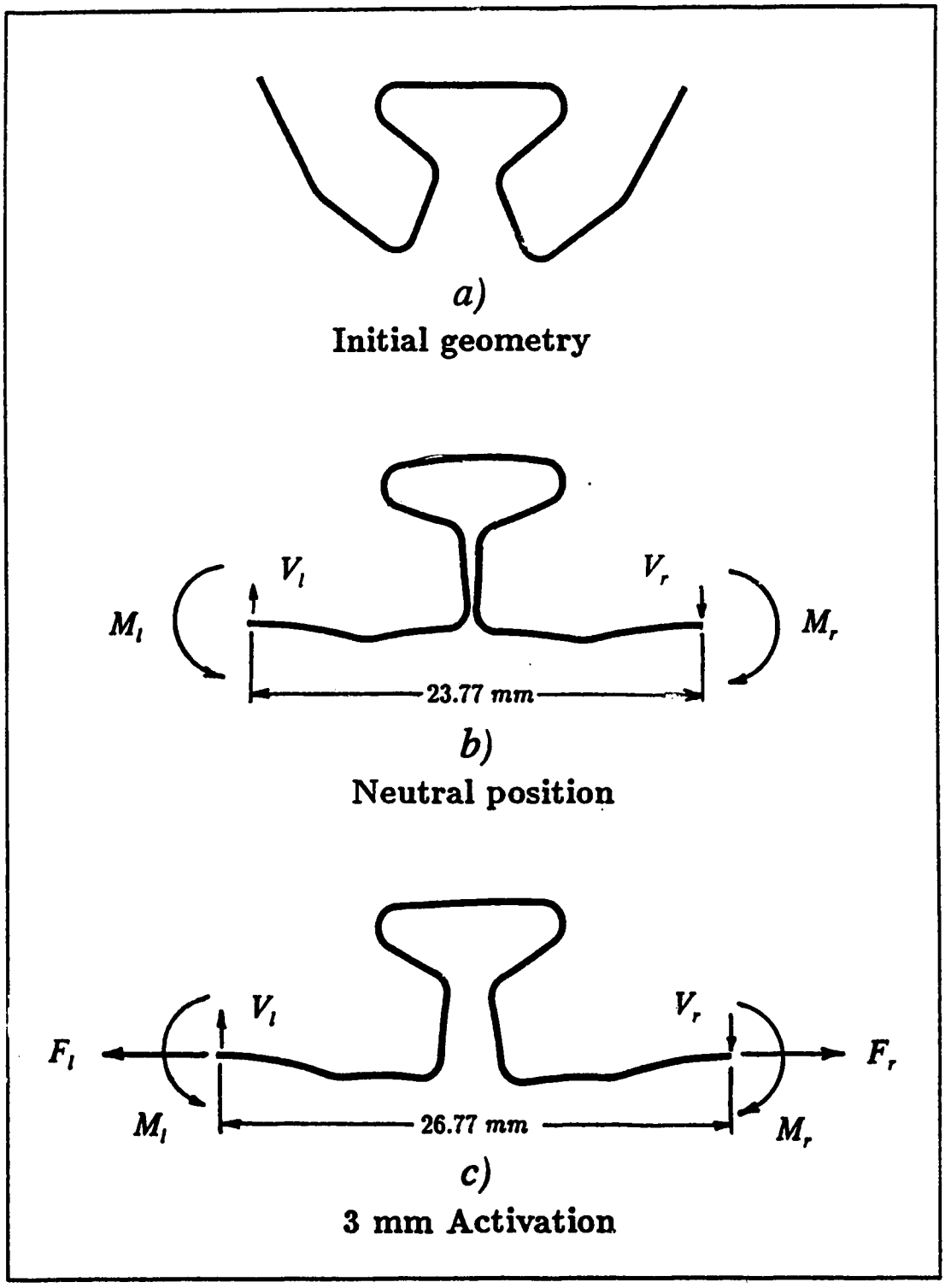

Figure 2.11: *Initial and deformed geometries of a typical T-spring*

2.4.2 Representation of Spring Geometry

In order to determine the force systems produced by the appliance throughout the patient's treatment, the initial shape of the appliance and its boundary conditions at the time in question must be known.

To evaluate the initial geometry of the spring, an enlarged photocopy is made of it in its unstressed condition. The photocopy of the spring is then divided into 17 sections, with each section recognized as either straight or curved with a constant radius of curvature, as shown in Figure 2.12. The lengths (ie. L_n: n = 1, 3, 5,.... 15, 17) of the straight sections and the lengths of the radii of curvature (ie. RoC_n: n = 2, 4, 6,.... 14, 16), as well as the angles that these radii "sweep through" (ie. θ_n: n = 2, 4, 6,.... 14, 16), of the curved sections are measured from the photocopy using a ruler and a protractor. These dimensions (with the cross-sectional dimensions and material properties of the spring) are then input into and stored by SEGTEC [22], the computer program used to calculate the force systems occurring at each end of the spring on the basis of the spring's geometric configuration.

Five characteristics of the geometry of the spring and brackets change from visit to visit. These are shown in Figure 2.13a: the inter-bracket distance (I.B.D.); the lengths of the first and last sections of the spring (L_1 and L_{17}); the vertical offset of the last node (y_{LAST}) (with respect to the first node); and the slope of the last node (also with respect to the first node), which happens to be equal to the angle α between the anterior segment and posterior segment. The inter-bracket distance, as stated in the clinical procedure, is measured *in vivo* by the orthodontist at each visit, and it is also verified by measuring

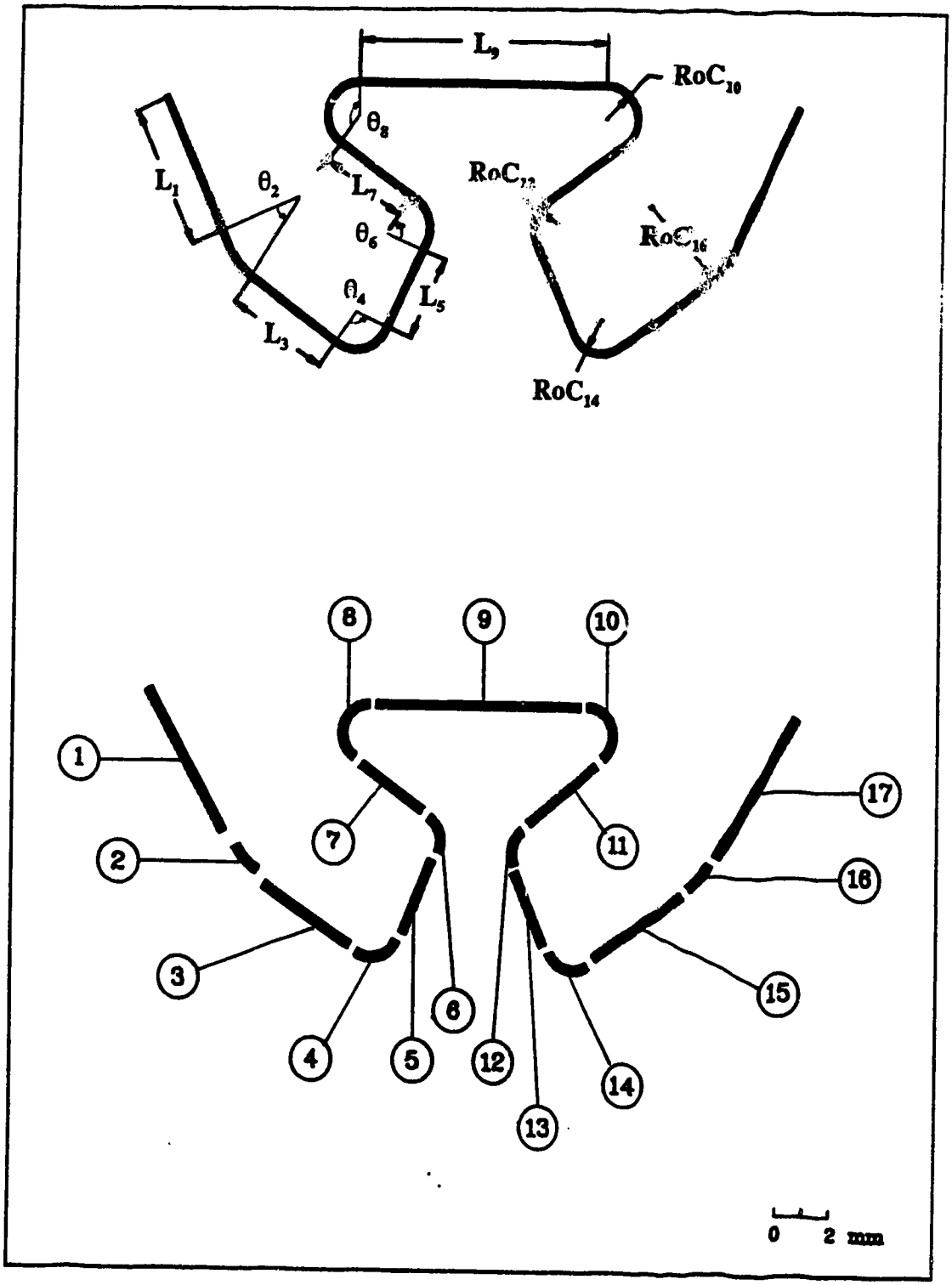

Figure 2.12: *Pre-activated T-loop spring sectioning*

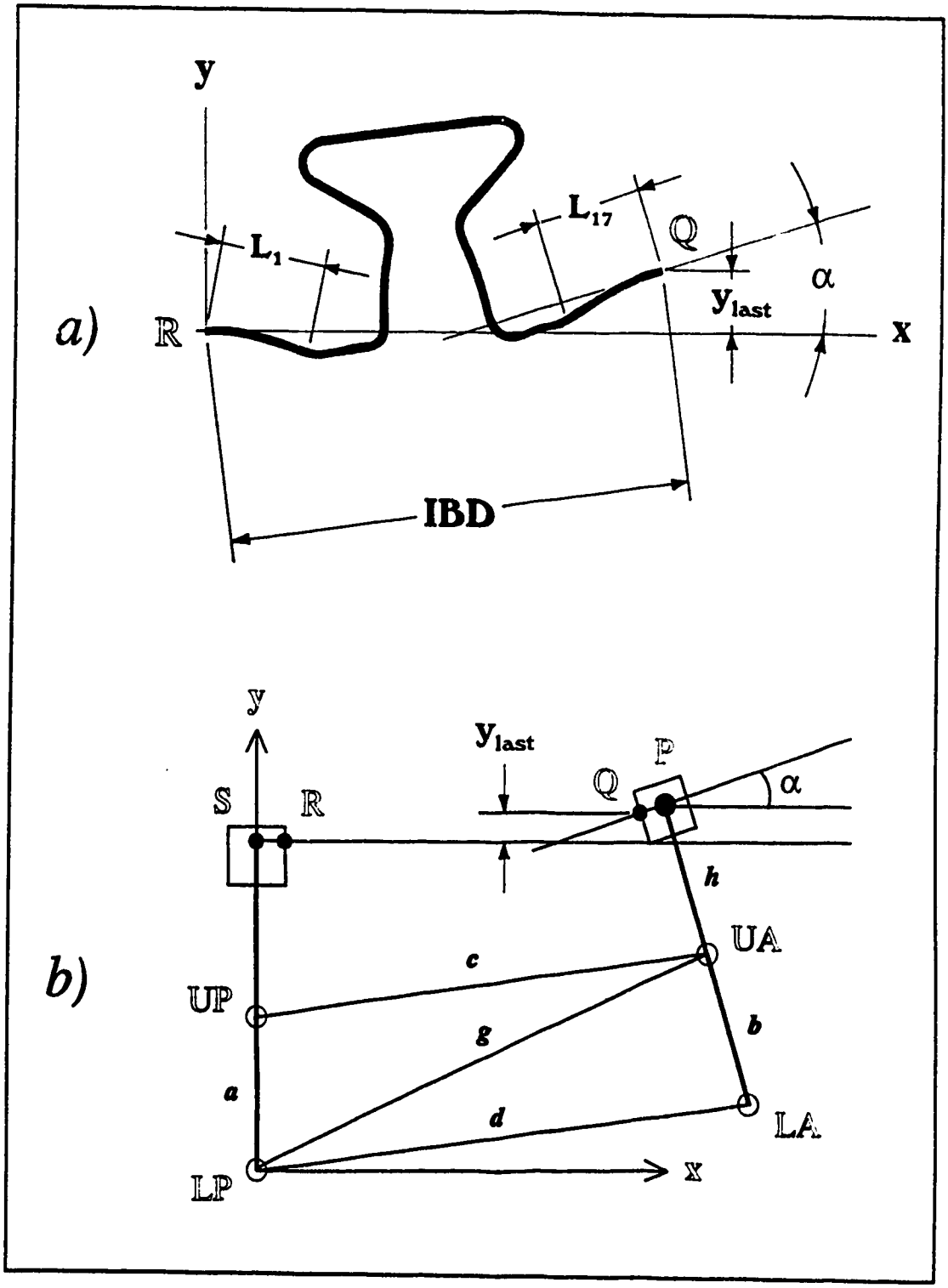

Figure 2.13: *Geometric properties of T-spring changing with time*

the I.B.D. on the impression. The lengths of the end sections are measured from the impression as well using the intraoral micrometer. They are the only dimensions of the spring itself that change every time it is reactivated. The full geometry of the spring and brackets in the impression is not used for any measurements other than the lengths of the end sections and the I.B.D., which serves to minimize errors due to varying impression depths, any possible distortion of the spring when the impression was made, and observer bias. The slope and offset of the last node of the spring are calculated from the inter-tooth distances and the dimensions of the measurement blocks, as described in Appendix A and shown in Figure 2.13b.

2.4.3 Sensitivity Analysis

The output from the computer program SEGTEC yields the force systems developed at each end of the spring, and this includes the axial forces (F_l and F_r), the shear forces (V_l and V_r), the moments (M_l and M_r), and the moment-to-axial force ratios ($\{M/F\}_l$ and $\{M/F\}_r$). Details concerning the background theory and function of SEGTEC can be found in the study by El-Rayes [22].

The results from SEGTEC, as with any other computer program, cannot be blindly regarded as correct. In a test for equilibrium errors, SEGTEC yielded discrepancies of only 2.6% in the axial force, less than 1% in the shear force, and 1.5% in the moment. When compared to the results of several experimental and finite element modeling studies, the results from SEGTEC were in good agreement with the other studies [22]. On the basis of this evidence, the results generated by SEGTEC are regarded as

sufficiently accurate for the purpose of this study.

Despite the established reliability of the results from SEGTEC, errors in the characteristics of the force systems could arise from inaccurate values being input to the program. The sources of such errors include: the dimensions of all of the spring's sections; the slope and vertical offset of its last node; the I.B.D.; the modulus of elasticity (E) of the spring's material (ie. TMA); and the cross-sectional dimensions of the spring. So as to appreciate the effects of errors in these parameters on the calculated force systems, a sensitivity analysis was performed on all sources of error individually.

For this sensitivity analysis, a symmetric "base case" T-spring was created, with its dimensions taken as average values of the springs used in this study. The primary boundary conditions of this standard T-spring were a zero slope and zero vertical offset for its last node (the spring's ends were collinear), as well as an I.B.D. of 22.5 mm. According to the neutral position of this T-spring, an I.B.D. of 22.5 mm indicates that its activation was approximately 7.0 mm, which is the average activation for all of the springs used throughout this study. Also common to all of the springs in this study, including this standard spring, is the value of the modulus of elasticity (E) of the TMA material. This was accepted to be 71.7 ± 2.92 GPa, and the yield strength of the material was set at 1240 MPa, as obtained from tension tests performed in a previous study [22].

For each parameter of the spring that is a potential source of error, its value was modified up to a maximum level of error, a "worst case", and the sensitivity of the force systems output to a discrepancy in that parameter was then quantified. The tables in Appendix B show the sensitivity of the force systems output from SEGTEC to 29

potential sources of error for the standard T-spring. For the axial force, six parameters (L_1, RoC_4, RoC_{14}, L_{17}, I.B.D. and the wire cross-section dimensions) produced errors greater than ±0.30 N, with four others above ±0.20 N. With the shear force, there were only two significant parameters, y_{LAST} and α, both of which produced errors of ±0.40 N or more, and few other parameters even approached the significance of these two parameters. The dominant parameters for errors in moment were L_1, y_{LAST} and α, all with absolute errors near ±3 N mm, and eight other parameters made errors around ±1 N mm. Last of all with the moment-to-force ratio, six parameters generated errors between ±0.50 mm and ±0.66 mm and six others made errors around ±0.30 mm.

Using the results of the sensitivity analysis, the overall error in each force system component (F, V, and M) and the M/F ratio can be estimated. To determine the overall error in either component or the M/F ratio, it was estimated that the average error which each parameter contributed to the overall error was half of the magnitude of the maximum value listed in Tables B.1 to B.3. Similar to the general equation (2.27), the estimated overall error for a force system component or the M/F ratio was then calculated to be the square root of the sum of the squares of the corresponding average errors due to errors in the parameters. In this study, there were 29 parameters which contributed to the overall error in a given force system component, such as the axial force, F, so let these parameters be called x_1, x_2, ..., x_{29} and the average errors that each of these parameters contributes to the overall error in F are δF_{x1}, δF_{x2}, ..., δF_{x29}. Assuming the average errors were random and independent of each other, the estimated overall error in the axial force, $\delta F_{overall}$, would be

$$\delta F_{overall} = \sqrt{(\delta F_{x1})^2 + (\delta F_{x2})^2 + \ldots\ldots + (\delta F_{x29})^2}\,, \qquad (2.31)$$

with δF_{x1}, for example, equal to half of the maximum error in F due to maximum variation in parameter x_1. The estimated overall errors in the force system components and the M/F ratio resulting from the approach that equation (2.31) represents are shown below in Table 2.3.

Table 2.3: *Estimated overall errors in force systems components and M/F ratio*

	F (N)	V (N)	M (N mm)	M/F (mm)
overall error	±0.5	±0.4	±3.2	±0.8

Chapter 3

RESULTS AND DISCUSSION

In Chapter 3, sign conventions for the directions of tooth displacements and force system components are set. Schematic representations of the movement of the anterior segment are shown for both sides of the dental arch of the five patients. These representations depict the quantitative nature of the anterior segment's movement with respect to the posterior segment. This is followed by analyses of the relationships between axial force and x displacement, shear force and y displacement, and M/F ratio and rotational displacement. The significance of the results of these analyses to current orthodontic practices is then discussed, specifically addressing the controversy concerning what force system is optimal for orthodontic treatment.

3.1 SIGN CONVENTIONS

For clarity and convenience, sign conventions for the tooth displacements and the force systems applied must be established. Figures 3.1 and 3.2 show the positive directions for tooth movements and force system components (on the ends of the spring, as well as on the teeth themselves) for the left and right sides of the maxillary dental arch. These figures are schematic representations of the left and right sides of the dental arch as observed in profile from the outside of the mouth.

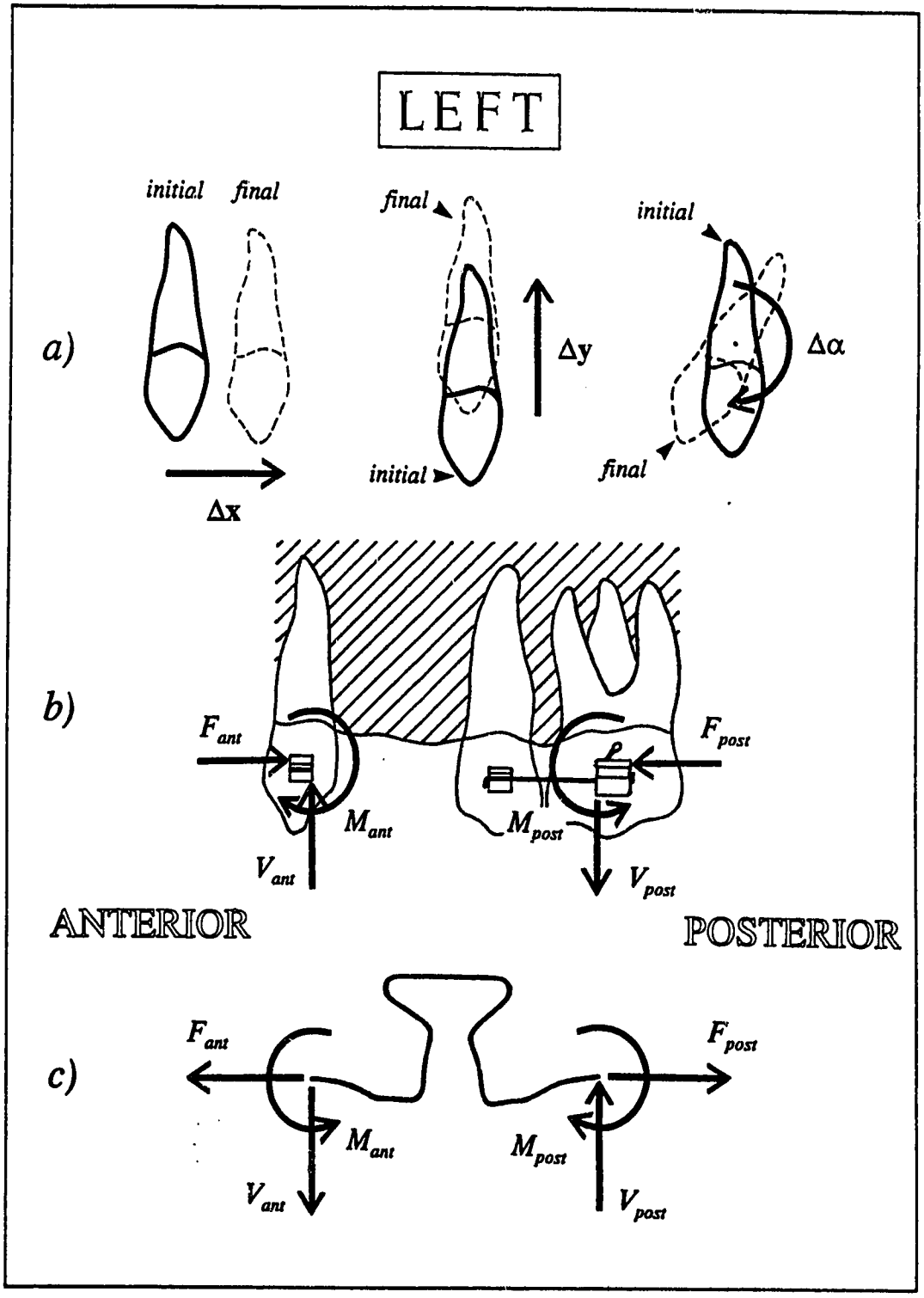

Figure 3.1: *Positive directions for force system components and tooth displacements for the patient's left side*

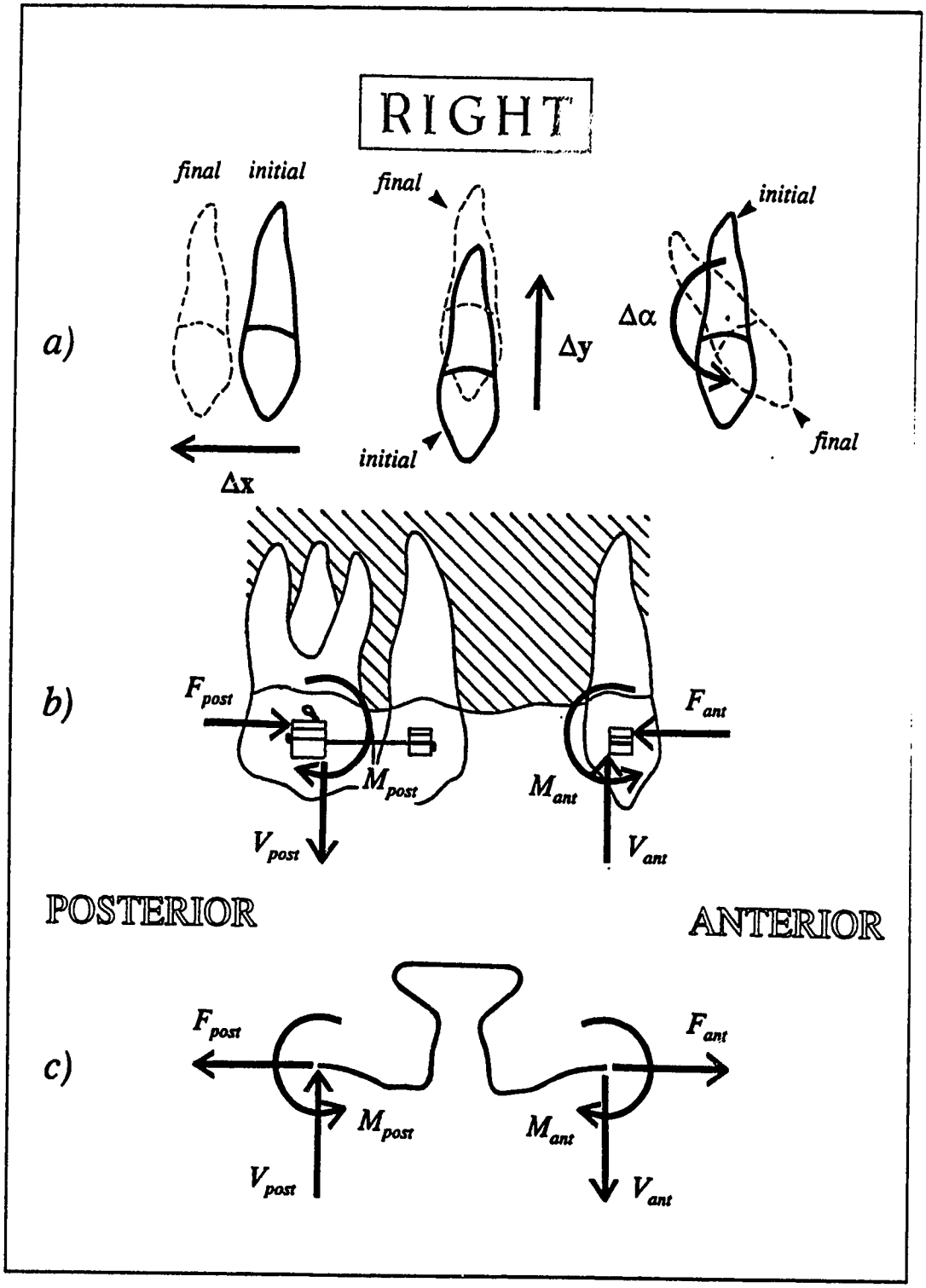

Figure 3.2: *Positive directions for force system components and tooth displacements for the patient's right side*

For the left side, Figure 3.1a indicates the positive directions of x, y, and rotational displacement respectively. For each displacement, the solid shape of the canine tooth represents its initial position, while the phantom (broken line) shape represents an arbitrary final position of the tooth, indicating movement of the tooth (and therefore the anterior segment) in the positive direction. The positive directions for the force system components acting on the brackets of the canine (F_{ant}, V_{ant}, and M_{ant}) and 1st molar (F_{post}, V_{post}, and M_{post}) are depicted in Figure 3.1b. These same force system components are shown in the positive sense as produced at the ends of the T-spring in Figure 3.1c. For the right side, Figures 3.2a, b, and c are arranged in the same manner as described above.

3.2 RESULTS

The results of this investigation were determined using the clinical data listed in Appendix C, which was collected from five patients referred to as RD, DK, NM, TT, and RZ. Both sides of the maxillary arch of each patient were observed for periods ranging from six to eleven months, with monthly visits for monitoring progress. For each patient, translation and rotation of the anterior segment is measured relative to the posterior segment, as the posterior segment is assumed to have moved considerably less than the anterior segment. All uncertainties in displacements of teeth, whether translational or rotational, were calculated by the error analysis described in Appendix A. As mentioned in sub-section 2.3.6, these uncertainties represent a 95% confidence interval with the Students t distribution of the data.

3.2.1 Movement of the Anterior Segment of Teeth

Figures 3.3 to 3.12 are schematic representations of the movement of the maxillary anterior segment as viewed extraorally (ie. from outside of the mouth) for the left and right sides of each patient. Each of these figures show the posterior segment as the vertical line passing through points $\mathbb{LP}$, $\mathbb{UP}$, and $\mathbb{S}$, and the position and orientation of the anterior segment is depicted at each clinical visit, numbered from the first visit, 1, in ascending order to the final visit. Point $\mathbb{S}$ is the midpoint of the first molar bracket's tube through which one end of the orthodontic spring passes. Similar to the posterior segment, the anterior segment is a line connecting the three points $\mathbb{LA}$, $\mathbb{UA}$, and $\mathbb{P}$, which can also be seen in Figure 2.13. With both sides of all of the patients, the anterior segment's movement was most often distal, or toward the posterior segment, so as to achieve space closure which signified the end of treatment. All translational movements of the anterior segment were measured from point $\mathbb{P}$ where the force systems were applied to the segment.

In Figures 3.3 and 3.4, the movement of the anterior segment in RD can be seen to be a combination of rotation and translation for both sides. With the root moving posteriorly, the amount of rotation of the segment appears to be somewhat different between the left and right sides. In addition to this, on the left side the vertical translation is generally intrusive or upward, while for the right side the y displacement oscillates, moving up and down until finally settling in a position 1 mm lower than the original position. This discrepancy in translation and rotation between sides of the same patient may be attributed to differences in the positions of the brackets adhered to the

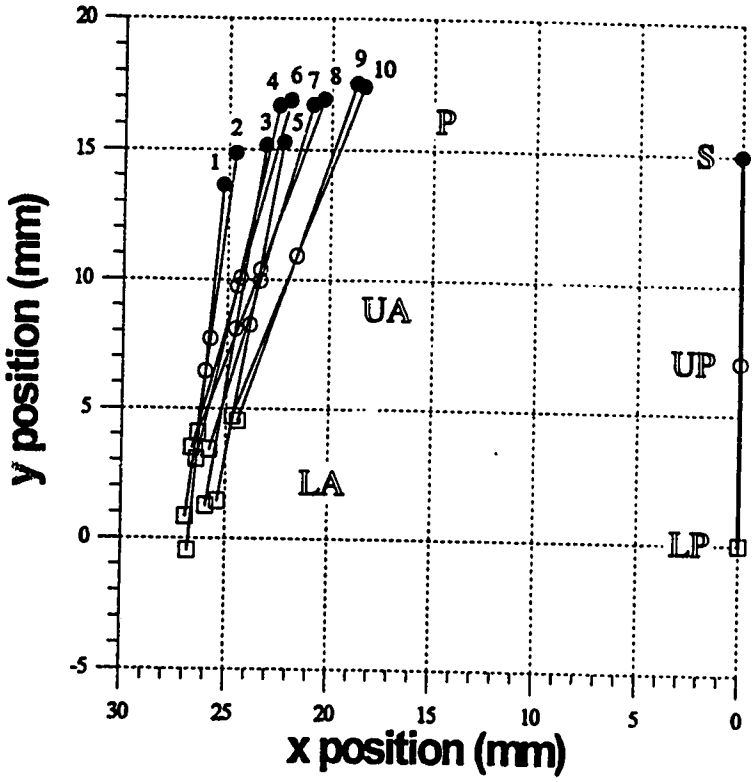

Figure 3.3: *Movement of anterior segment for RD (left)*

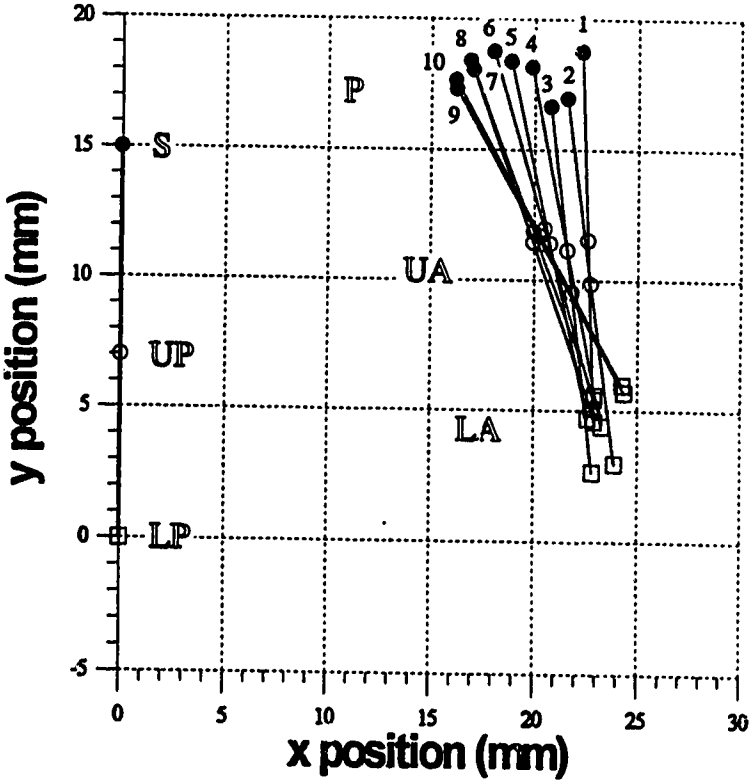

Figure 3.4: *Movement of anterior segment for RD (right)*

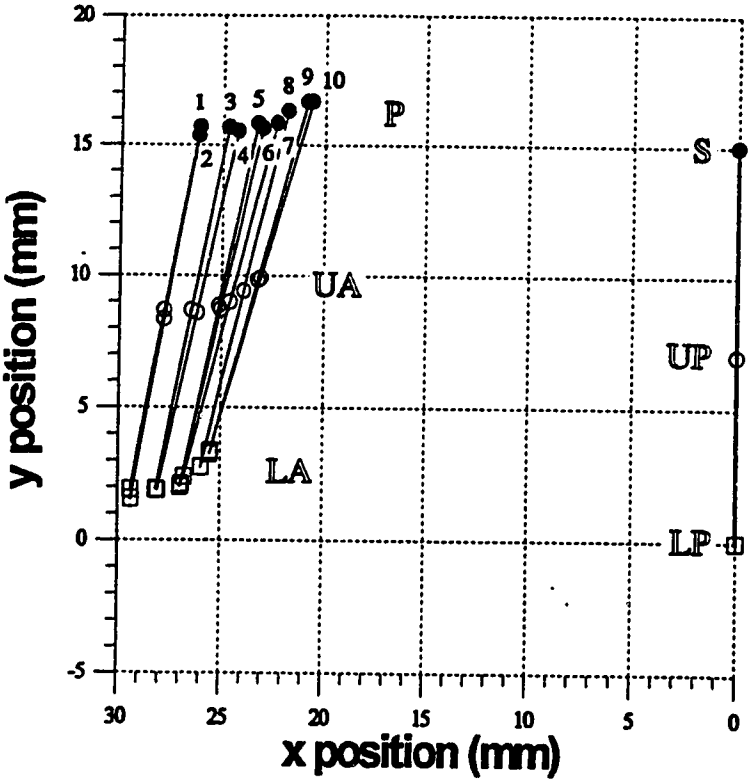

Figure 3.5: *Movement of anterior segment for DK (left)*

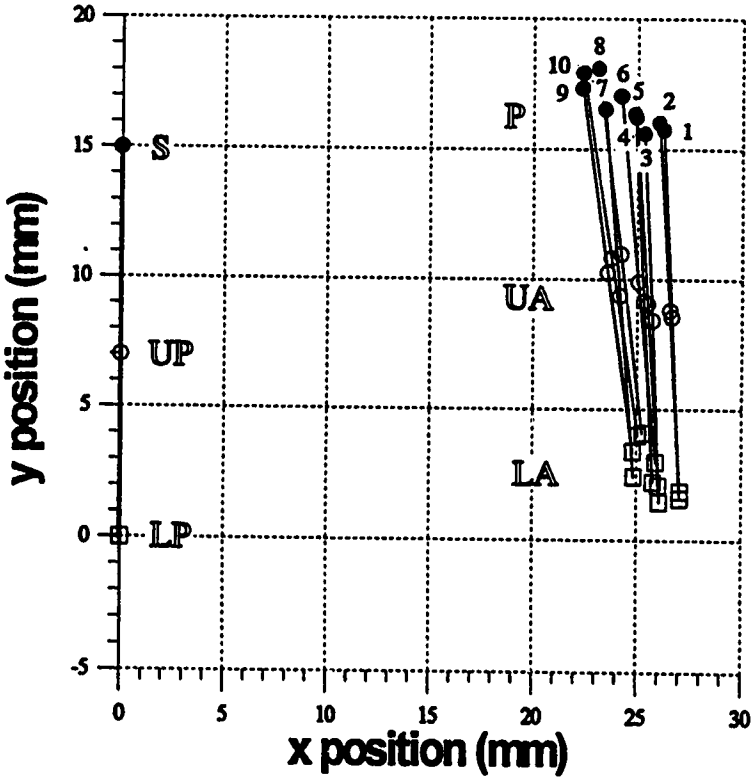

Figure 3.6: *Movement of anterior segment for DK (right)*

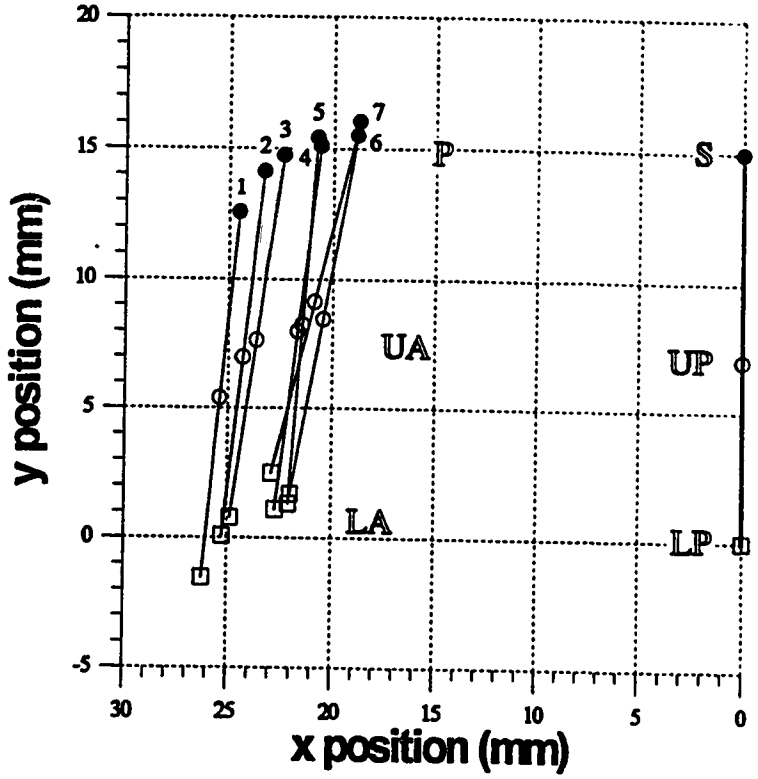

Figure 3.7: *Movement of anterior segment for NM (left)*

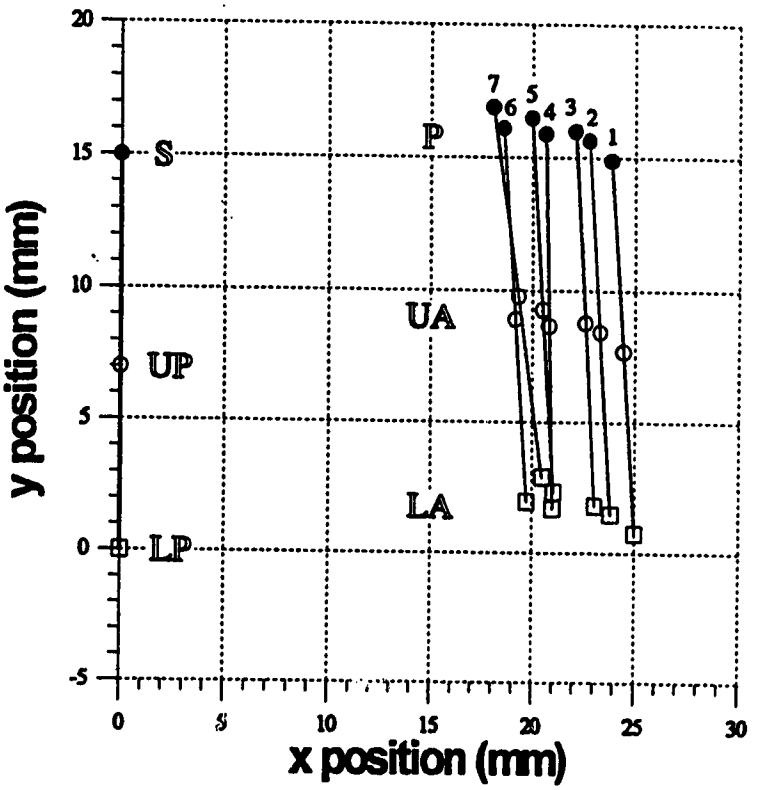

Figure 3.8: *Movement of anterior segment for NM (right)*

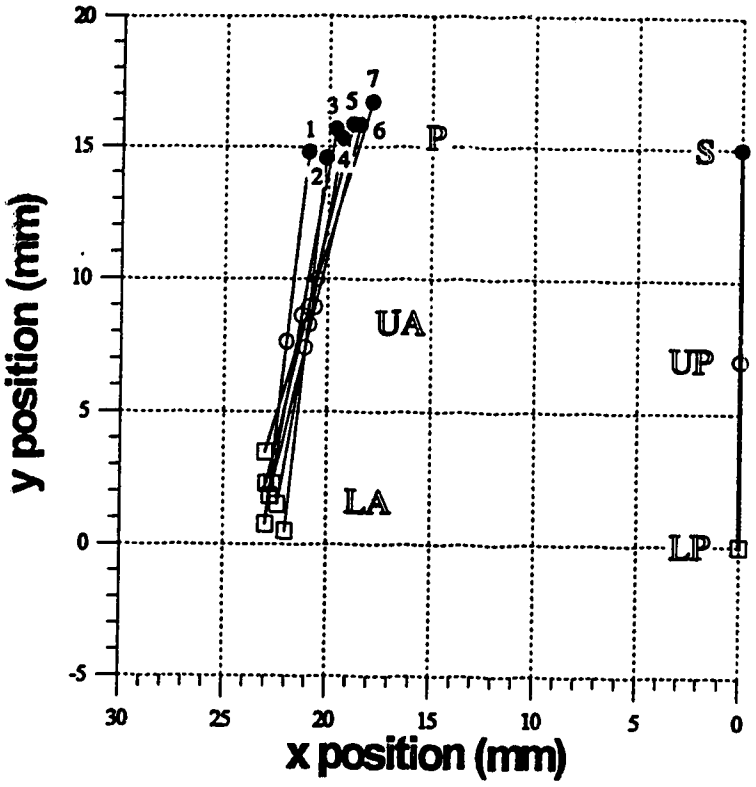

Figure 3.9: *Movement of anterior segment for TT (left)*

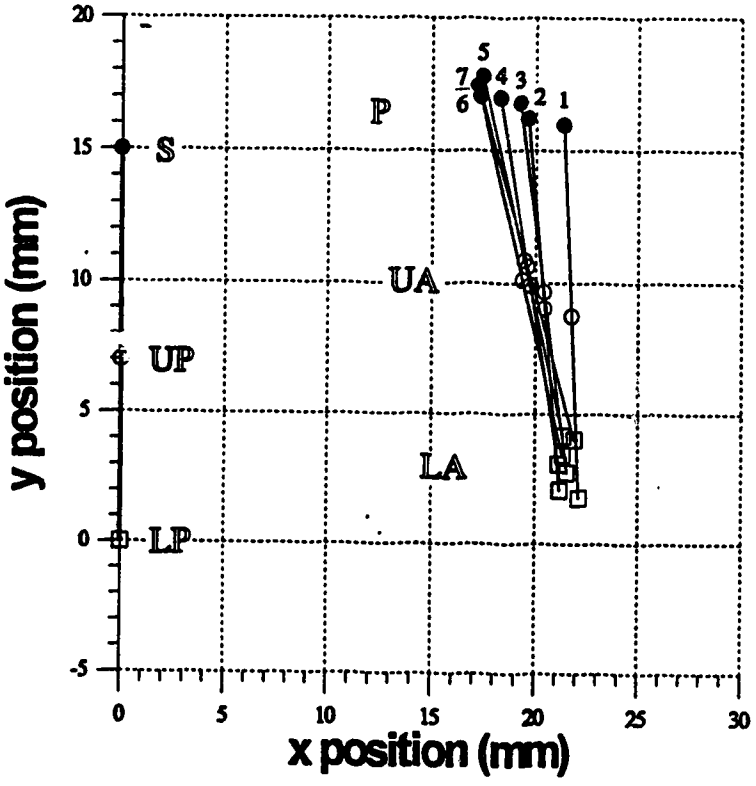

Figure 3.10: *Movement of anterior segment for TT (right)*

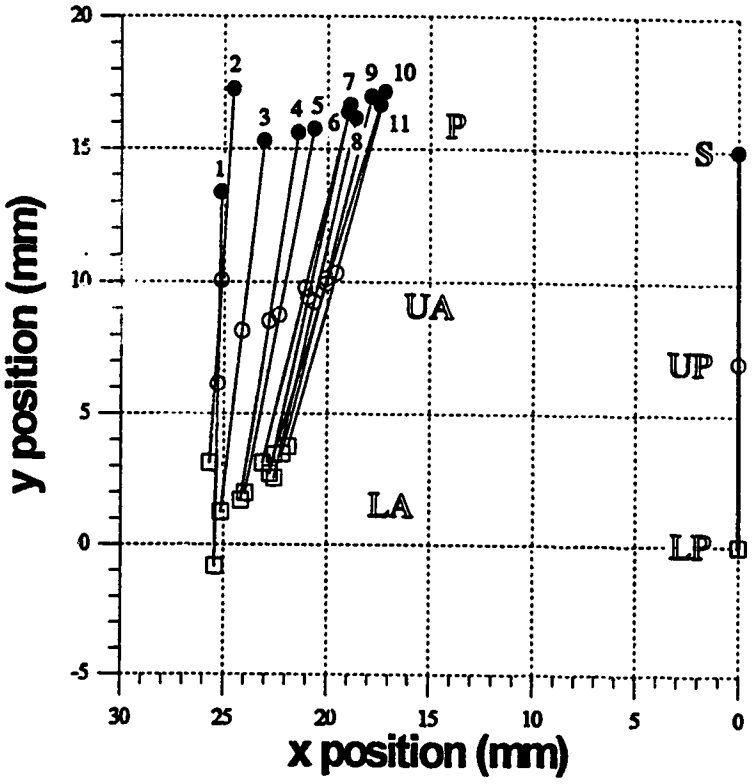

Figure 3.11: *Movement of anterior segment for RZ (left)*

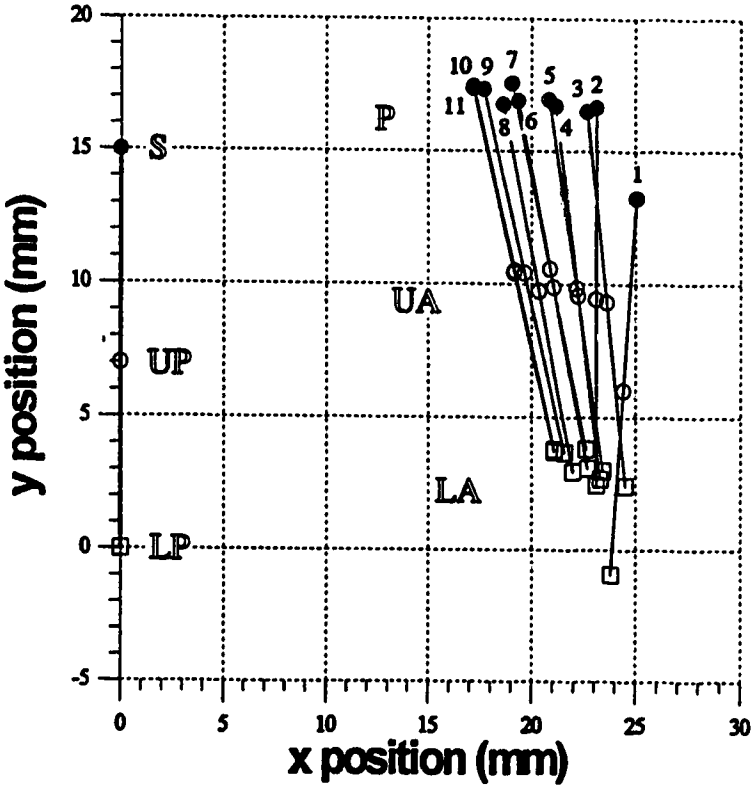

Figure 3.12: *Movement of anterior segment for RZ (right)*

labial surfaces of the canine teeth relative to their 1st molar counterparts, or unexpected tipping and positive y displacement of the posterior segment.

Figures 3.5 and 3.6 reveal that the anterior segment of patient DK did not experience any significant rotation. Both sides show only translation took place, with the right side moving intrusively about 1 mm more than the left side. This difference is of no consequence when the uncertainty in the y position of the anterior segment is considered, and this shall be addressed later. A comparison of the x displacements on the left and right sides shows a greater amount of total distal movement on the left side.

Movement of the anterior segment of patient NM is shown in Figures 3.7 and 3.8. For both sides, it can be seen that the anterior segment strictly translated intrusively and distally from the 1st to the 4th clinical visit. From the 4th to the 7th visit, there was some limited positive rotation and additional translation. The total distal translation of the anterior segment was about the same for the left and right sides.

Figures 3.9 and 3.10 depict the movement of patient TT's anterior segment as seen from left and right profile views. After some pure distal translation between the 1st and 2nd visits, the anterior segment rotated in the positive direction while slowly moving upward about 2 mm. The total distal translation of the anterior segment was greater on the right side than the left, with a difference of 1 mm.

For the movement of the anterior segment of RZ, Figures 3.11 and 3.12 show its displacement from the left and right sides respectively. As observed from both sides, the anterior segment experienced a large upward displacement of about 3.5 mm, along with a slight positive rotation, between the 1st and 2nd visits. This was followed by a

combination of small amounts of positive rotation and generally positive x and y displacement from the 3rd to the 11th visit. Both sides of the anterior segment of RZ had a total distal translation of nearly 8 mm.

3.2.2 Axial Force and X Displacement

As indicated in the literature review in Chapter 1, the relationship most often investigated in orthodontic studies is that between the mesial/distal or axial force, F, and the tooth movement in the direction of that force, otherwise known as x displacement, Δx. Figures 3.13 to 3.22 show the changes in axial force applied to and the displacement of point $\mathbb{P}$ in the x direction over time for both sides of the five patients in this study. The times at which the orthodontic spring was reactivated (approximately every two months) are identified in these figures by abrupt increases in the magnitude of the axial force applied on the same day. When space closure was completed early, this is indicated in Figures 3.13 to 3.22 with the label "SC" (meaning Space closure Complete) above the error bars of the x displacement curve on the days that closure was observed during the clinical visit. Space closure was regarded to be complete once the crowns of the canine and 2nd premolar made first contact with each other. Error bars for the axial force are not shown in these figures in order to avoid clutter with the error bars for the x displacements. Uncertainty in the axial force at any given time during treatment was estimated to be about ±0.5 N, as determined through the sensitivity analysis described in Chapter 2 and Appendix B.

Some of the primary concerns in orthodontic treatment are what axial force levels

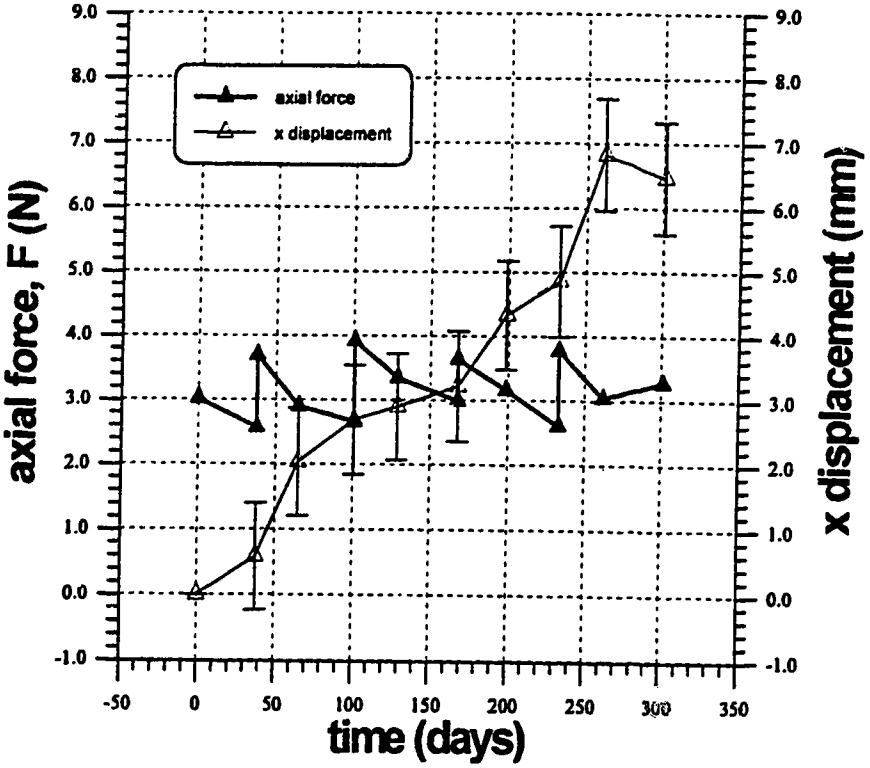

Figure 3.13: *Axial force and x displacement of point P over time for RD (left)*

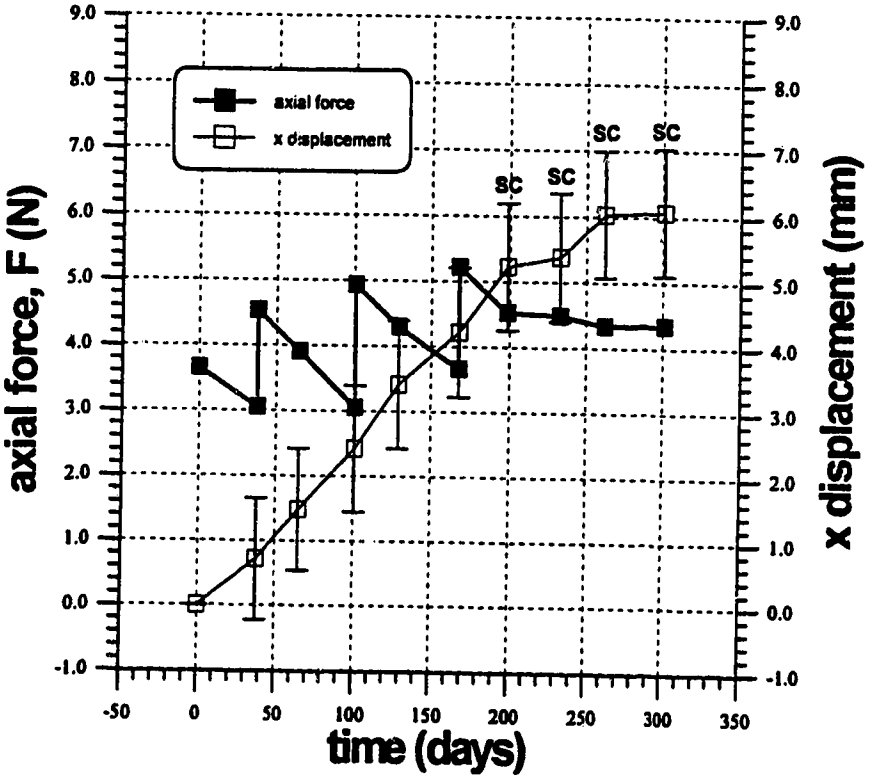

Figure 3.14: *Axial force and x displacement of point P over time for RD (right)*

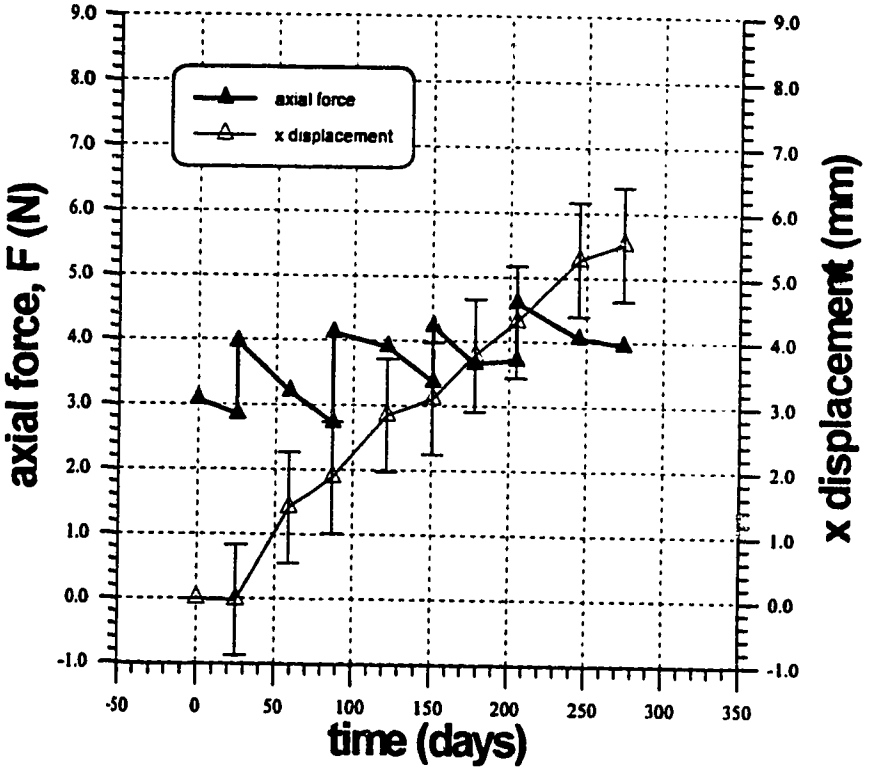

Figure 3.15: *Axial force and x displacement of point P over time for DK (left)*

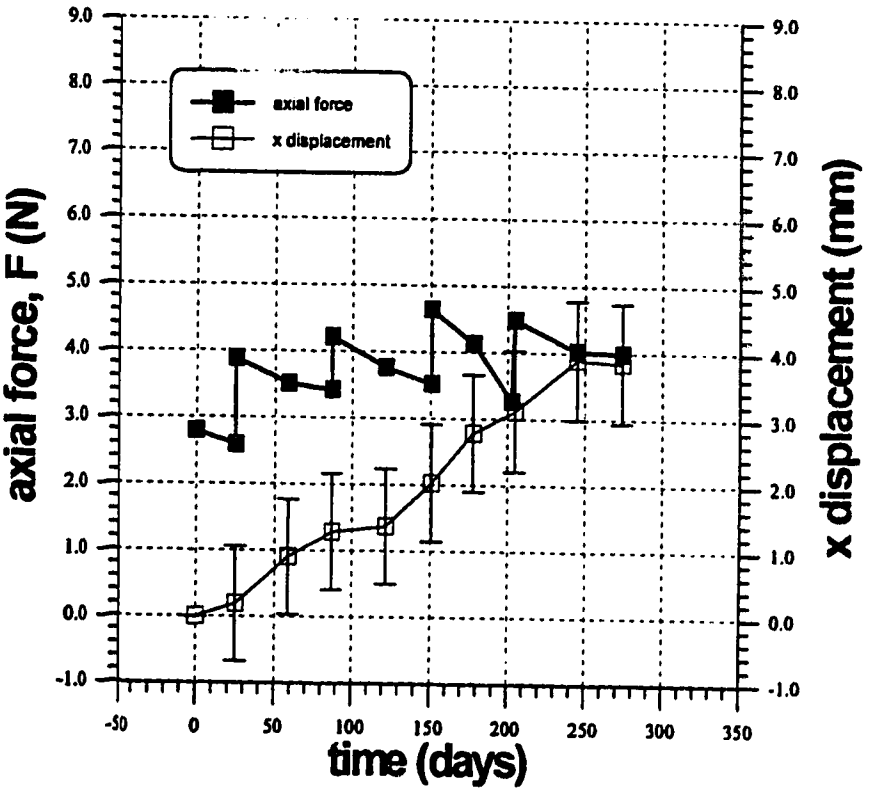

Figure 3.16: *Axial force and x displacement of point P over time for DK (right)*

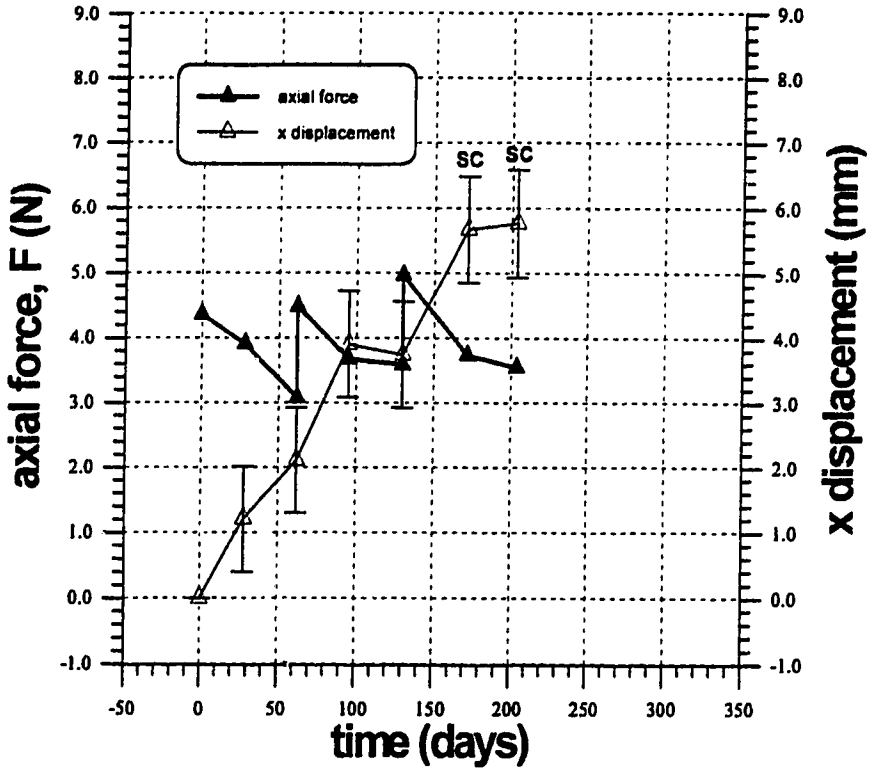

Figure 3.17: *Axial force and x displacement of point P over time for NM (left)*

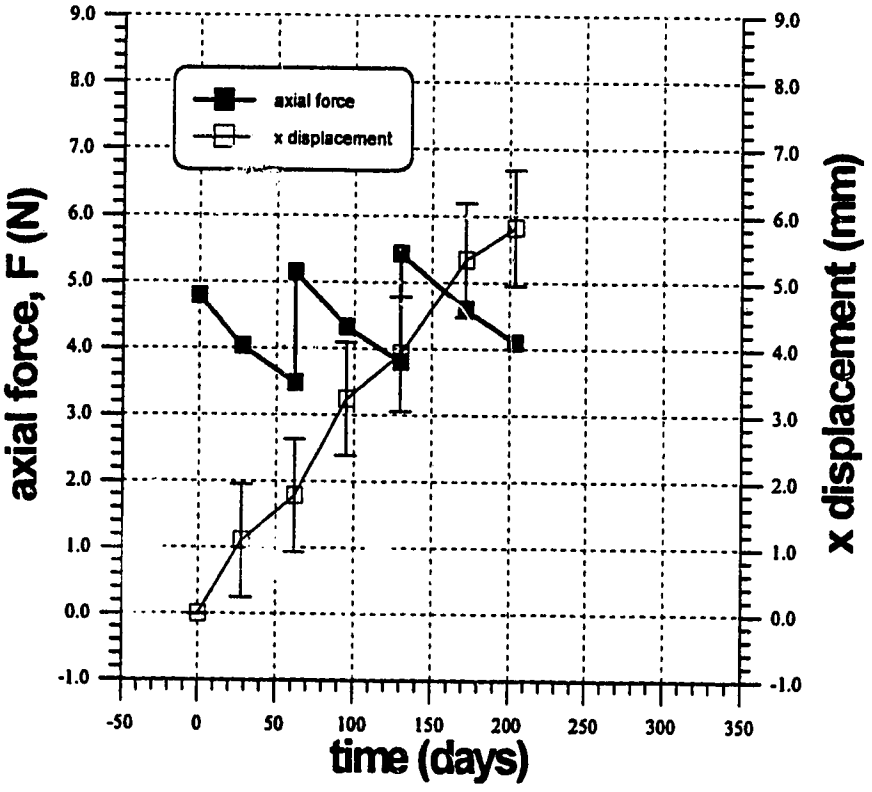

Figure 3.18: *Axial force and x displacement of point P over time for NM (right)*

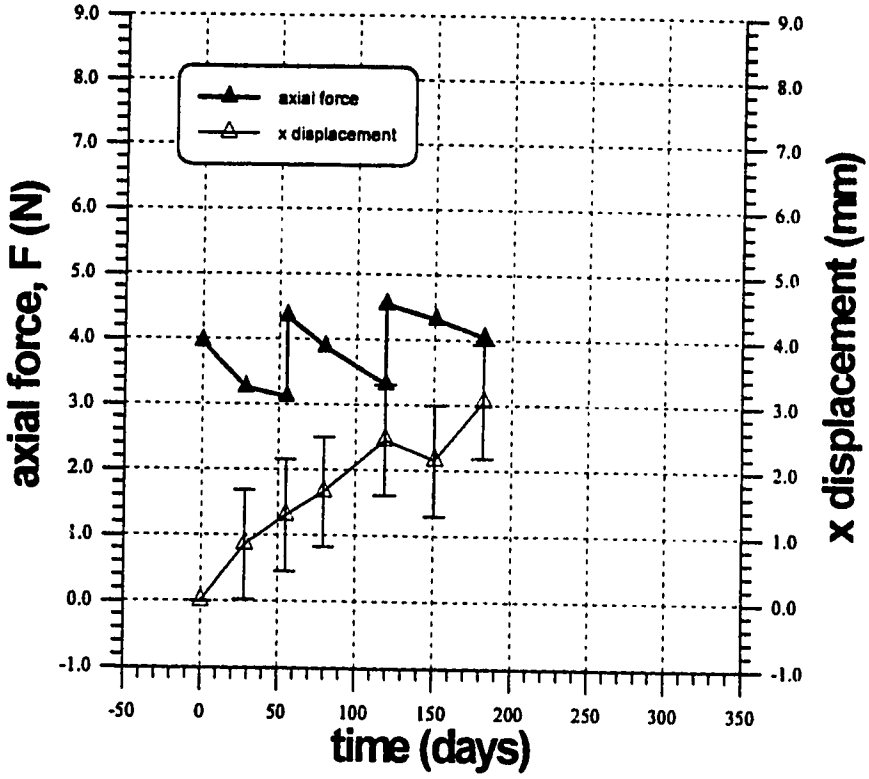

Figure 3.19: *Axial force and x displacement of point P over time for TT (left)*

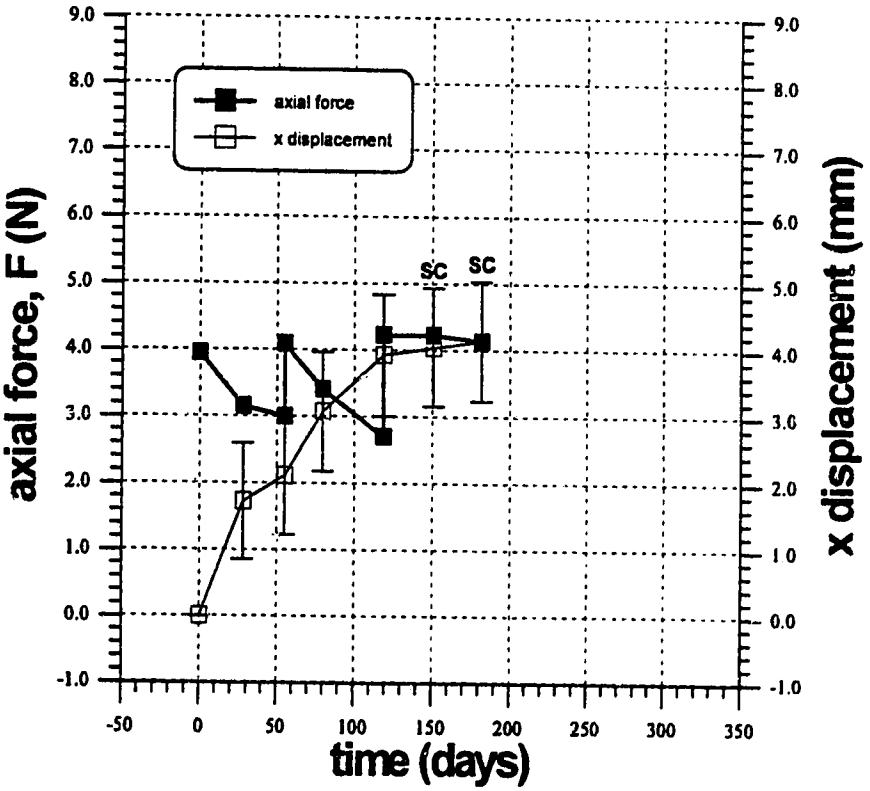

Figure 3.20: *Axial force and x displacement of point P over time for TT (right)*

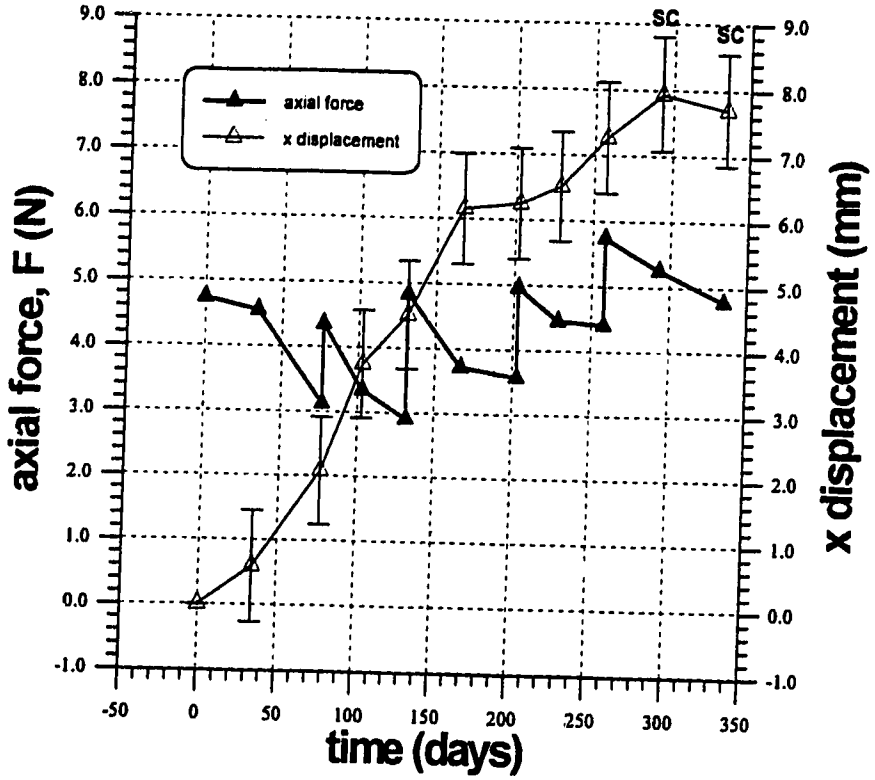

Figure 3.21: *Axial force and x displacement of point P over time for RZ (left)*

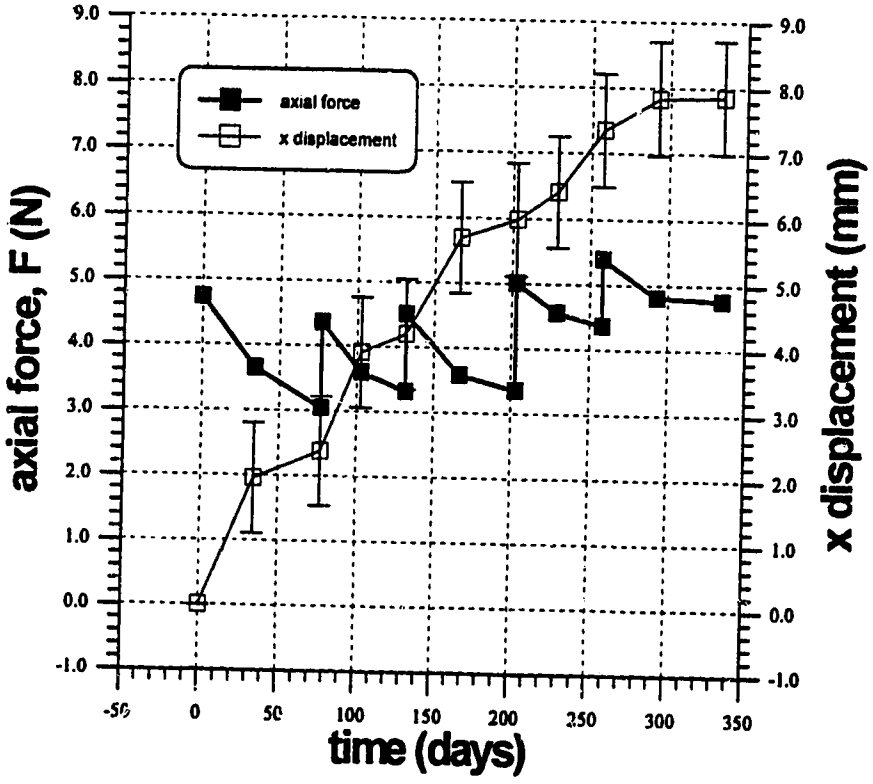

Figure 3.22: *Axial force and x displacement of point P over time for RZ (right)*

produce optimal tooth movement and what is the rate of tooth movement in such a case. The preactivated T-loop spring decreases the axial force it produces as the two tooth segments come closer together, thus requiring the spring to be reactivated in order for the axial forces to be increased to previous levels. This results in an oscillation in the axial force with a period of approximately two months, so a range of axial force levels must be considered instead of a single force level. Table 3.1 shows the total range of axial force applied, the average axial force applied and the average rate of space closure (or distal movement of the anterior segment) for both sides of all five patients. The number of days after the start of treatment at which full space closure was complete on each side of each patient is also listed in this table. For example, Figure 3.14 shows that for the right side of patient RD, an axial force range of 3.1 to 5.2 N was applied to the anterior segment, resulting in an average rate of distal movement of 0.76 mm/30 days up until day 199 when space closure was complete.

From the evidence in Table 3.1, it may be noted that for patients with whom full space closure was achieved early on one side of the dental arch, the average rate of distal movement was higher on the side with the early space closure than on the opposite side. However for the right side of patient RD, space closure was complete on day 199, 102 days earlier than for the left side, and assuming the space to be closed was approximately the same on both sides of the patient, the rate of space closure or x displacement should have been considerably greater on the right than on the left. Yet the difference in rate between both sides was less than 0.10 mm/30 days. The right side of RD also appeared to continue moving distally from days 233 to 262 despite the observation that space

closure was complete during this interval. Conversely, the space on the right side of patient TT closed only about 30 days before the left side, but the difference in the average rate of space closure was more than 0.40 mm/30 days. These cases imply that for some patients, full space closure may not have actually occurred when it was observed during the clinical visit.

Table 3.1: *Averages of axial force and rate of space closure*

patient	days to space closure	axial force range (N)	average axial force (N)	average rate of closure (mm/30 days)
RD (left)	301	2.6 - 3.9	3.2	0.68
RD (right)	199	3.1 - 5.2	4.1	0.76
DK (left)	274	2.7 - 4.6	3.7	0.63
DK (right)	274	2.6 - 4.6	3.7	0.44
NM (left)	172	3.1 - 5.0	4.0	1.00
NM (right)	204	3.5 - 5.4	4.4	0.90
TT (left)	182	3.1 - 4.5	3.9	0.52
TT (right)	151	2.7 - 4.2	3.6	0.95
RZ (left)	293	2.9 - 5.7	4.3	0.89
RZ (right)	335	3.0 - 5.4	4.2	0.83
total avg.	-	2.9 - 4.9	3.9	0.76

It is important to know when space closure is complete. Once full space closure has been achieved, it is futile to attempt to correlate the force systems applied to the

anterior segment with the segment's movement because the orthodontic spring has become statically indeterminate. Under these circumstances, the canine and the 2nd premolar (hence, the anterior and posterior segments, respectively) are in contact at some point, exerting an unknown contact force on each other. This contact force makes it impossible to determine the force systems produced at the ends of the spring using free body diagrams and corresponding equations of static equilibrium, which is essentially how SEGTEC performs this task. Therefore, the force systems imparted to the anterior segment are no longer predictable after space closure is complete.

3.2.3 Shear Force and Y Displacement

A relationship that has not been commonly considered in past studies is one between the vertical or extrusive/intrusive force and displacements in that direction. The investigation by Cohen [16] was the only study referred to in the literature review in Chapter 1, which considered vertical forces and movements. With the application of intrusive (gingival) forces ranging from about 0 to 1.0 N, Cohen observed the range of total movement was from 0.33 mm intrusively to 0.22 mm extrusively over a period of 6 to 8 weeks, with fluctuations in vertical position of the cuspid from 0.64 mm intrusive to 0.67 mm extrusive. As mentioned in the literature review, these fluctuations were attributed to tipping and uprighting of the tooth throughout treatment. Cohen believed that the natural occlusal forces affected the vertical tooth positions sufficiently so that no substantial net intrusive or extrusive movement occurred.

In this study, the extrusive/intrusive force is referred to as the shear force, V, and

the corresponding tooth displacement is called y displacement, Δy. Figures 3.23 to 3.32 and Table 3.2 show the shear force applied to point ℙ of the anterior segment was typically between 0 and 2.0 N upward on both sides of all the patients. As with the axial forces in the previous sub-section, the error bars for the shear force are not displayed to prevent clutter with the error bars for the y displacements. The uncertainty in the shear force at any given time was estimated to be ±0.4 N by the sensitivity analysis in Chapter 2 and Appendix B. Times of reactivation are again indicated where abrupt changes in the shear force take place on the same day, though in some instances the change is not significant and therefore more difficult to notice.

With the exception of the right side of patient RD (Figure 3.24), the y displacement of the anterior segment for both sides of all of the patients was generally intrusive, ie. upward into the gingiva. Though the y displacement is rather unpredictable on a month-to-month basis, there are some specific examples in which there appears to be a correlation between the shear force and the y displacement. For instance, on the left side of RZ in Figure 3.31, the shear force switched from +1.0 N (upward) on day 0 to -0.9 N (downward) on day 34. For the first 34 days, the anterior segment moved upward 4 mm, then moved downward 2 mm from day 34 to day 77. This upward/downward displacement is consistent with the change in sign of the shear force.

In the contradictory case of patient RD's right side, Figure 3.24 depicts extrusive or negative displacement of the anterior segment at point ℙ in the first 38 days, despite the application of a high positive shear force. With the right side of patient RZ in Figure 3.32, an initially extrusive or negative shear force at the beginning of treatment produced

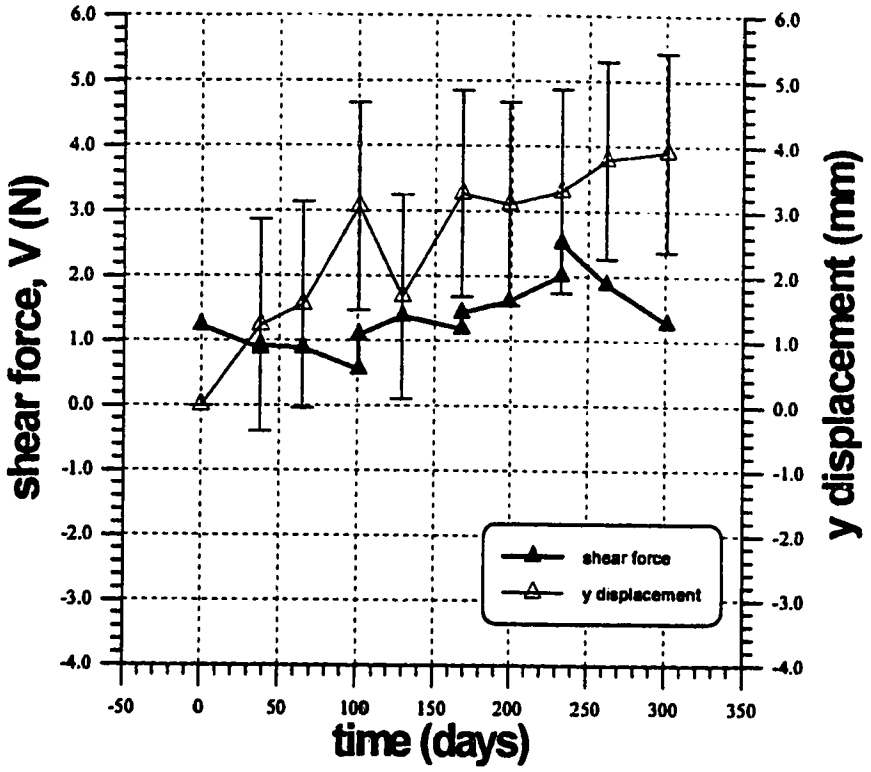

Figure 3.23: *Shear force and y displacement of point P over time for RD (left)*

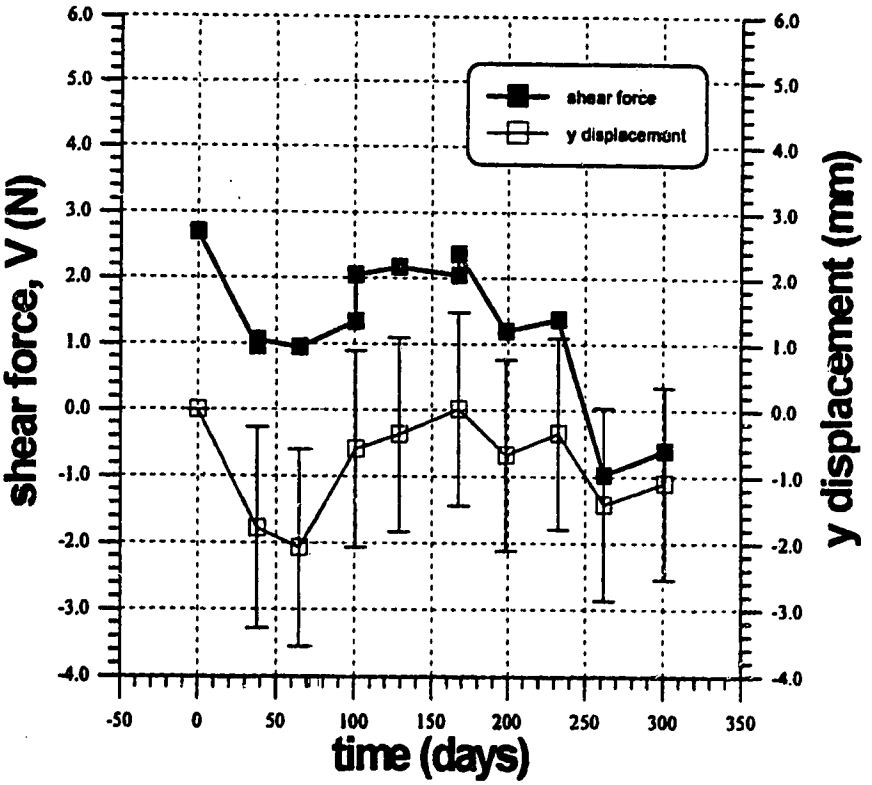

Figure 3.24: *Shear force and y displacement of point P over time for RD (right)*

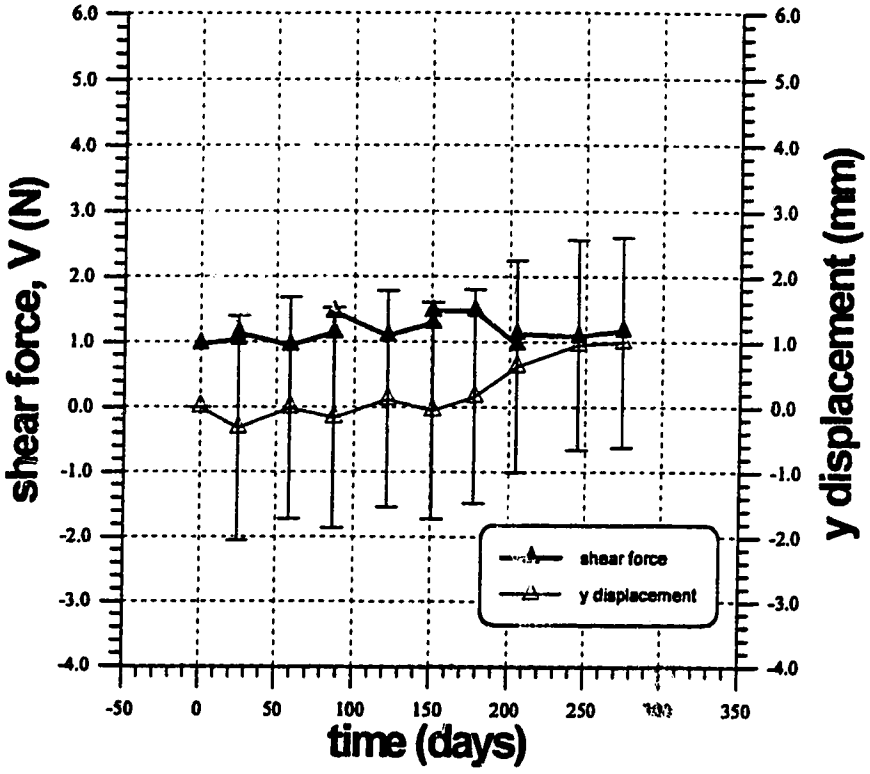

Figure 3.25: *Shear force and y displacement of point P over time for DK (left)*

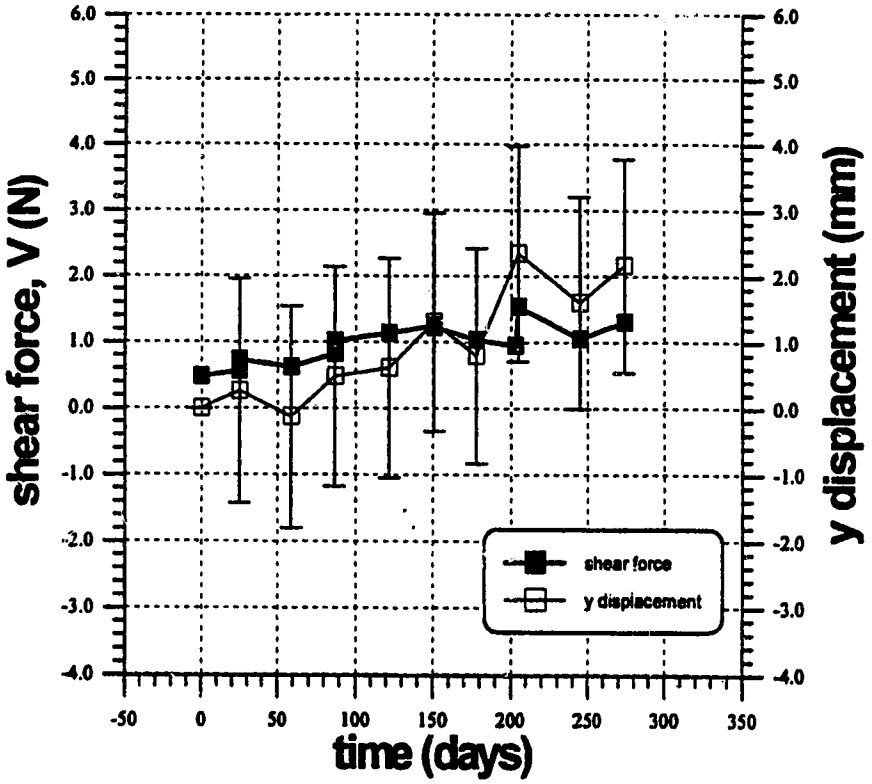

Figure 3.26: *Shear force and y displacement of point P over time for DK (right)*

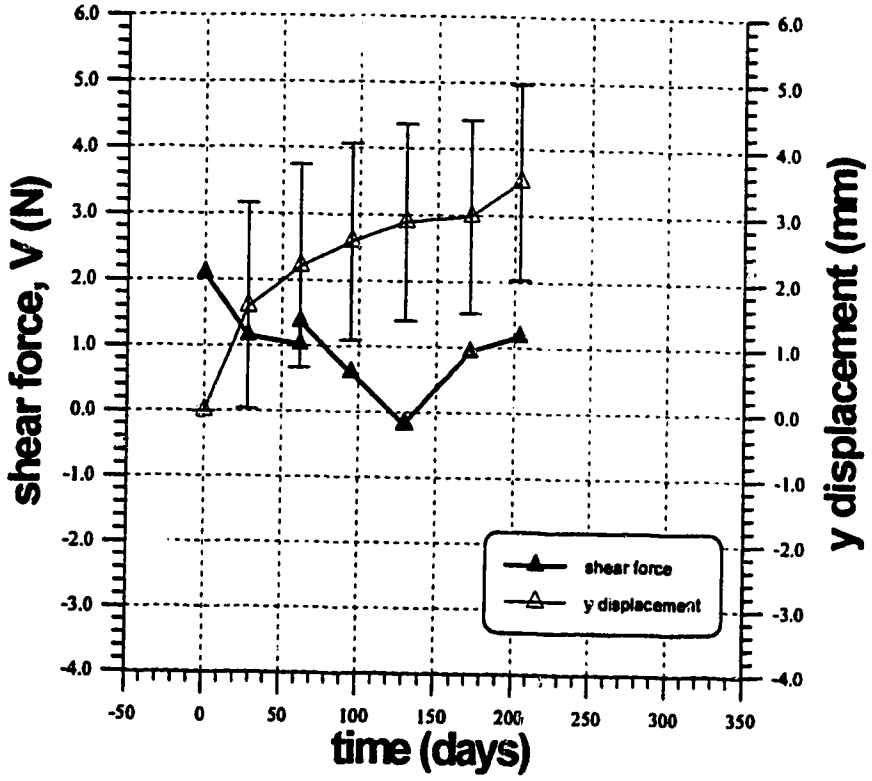

Figure 3.27: *Shear force and y displacement of point P over time for NM (left)*

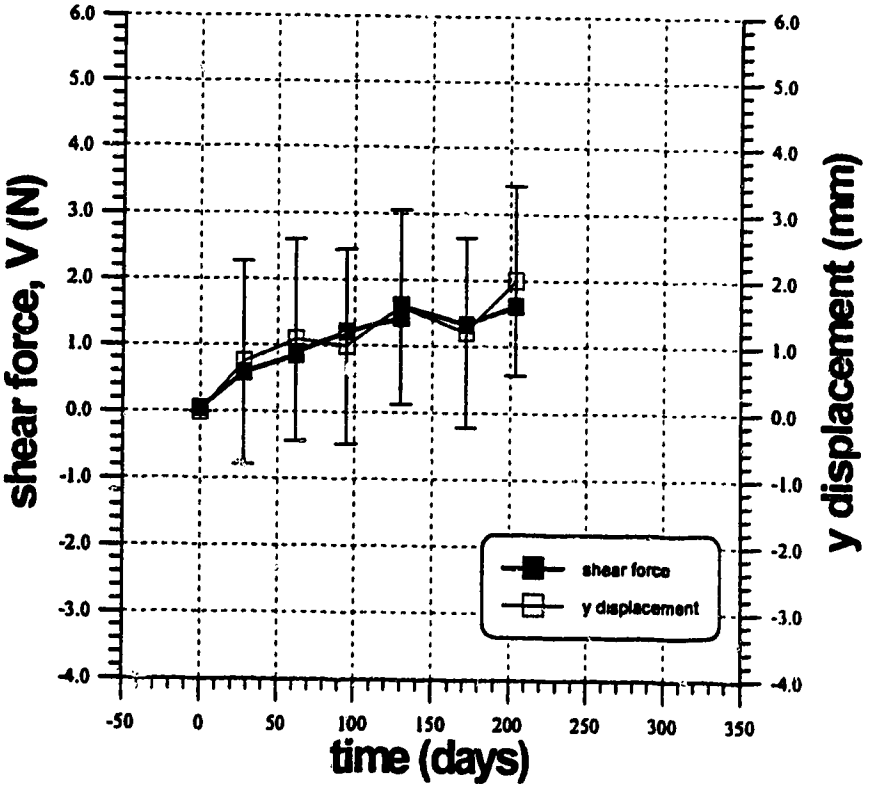

Figure 3.28: *Shear force and y displacement of point P over time for NM (right)*

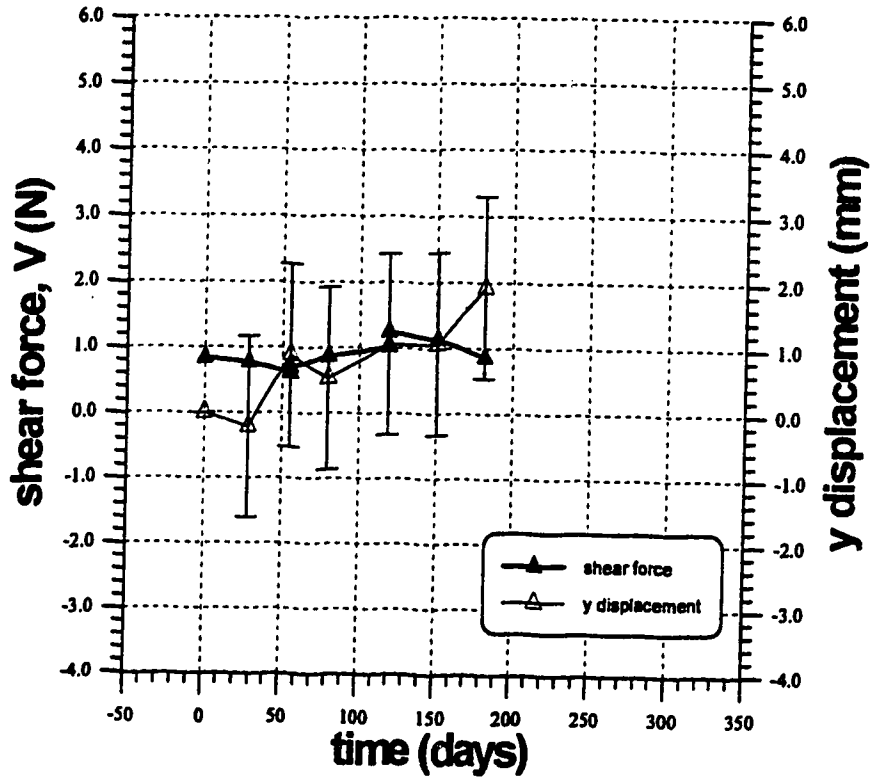

Figure 3.29: *Shear force and y displacement of point P over time for TT (left)*

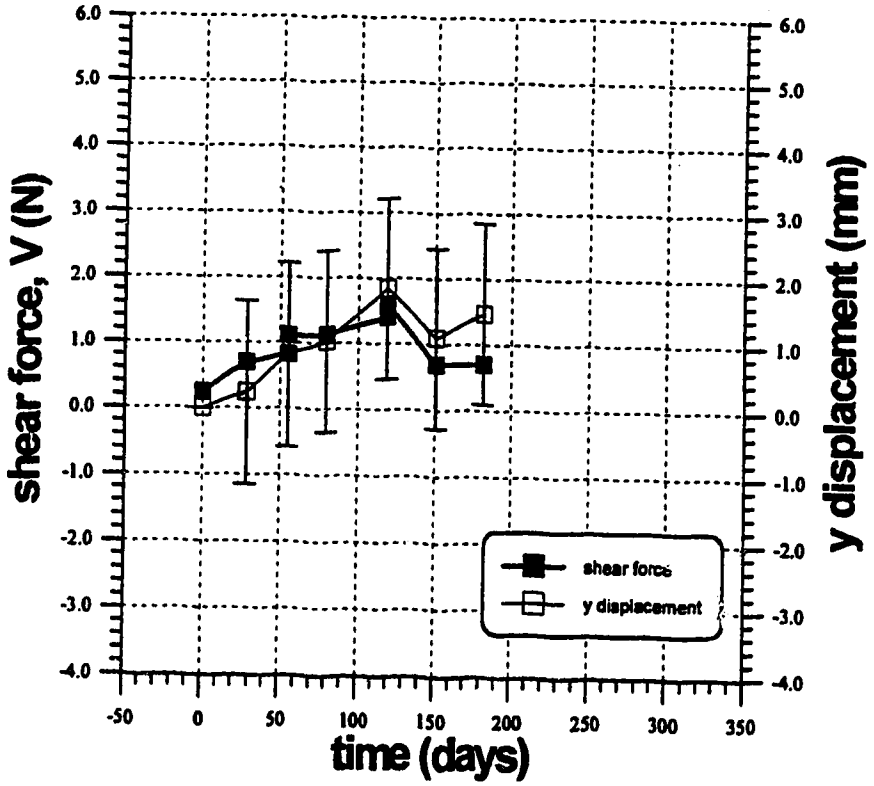

Figure 3.30: *Shear force and y displacement of point P over time for TT (right)*

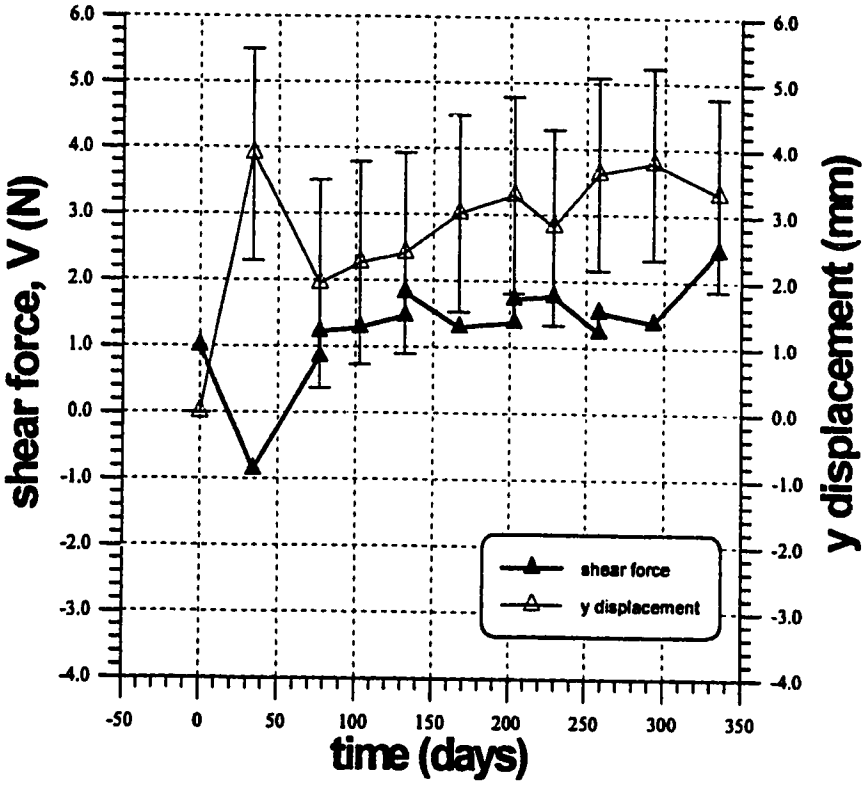

Figure 3.31: *Shear force and y displacement of point Ṗ over time for RZ (left)*

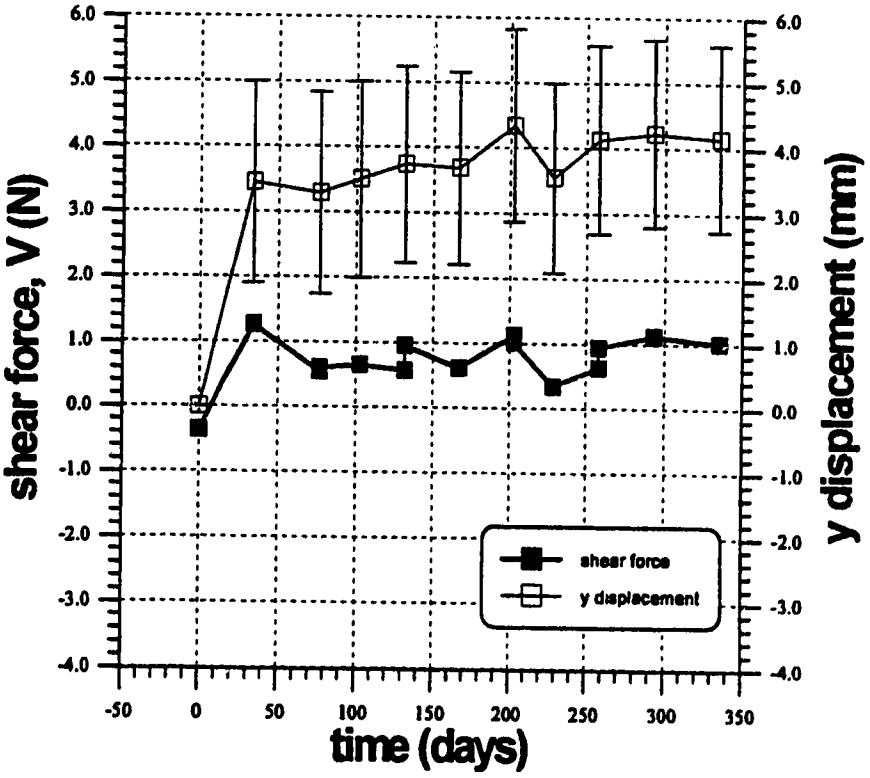

Figure 3.32: *Shear force and y displacement of point P over time for RZ (right)*

an exceptional intrusive movement of the anterior segment. Other such contradictions can be attributed to the high uncertainty in the y displacement, which was typically the same magnitude as the total y displacement in the patient. This created the difficulty in determining if the anterior segment was moving intrusively or extrusively between clinical visits.

Table 3.2: *Averages of shear force and rate of intrusion*

patient	shear force range (N)	average shear force (N)	average rate of intrusion (mm/30 days)
RD (left)	0.6 - 2.5	1.4	0.46
RD (right)	-1.0 - 2.7	1.3	-0.12
DK (left)	0.9 - 1.5	1.2	0.07
DK (right)	0.5 - 1.6	1.0	0.22
NM (left)	-0.2 - 2.1	0.9	0.60
NM (right)	0.1 - 1.6	1.1	0.30
TT (left)	0.6 - 1.2	0.9	0.27
TT (right)	0.7 - 1.6	0.9	0.29
RZ (left)	0.9 - 2.5	1.3	0.41
RZ (right)	-0.4 - 1.3	0.7	0.52
total avg.	0.3 - 1.9	1.1	0.30

3.2.4 M/F Ratio and Rotational Displacement

Last of all, there is the relationship between the moment-to-axial force ratio, M/F, and the rotational displacement of the anterior segment of teeth. Unlike the axial force, shear force, and moment, the M/F ratio typically decreases whenever the spring is reactivated. Even though both the moment and the axial force increase in magnitude with each reactivation, the increase in the axial force is often greater than that of the moment on a percentage basis, thus causing the ratio to decrease. The uncertainty in the M/F ratio at any given time was estimated to be ±0.8 mm, based on the sensitivity analysis in Chapter 2 and Appendix B.

Figures 3.33 to 3.42 present the changes in the M/F ratio and in the angle of the anterior segment with respect to the posterior segment on each side of the five patients in this study. Table 3.3 provides a synopsis of the data in these figures, showing the range of M/F ratio, the average M/F ratio, and average rate of positive rotation or root movement. All of the patients generally experienced root movement to some extent, though tipping and translation of the segment were occasionally observed.

It is expected that if both sides of the dental arch in a patient moved in the same general manner and the same rate, the M/F ratio should have been similar on both sides as well. For all five patients, the average M/F ratios of left and right sides were within 1 mm of each other, which is accommodated by the estimated error in the M/F ratio. Despite this, only three patients (DK, NM, and RZ) also had average rates of rotation that were similar on both sides. The average values of the M/F ratio on both sides of patient RD were close to each other, but the average rate of rotation on the right side was

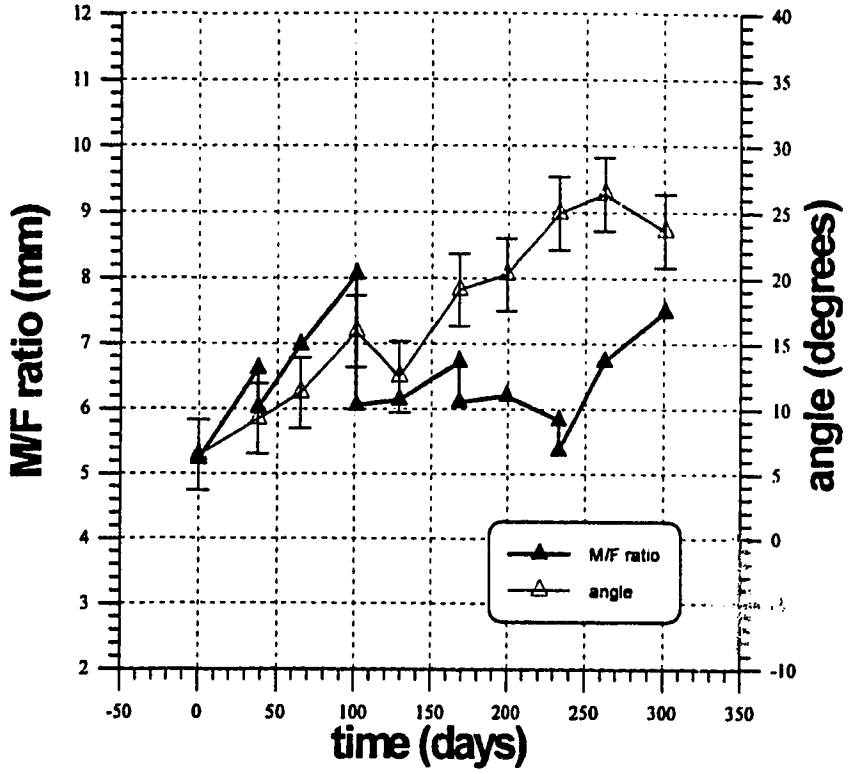

Figure 3.33: *M/F ratio and angle of anterior segment over time for RD (left)*

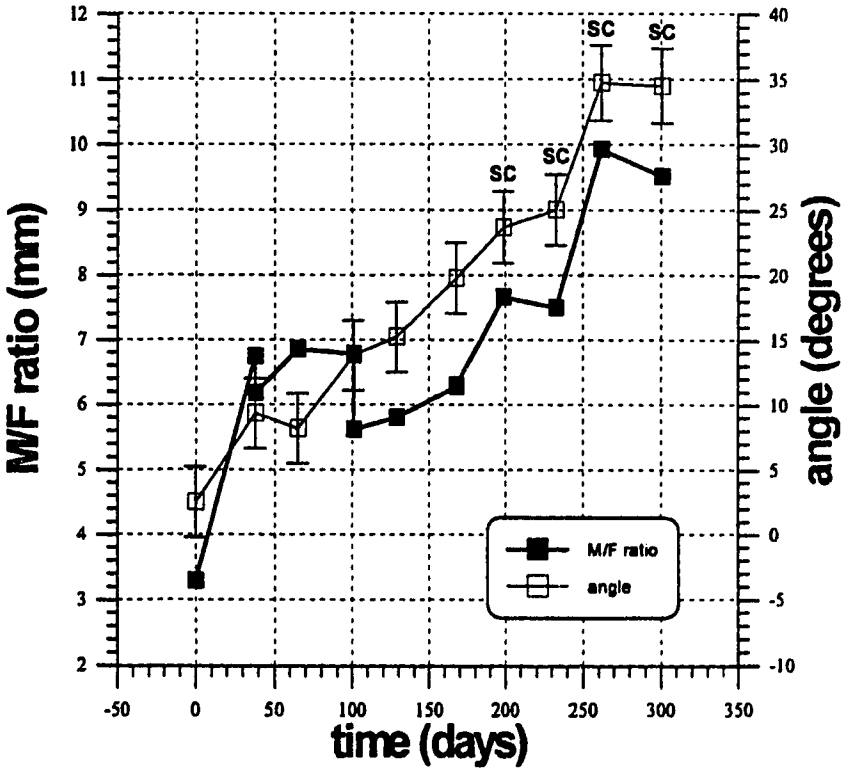

Figure 3.34: *M/F ratio and angle of anterior segment over time for RD (right)*

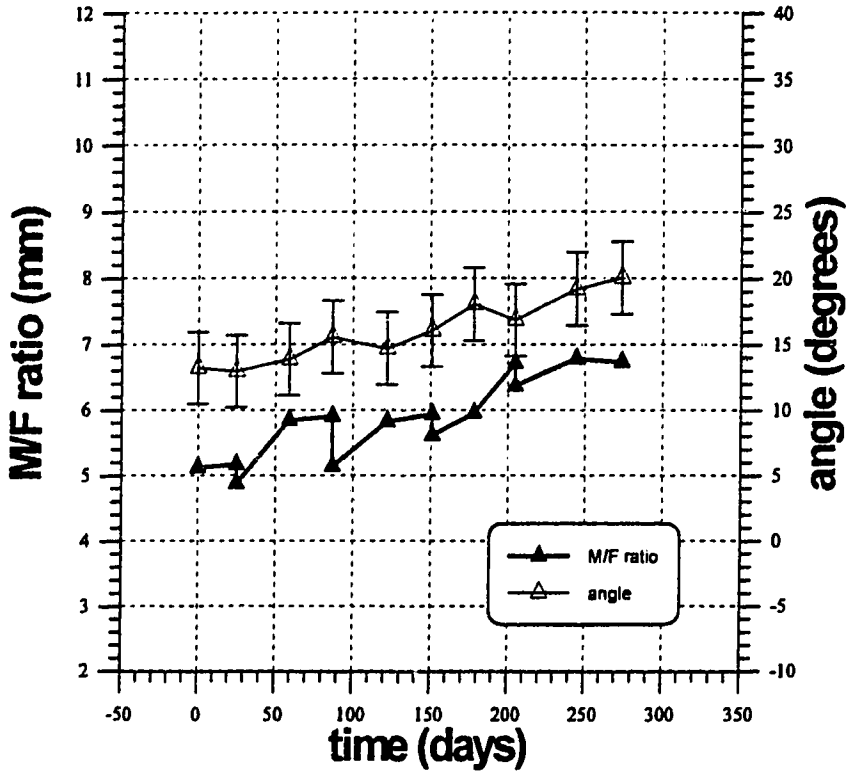

Figure 3.35: *M/F ratio and angle of anterior segment over time for DK (left)*

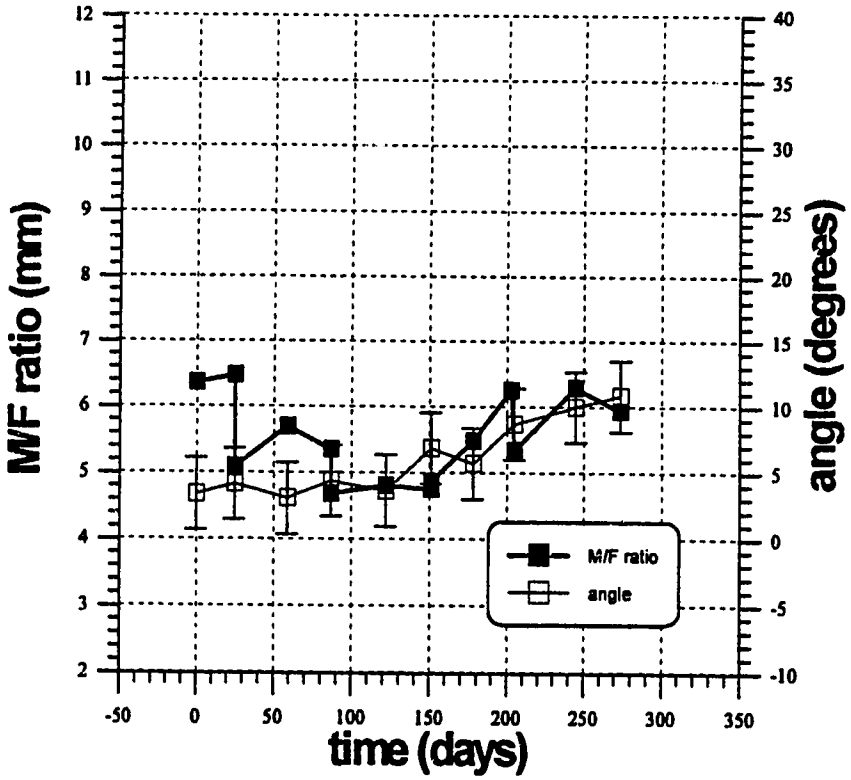

Figure 3.36: *M/F ratio and angle of anterior segment over time for DK (right)*

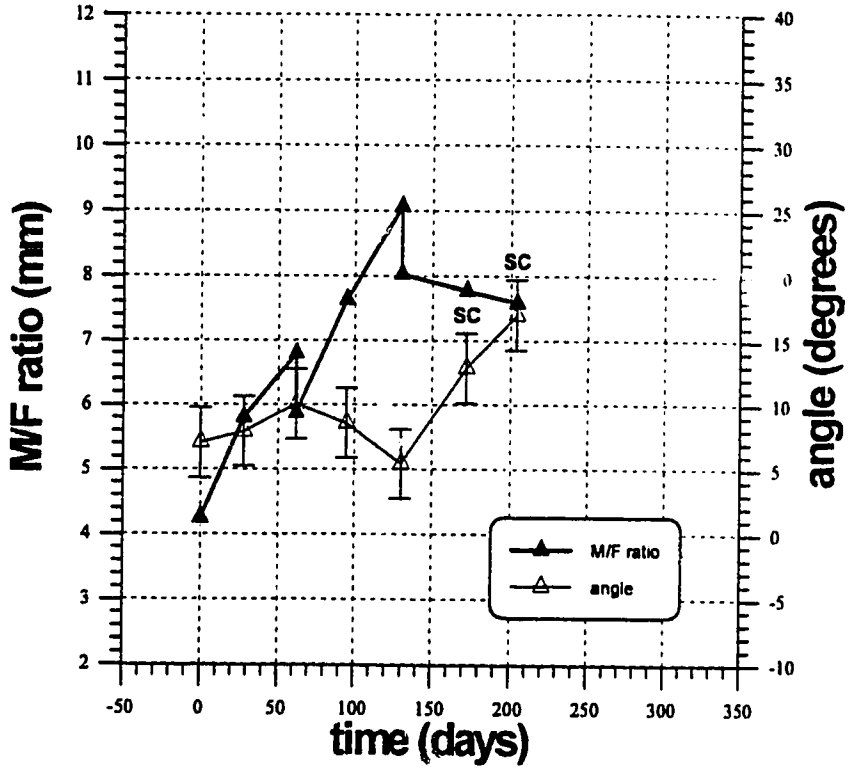

Figure 3.37: *M/F ratio and angle of anterior segment over time for NM (left)*

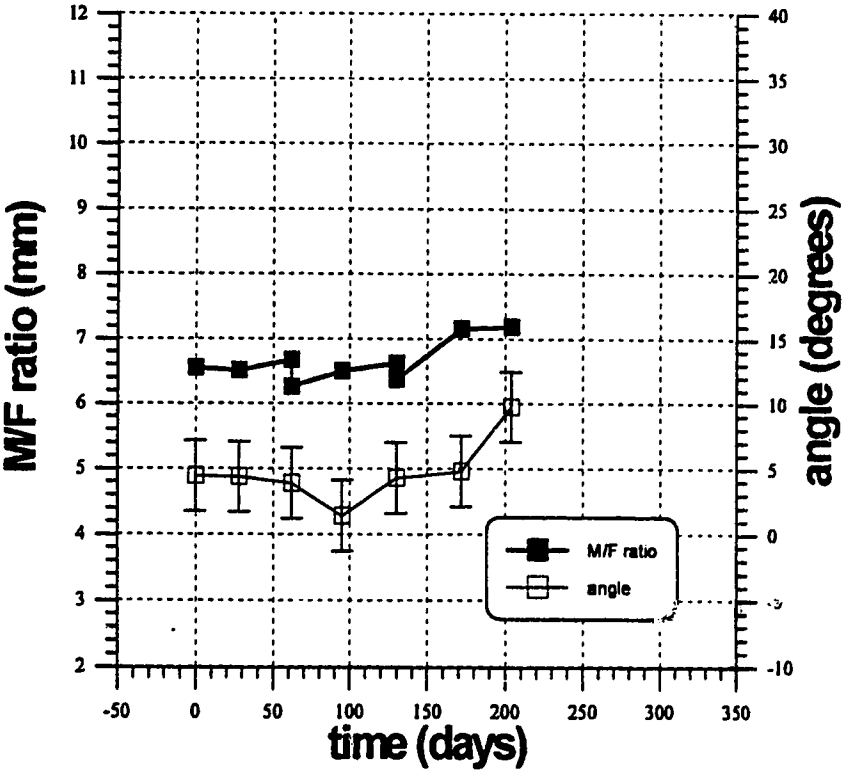

Figure 3.38: *M/F ratio and angle of anterior segment over time for NM (right)*

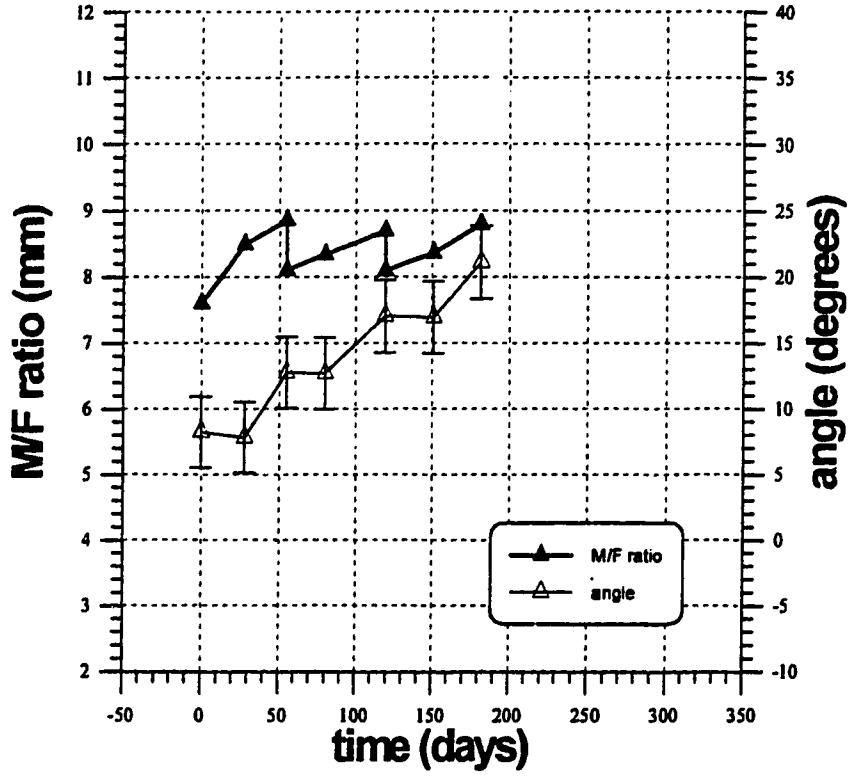

Figure 3.39: *M/F ratio and angle of anterior segment over time for TT (left)*

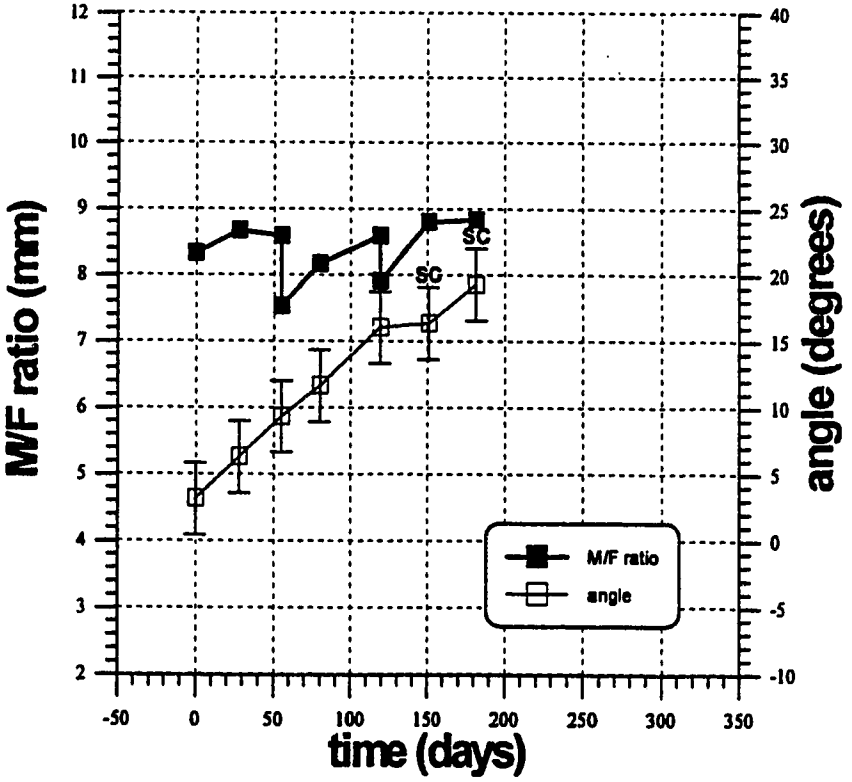

Figure 3.40: *M/F ratio and angle of anterior segment over time for TT (right)*

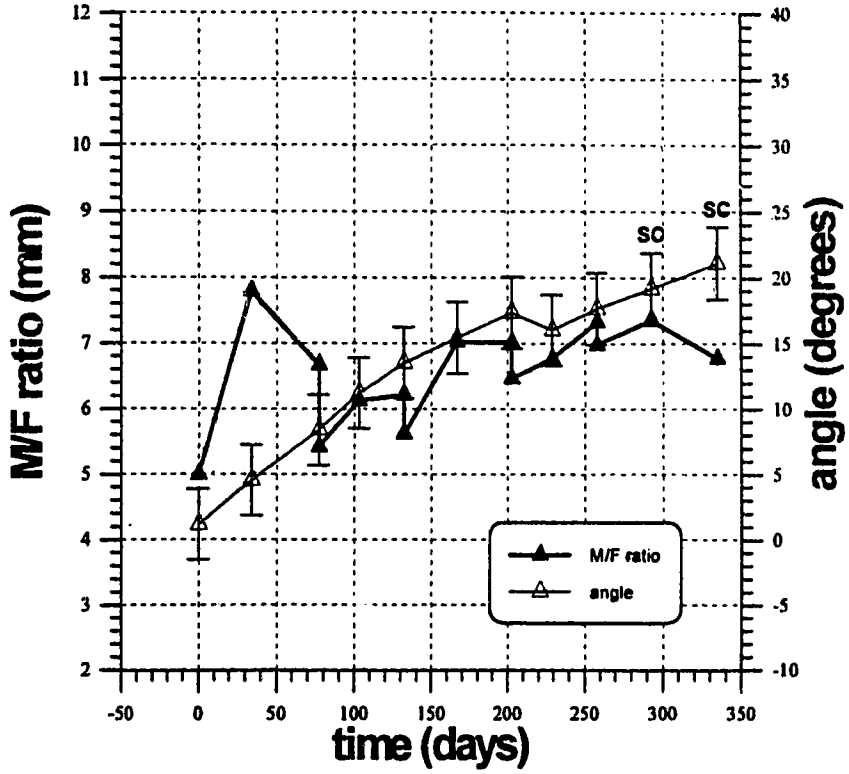

Figure 3.41: *M/F ratio and angle of anterior segment over time for RZ (left)*

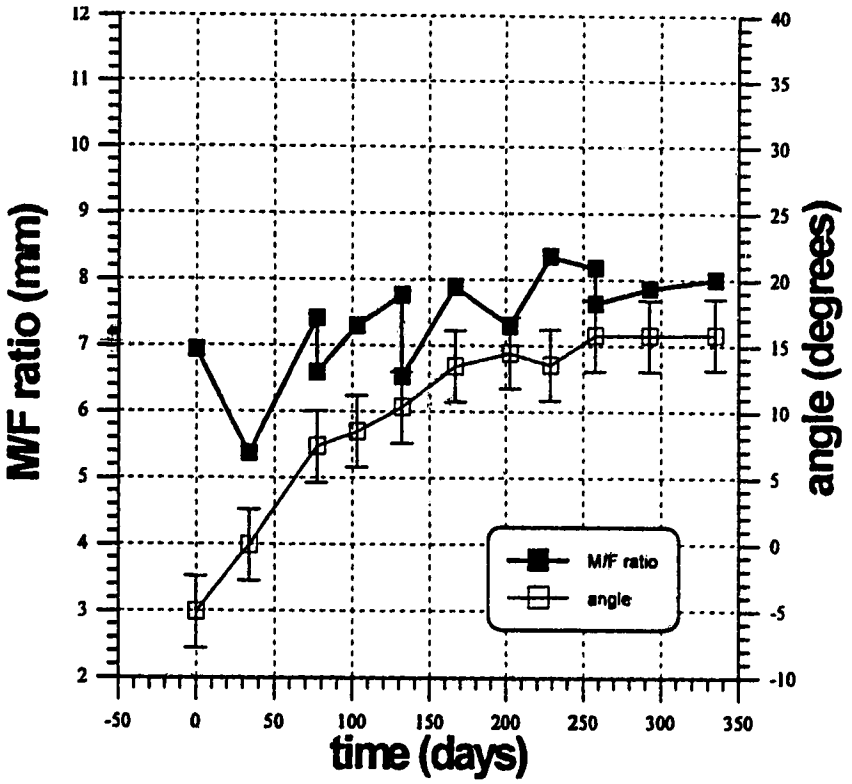

Figure 3.42: *M/F ratio and angle of anterior segment over time for RZ (right)*

1.0°/30 days more than on the left, and this is a significant difference when compared to the other patients. Though the average M/F ratio was virtually the same on both sides of patient TT, there was a difference of about 0.6°/30 days in average rate of rotation.

Table 3.3: *Averages of M/F ratio and rate of rotation*

patient	M/F ratio range (mm)	average M/F ratio (mm)	total rotation (°)	average rate of rotation (°/30 days)
RD (left)	5.2 - 8.1	6.4	17.2	2.00
RD (right)	3.3 - 9.9	6.2	32.0	3.00
DK (left)	4.9 - 6.8	5.9	6.8	0.77
DK (right)	4.7 - 6.5	5.5	7.4	0.85
NM (left)	4.3 - 9.1	6.9	10.0	0.53
NM (right)	6.3 - 7.2	6.7	5.3	0.55
TT (left)	7.8 - 8.9	8.4	12.9	2.14
TT (right)	7.5 - 8.8	8.3	16.1	2.76
RZ (left)	5.0 - 7.8	6.6	20.0	1.78
RZ (right)	5.4 - 8.4	7.4	20.9	1.75
total avg.	5.4 - 8.2	6.8	-	1.61

The total rotation experienced by the anterior segment as observed from the left and right sides of each patient is also provided in Table 3.3. Aside from patient RD, the anterior segment was seen from both sides to rotate about the same amount. Somehow the anterior segment of patient RD was observed to rotate nearly twice as much from the

right side than from the left side. This could be attributed to an eccentric application of moments to the segment, in which the higher magnitudes of moment were applied to the right side than the left. The fact that space closure was accomplished on the right side rather early in patient RD's treatment may also have been a factor, as well as unanticipated occlusal/gingival movement of the posterior segment.

3.3 DISCUSSION OF RESULTS

The general objective of this study has been to relate the forces applied to the tooth movement which occurred. The axial and shear force components of the force systems applied were compared individually with their corresponding displacements, then the combined effects of the axial force and the moment acting together were studied in the form of the M/F ratio, elucidating the quantitative relationship between the force system applied and the resulting movement of the anterior segment. Displacement of the anterior segment in the x and y directions was measured from point $\mathbb{P}$, the point at which the force systems were applied to the segment. Rotation of the anterior segment was measured by the change in angle of the canine tooth axis (represented by points $\mathbb{LA}$, $\mathbb{UA}$, and $\mathbb{P}$ in Figure 2.13) with respect to the 1st molar axis (represented by points $\mathbb{LP}$, $\mathbb{UP}$, and $\mathbb{S}$ also shown in Figure 2.13).

3.3.1 Axial Force and Rate of Space Closure

The axial or mesial/distal force has often been the main subject of analysis in studies of tooth movement, which is evident from the literature review in Chapter 1. It is commonly believed in orthodontics that an increase in axial force results in an increase in the rate of distal movement up to some force value, at which the rate of movement reaches a maximum and perhaps decreases with any further increases in force. In this study, axial forces ranging from approximately 2.5 to 6.0 N were tested, as seen in Figure 3.43, and resulted in average rates of space closure from 0.44 to 1.00 mm/30 days.

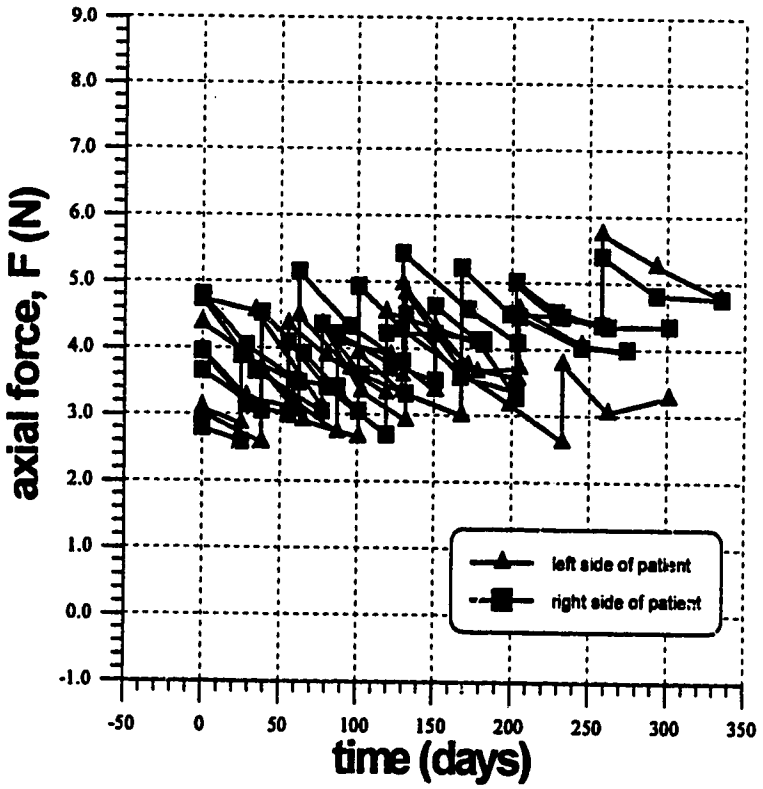

Figure 3.43: *Axial force over time for both sides of all patients*

Using the values from Table 3.1, Figure 3.44 shows the average axial force against the average rate of space closure for both sides of the five patients. The side of the patient to which the data point refers is indicated in the figure. An attempt to fit a linear relationship to the data yielded a best-fit line with a correlation coefficient of only 0.165. This low coefficient signifies that, according to the data collected in this study, there is a very weak linear relationship between the average axial force applied to the anterior segment and the average rate of space closure. From this statistical indicator, it may be concluded that the segment's distal movement is insensitive to changes in the magnitude of the axial force in this range.

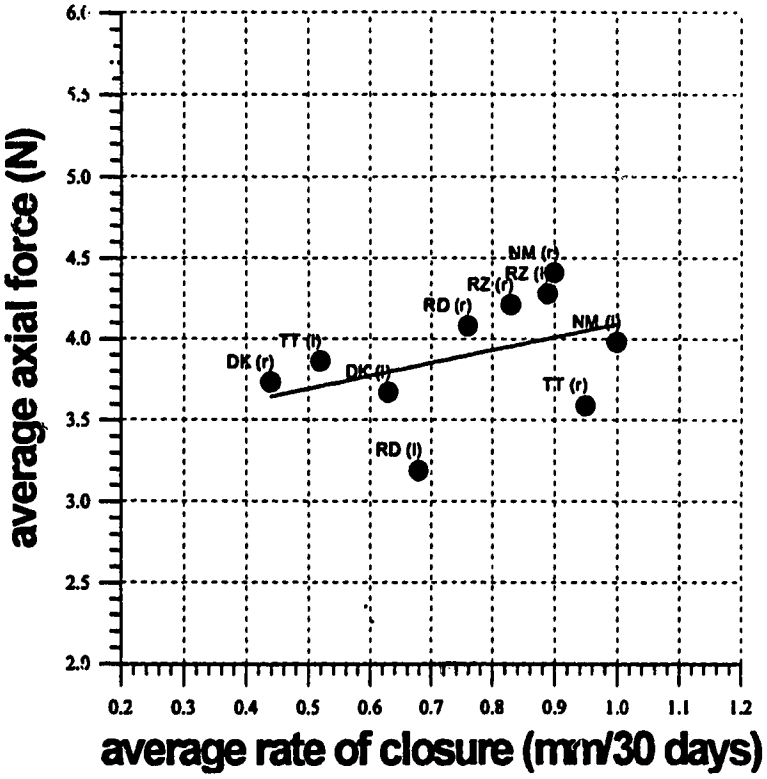

Figure 3.44: *Average axial force versus average rate of space closure*

Based on the distribution of data points in Figure 3.44, the lack of correlation was not only due to the great variation in the rate of response to axial force between patients, but also between sides of the same patient. However, for the majority of the sides of the patients with force levels closer to the low end of the average range throughout treatment (3.0 to 4.0 N), the rates of tooth movement were relatively low as well, lying between 0.44 and 0.70 mm/30 days. At the higher end of the average range (4.0 to 4.5 N), the rates of tooth movement were higher, ranging from about 0.70 to 1.00 mm/30 days. Therefore with most of the patients, an average axial force of 4.0 to 4.5 N closed the space as much as 0.5 mm/30 days faster than average forces below 4.0 N. The error in the axial force and the narrow range of average axial forces applied in this study make it impossible to suggest a universally applicable axial force level for optimal orthodontic treatment using the anterior retraction technique.

There were many factors, both biological and measuremental, that could have significantly biased the data from the patients in this study. An important consideration for the analysis of the results is knowing when space closure was truly first achieved. One case in point is patient RD. On the left side, space closure appears to have actually occurred at day 262. Figures 3.13 and 3.33 respectively provide evidence that negative x displacement (mesial movement) and rotation (tipping) took place between days 262 and 301. One can infer from this evidence that perhaps the 2nd premolar and the canine made contact with each other around day 262 at a point above the alveolar crest near the roots of the teeth where the orthodontist could not observe the contact. But if full space closure was achieved and the two teeth made contact, a tipping rotation of the anterior

segment should have caused a slight distal movement of point $\mathbb{P}$ instead. The anterior segment falsely appears to move mesially or in the negative direction. On the right side of the same patient, Figure 3.14 shows that there was substantial distal movement of point $\mathbb{P}$ in the anterior segment between days 233 and 262 even though it was noted that space closure was complete by day 199. This movement could be accounted for by the uncertainty in x displacement, yet the high amount of root movement that occurred during the interval, as shown in Figure 3.34, should have produced mesial, not distal, movement at point $\mathbb{P}$. Such cases emphasize the need to monitor the x and y displacement of the anterior segment from some point other than the point of force system application. The center of resistance would be more appropriate since its movement is representative of the movement of all the teeth in the anterior segment, and the type of movement experienced by the segment is identified by the location of the center of rotation with respect to the center of resistance, as described in Figure 1.3 in Section 1.1. Unfortunately, the location of the center of resistance is unknown, and its position may be subject to significant change while the anterior segment moves.

3.3.2 Shear Force and Rate of Intrusion

The shear or intrusive/extrusive force in orthodontic treatment has not undergone nearly as much analysis as its axial counterpart. Nonetheless, vertical movement of the anterior segment is also important, since its vertical position relative to the posterior segment affects the occlusal plane, or biting surface, and the relation between the maxillary and mandibular dental arches when in contact with each other. Therefore, the

orthodontist may also need to intrusively or extrusively move the anterior segment as well to improve occlusion.

Reitan [23] discovered that a downward force of about 0.25 N was sufficient for the extrusion of an individual tooth, and a similar upward force was found to be enough for intrusive movement of an incisor by Burstone [24]. Unfortunately, according to Figures 3.23 to 3.32, uncertainty in the y displacement of the anterior segment was often of the same magnitude as the displacement itself. The effect of this high uncertainty in the y displacement is obvious in Figure 3.45, in which an attempt to correlate the average shear force applied and the rate of intrusion was made. The best fit line to the data has a correlation coefficient of 0.150, representing once again a very weak linear relationship. Therefore, this attempt to correlate shear force with y displacement proves to be generally inconclusive. However for the majority of the patients, an average upward shear force of about 1.0 N resulted in some intrusive displacement of the anterior segment. This statement is in agreement with the observations of Reitan and Burstone because one would expect that the total force applied to a segment of teeth would need to be greater than the force acting on an individual tooth in order to achieve the same displacement [25].

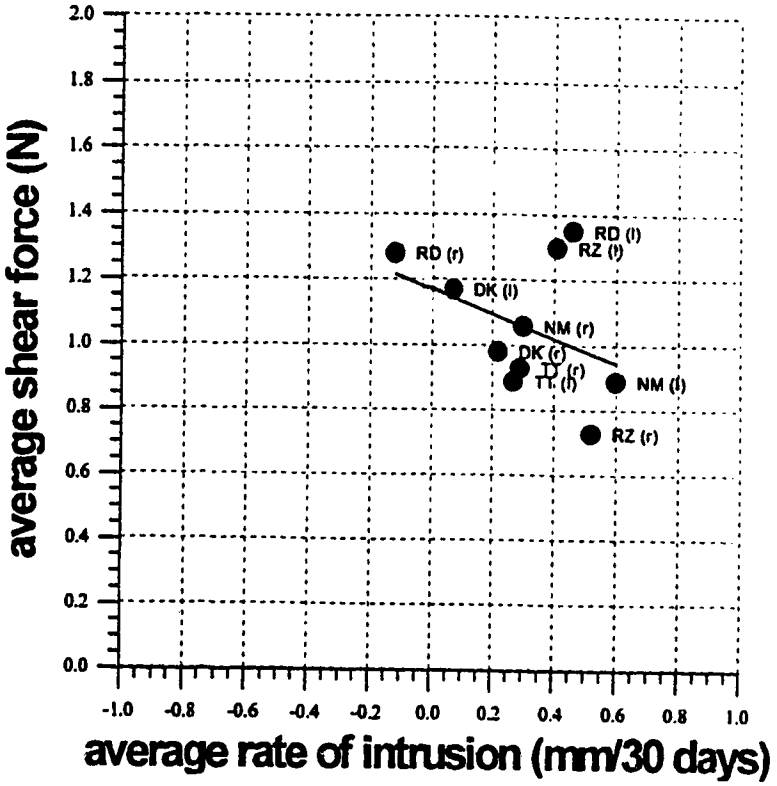

Figure 3.45: *Average shear force versus average rate of intrusion*

3.3.3 M/F Ratio and Rate of Rotation

There has been considerable research conducted on the relationship between the moment-to-axial force ratio (M/F) and the rotational displacement of teeth. The M/F ratio can potentially determine the type of movement that will be experienced by the anterior segment. From the data in Table 3.3, Figure 3.46 shows the average M/F ratio observed on each side of each patient plotted against their corresponding average rates of positive rotation (root movement). Yet again, a low correlation coefficient of 0.188 for the best fit line to the data reveals that there is only a very weak linear relationship between M/F ratio and rate of rotation. Fortunately, it can be seen in Figure 3.46 that there is some grouping of the data points on a per patient basis. For example, patients

DK, NM, and RZ exhibited average M/F ratios on each side within 1.0 mm of each other for approximately the same rate of rotation.

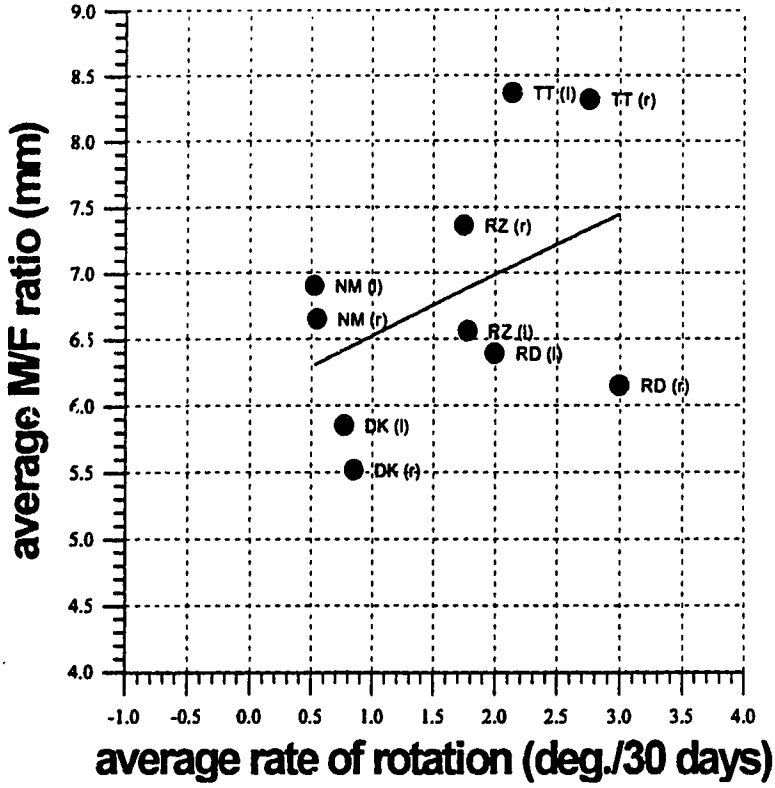

Figure 3.46: *Average M/F ratio versus average rate of rotation*

Average rates of rotation do not necessarily represent the various types of movement experienced by the anterior segment during treatment. In the case of translation, the M/F ratio signifies the length of the "moment arm", or the distance from the center of resistance of the anterior segment to the point at which the force system is applied to the segment. When the value of the M/F ratio is approximately equal to the length of the "moment arm", small changes in the M/F ratio could shift the type of movement of the segment from tipping to root movement, thereby missing the opportunity to translate the segment. Therefore, it is more appropriate to examine the

discrete intervals at which translation or near translation (a rotation of less than half the uncertainty in the angle of the anterior segment, which is about 1.5°) occurred on both sides of each patient. For example, according to Figures 3.35 and 3.36, both sides of patient DK experienced very little rotation and the M/F ratio fluctuated around 6.0 mm, so the M/F ratio required for translation by patient DK was estimated to be about 6.0 mm. Table 3.4 lists the estimated values for the M/F ratios in order to produce translation of the anterior segment, showing the left and right sides respectively.

Table 3.4: *Estimated M/F ratios required for translation (in mm)*

patient	RD	DK	NM	TT	RZ
M/F ratio	6.0/6.0	6.0/5.5	6.0/6.5	8.0/8.0	5.0/5.0

As expected, the estimates of the M/F ratio for translation were similar for both sides of the patient with all five patients. With patient RZ, the estimates were not based on any translatory movement observed. This was because the M/F ratio progressively increased throughout the first seven or eight months of treatment, and only root movement was seen during this period on both sides. From the predicted relationship between M/F ratio, the length of the "moment arm", and type of tooth movement, the M/F ratio required for translation of the anterior segment of patient RZ was assumed to be below the lowest M/F value, which was about 5.0 mm.

Both sides of patient TT had considerably higher estimates of the M/F ratio

required for translation when compared with the other patients in this study. This may be a false indication of the position of the center of resistance with respect to the point of force application for two possible reasons. First, Table 3.3 shows that despite a narrow range of M/F ratios, the anterior segment experienced as much as 16° of positive rotation (root movement) at an average rate of 2 to 3°/30 days. The "translation" that appears to have occurred on both sides of TT in Figures 3.39 and 3.40 may have been reduced root movement (between 1 and 2°/30 days) concealed by the magnitude of uncertainty in the angle, which was about ±3°. Therefore, the M/F ratio required for translation for TT might have actually been lower, such as 6 or 7 mm. Second, the placement of the bracket on the labial surface of the canine's crown may have been further away from the alveolar crest (and perhaps the center of resistance as well) in comparison with the other patients.

Unfortunately, as an estimated value often insinuates, there are some examples of unanticipated behavior to the force systems applied in this study. For the left side of patient NM, there were two intervals where the movement of the anterior segment in response to the force systems applied was contrary to expectations. From days 0 to 28, the M/F ratio changed from an extraordinarily low value of 4.3 mm to 5.8 mm, yet Figure 3.37 shows some positive rotation (root movement) took place (about 1°). Assuming that the M/F ratio for translation of the anterior segment is around 6.5 mm as estimated from the near-translatory behavior observed in Figure 3.37, the M/F ratios observed during this interval should have corresponded with tipping and not root movement. The second interval in question is between days 62 and 130, in which the

higher range of ratios (5.9 to 9.1 mm) would be expected to produce root movement instead of tipping as depicted in Figure 3.37.

Without knowledge of the anatomy of each patient and the positioning of the orthodontic appliances, combining the evidence from five different patients cannot yield conclusive results concerning M/F ratios and the type of movement of the anterior segment. The length of the "moment arm" cannot be determined if the size of the teeth in the segment and the positions at which the brackets are adhered to the labial crown of the canines are not known. In addition to this, the concept of root length loses its effectiveness in conveying the position of the center of resistance when dealing with the "multi-rooted" anterior segment. The center of resistance depends on the portion of the tooth or segment of teeth that is recessed into the periodontium, as well as the size of the tooth or teeth in the segment, and this makes the absolute location of the center of resistance in each individual highly variable.

The absolute movement of the posterior segment in all of the patients of this study was considered small when compared to the anterior segment's movement. However, evidence such as the differences in movement between sides for patient RD raises the question of whether or not this assumption is justified. In the x direction (mesial/distal), the posterior segment's translation was most likely substantially less than the translation of its anterior counterpart. Yet in the y direction (intrusive/extrusive), it is highly probable that the magnitude of displacement for the posterior segment was approximately the same as what was observed with the anterior segment in the results. Since

displacements of the anterior segment were calculated relative to the posterior segment, some of the y displacement of the anterior segment may have been partially due to absolute y displacement of the posterior segment. Similar circumstances could also apply to the rotation of the anterior segment.

This study also ignored the biological responses of the surrounding bone and tissue to the application of force systems to the teeth. As noted by Burstone [9], "force systems operate by producing stress and strain patterns in the periodontium and bone, which in turn produce tooth and bone displacements concomitant with a biological bone response. Thus, an optimal force system requires a consideration not only of what can be produced by an appliance but also the variation in the bony support, root length, and the biological response."

Chapter 4

CONCLUSIONS

4.1 SUMMARY

The main objective of this research was to study the relationship between force systems applied to teeth and subsequent movement of those teeth during orthodontic treatment. To investigate this, the maxillary dental arches of five patients undergoing orthodontic therapy by anterior segment retraction were studied during treatment. The force systems applied to the anterior segment of teeth and the resulting displacements of the segment were determined entirely from geometric relationships. Measurements of inter-tooth distances between the anterior and posterior segments and impressions of the geometries of the orthodontic springs with the brackets they were connected to were made *in vivo* at approximately monthly intervals. Impressions of the spring/brackets geometries, along with the spring's initial geometry, were employed to determine the force systems through the use of the computer program SEGTEC. With the initial geometry and various boundary conditions of the spring for a given time, SEGTEC calculated the force systems produced at both ends of the spring. Together with some known static dimensions in the measurement apparatus, the inter-tooth distances were used to determine the position and orientation of the anterior segment with respect to the posterior segment. The posterior segment was assumed to be sufficiently anchored so that it moved considerably less than the anterior segment had throughout treatment. By

this assumption, the anterior segment was expected to have experienced the most of the movement indicated by changes in its position and orientation. After compiling all of the results from both sides of the five patients, attempts were made to discern any relationships between the known forces (ie. F and V) or characteristics (ie. M/F) and the movements of the anterior segment they caused.

From the results of this study, there was no strong linear relationship between the axial force applied to the anterior segment and the rate of space closure. The difficulty in establishing a correlation might be attributed to the fact that displacement of the segment should be measured at its center of resistance and not the point of force application. However, the rate of space closure seemed generally faster (from 0.1 to 0.5 mm/30 days difference) at axial force levels averaging between 4.0 to 4.5 N than with average force levels below 4.0 N. Due to excessive uncertainty in the y position of the anterior segment, the only statement that could be made about the results concerning shear force and y displacement was that an average intrusive (upward) shear force of 1.0 N caused intrusive movement of the segment. Analysis of the relationship between the M/F ratio and rotational displacement of the segment showed significantly different magnitudes of M/F ratio associated with translation between five patients, ranging from 5 to 8 mm. But before using these values to determine the distance from the point of force application to the segment's center of resistance, it is necessary to know the sizes and lengths of the roots of the teeth in the anterior segment in order to compare the M/F ratios for translation amongst the patients. There is also the question of where on the labial surface of the canine tooth's crown that the bracket is placed, so the point at which

the force system is applied to the anterior segment may vary substantially between patients.

There were numerous limitations to this study, not the least of which was the small sample population. With both sides of five patients under observation, the integrity of the results of this study was highly vulnerable to biological variability between patients and between sides of the same patient. The range of average axial forces applied to the anterior segment was also small, about 3.0 to 4.5 N, so with an estimated error of ±0.5 N, it was hard to distinguish the force values between patients and sides of patients to uncover relationships. The actual amount of absolute movement of the posterior segment in each patient was not explicitly determined as well. This could have introduced significant errors to the calculated displacements of the anterior segment, especially with intrusive/extrusive translations and rotations. As are most investigations of tooth movement phenomena, this study was also ignorant of histological responses of the bone and tissue surrounding the teeth. Knowledge of how the known forces applied to teeth affect bone resorption and deposition could help reduce discomfort and shorten treatment.

4.2 RECOMMENDATIONS FOR FURTHER STUDY

The primary assumption in this study was that the posterior segment of teeth moved very little as compared to the anterior segment's movement. In truth, there must have been some movement in the posterior segment, even if it was only a fraction of the anterior segment's displacement. For greater confidence in the tooth movements measured, future studies should determine how much the posterior segment moves during

treatment. This can be determined using moulds of the dental arch and/or cephalometric radiographs (profile X-rays of the head around the mouth). The discouraging factors to these approaches are the expenses and the discomfort that the patients would confront. However, the radiographs also provide information about the teeth that cannot be found by any other conventional means, such as the root sizes of the teeth in the patients. This would prove to be valuable for analyzing the relationship between the M/F ratio and the type of tooth movement. This relationship also requires a new way of locating the center of resistance for multiple tooth segments, since previous studies base its location on the root length of one tooth.

The measurement blocks used in this study to measure the inter-tooth distances were fairly effective in determining the x position and orientation of the anterior segment, but the uncertainty in the y position was excessively high. From the error analysis of the geometry for determining the position of the anterior segment with respect to the posterior segment, an improved geometry could be devised with which tooth displacement could be measured with less uncertainty and more confidence. For example, to simplify the determination of the x,y position of the anterior segment, another pair of measurements could be made from each of the points of the posterior measurement block directly to the actual point at which the force systems are applied to the segment. Using these distances, the uncertainty in the x position is half as much as with previous method, but the uncertainty in the y position is essentially unchanged. This other method was not used independently because the the anterior segment's rotation could not be determined (two points on the segment are required for this). However, with this other method, it

was discovered that if the distance between the segments of teeth roughly equaled two times (instead of three times with the current set-up) the distance between the points on the posterior measurement block, uncertainty in the y position typically decreased by 33%.

One of the tenets of statistics is to maximize the amount of data accumulated, specifically maximizing the population of your sample, and this is very critical in studies of biological systems. With a greater number of subjects in the experiment, the results and the conclusions derived from these results have more integrity. Under ideal circumstances, it would be most enlightening to observe changes in the force systems applied and the subsequent tooth movements on a daily basis for several months in one hundred patients. However there are practical considerations, including the comfort of the patients and the limited time and resources in which to acquire such vast amounts of data. Nonetheless, it is evident from the difficulties in reaching firm conclusions with this study that the sample population must be much larger (>> 5) to better represent the wide variety of dentitions that exist in the whole population. In addition, clinical visits should be made bi-monthly for the duration of treatment to improve resolution. This would aid in developing a universal strategy of orthodontic therapy through anterior segment retraction.

Many previous studies have monitored the movement of single cuspids with force systems applied to them, but no general consensus has been arrived at for the optimal force system to apply. Once solid conclusions are reached concerning movement of single teeth, movement of multi-toothed segments could be studied with more confidence.

References

[1] **Burstone, C.J.** "The Segmented Arch Approach to Space Closure", *American Journal of Orthodontics*, Vol. 82, No. 5, pp. 361-378, 1982.

[2] **Faulkner, M.G., Lipsett, A.W., El-Rayes, K. and Haberstock, D.L.**, "On the Use of Vertical Loops in Retraction Systems", *American Journal of Orthodontics and Dentofacial Orthopedics*, Vol. 99, No. 4, pp. 328-336, 1991.

[3] **Burstone, C.J.** "Application of Bioengineering to Clinical Orthodontics", In: Graber, T.M. and Swain, B.F. (eds.), Current Orthodontic Concepts and Techniques, Vol. 1, Ch. 5, W.B. Sanders Co., 1975.

[4] **Smith, R.J. and Burstone, C.J.**, "Mechanics of Tooth Movement", *American Journal of Orthodontics*, Vol. 85, No. 4, pp. 294-307, 1984.

[5] **Faulkner, M.G., Fuchshuber, P., Haberstock, D. and Mioduchowski, A.**, "A Parametric Study of the Force/Moment Systems Produced by T-Loop Retraction Springs", *Journal of Biomechanics*, Vol. 22, No. 6/7, pp. 637-647, 1989.

[6] **Nägerl, H., Burstone, C.J., Becker, B. and Kubein-Messenburg, D.**, "Centers of Rotation with Transverse Forces: An Experimental Study", *American Journal of Orthodontics and Dentofacial Orthopedics*, Vol. 99, No. 4, pp. 337-345, 1991.

[7] **Quinn, R.S. and Yoshikawa, D.**, "A Reassessment of Force Magnitude in Orthodontics", *American Journal of Orthodontics*, Vol. 88, No. 3, pp. 252-260, 1985.

[8] **Burstone, C.J.**, "The Biomechanical Rationale of Orthodontic Therapy", In: Melsen, B. (ed.), Current Controversies in Orthodontics, Ch. 6, Quintessence Publishing Co. Ltd., 1991.

[9] **Smith, S. and Storey, E.**, "The Importance of Force in Orthodontics: The Design of Cuspid Retraction Springs", *Australian Journal of Dentistry*, Vol. 56, No. 6, pp. 291-304, 1952.

[10] **Andreasen, G.F. and Johnson, P.**, "Experimental Findings on Tooth Movements Under Two Conditions of Applied Force", *The Angle Orthodontist*, Vol. 37, No. 1, pp. 9-12, 1967.

[11] **Hixon, E.H., Atikian, H., Callow, G.E., McDonald, H.W. and Tacy, R.J.**, "Optimal Force, Differential Force, and Anchorage", *American Journal of Orthodontics*, Vol. 55, No. 1, pp. 437-457, 1969.

[12] **Hixon, E.H., Aasen, T.O., Arango, J., Clark, R.A., Klosterman, R., Miller, S.S. and Odom, W.M.**, "On Force and Tooth Movement", *American Journal of Orthodontics*, Vol. 57, No. 5, pp. 476-489, 1970.

[13] **Boester, C.H. and Johnston, L.E.**, "A Clinical Investigation of the Concepts of Differential and Optimal Force in Canine Retraction", *The Angle Orthodontist*, Vol. 44, No. 2, pp. 113-119, 1974.

[14] **Andreasen, G.F. and Zwanziger, D.**, "A Clinical Evaluation of the Differential Force Concept as applied to the Edgewise Bracket", *American Journal of Orthodontics*, Vol. 78, No. 1, pp. 25-40, 1980.

[15] **Nikolai, R.J.**, "On Optimum Orthodontic Force Theory as applied to Canine Retraction", *American Journal of Orthodontics*, Vol. 68, No. 3, pp. 290-302, 1975.

[16] **Cohen, B.**, "The Rate of Tooth Movement in Response to Known Applied Force Systems", M.Sc. Thesis, Department of Preventive Dental Science, University of Manitoba, 1991.

[17] **Tanne, K., Koenig, H.K. and Burstone, C.J.**, "Moment to Force Ratios and the Center of Rotation", *American Journal of Orthodontics and Dentofacial Orthopedics*, Vol. 94, No. 5, pp. 426-431, 1988.

[18] **Vanden Bulcke, M.M., Burstone, C.J., Sachdeva, R.C.L. and Dermaut, L.R.**, "Location of the Centers of Resistance for Anterior Teeth During Retraction using the Laser Reflection Technique", *American Journal of Orthodontics and Dentofacial Orthopedics*, Vol. 91, No. 5, pp. 375-384, 1987.

[19] **Taylor, J.R.**, "Propagation of Uncertainties", In: Taylor, J.R., An Introduction to Error Analysis: The Study of Uncertainties in Physical Measurements, Ch. 3, University Science Books, 1982.

[20] **Hayward, A.T.J.**, Repeatability and Accuracy, Mechanical Engineering Publications Ltd., 1977.

[21] Micro Validator Series Machines User's Manual, Brown & Sharpe Mfg. Co., 1986.

[22] **El-Rayes, K.**, "Numerical Analysis of Orthodontic Appliances", M.Sc. Thesis, Department of Mechanical Engineering, University of Alberta, 1989.

[23] **Reitan, K.**, "Some Factors Determining the Evaluation of Forces in Orthodontics", *American Journal of Orthodontics*, Vol. 43, No. , pp. 32-45, 1957.

[24] **Burstone, C.J.**, "Deep Overbite Correction by Intrusion", *American Journal of Orthodontics*, Vol. 72, No. 1, pp. 1-22, 1977.

[25] **Foster, T.D.**, "Orthodontic Tooth Movement", In: A Textbook of Orthodontics, Ch. 9, 3rd ed., Blackwell Scientific Publications, 1990.

Appendix A

ERROR ANALYSIS

Performing an error analysis on the displacements of teeth in this study serves two purposes. The first is to quantify the uncertainties in displacements at a specified level of confidence, and the second is to determine which measurements that are subject to error contribute the most to the uncertainty in the displacements. However before the uncertainty in translational and rotational displacement can be determined, the uncertainty in the cartesian coordinates of point P (δx_p, δy_p) and in the orientation of the canine tooth axis (and hence the anterior segment, $\delta\alpha$) must be calculated first.

A.1 Error Analysis of Translational Displacements

Translational displacement in the x and y directions are observed individually in this study, since the axial and shear force components are treated the same. With this approach, attempts are made to correlate axial force with x displacements and shear force with y displacements. The formula for calculating the x coordinate of point P is

$$x_p(a,b,c,d,g,h) = g\left(1+\frac{h}{b}\right)\sqrt{1-p^2} - \frac{d\,h}{b}\left(p\sqrt{1-s^2} + s\sqrt{1-p^2}\right), \quad (2.21)$$

with p and s defined by equations (2.3) and (2.5). According to the general equation (2.27), the uncertainty in the x coordinate of point P is

$$\delta x_P = \sqrt{\begin{array}{l}\left(\frac{\partial x_P}{\partial a}\right)^2(\delta a)^2 + \left(\frac{\partial x_P}{\partial b}\right)^2(\delta b)^2 + \left(\frac{\partial x_P}{\partial c}\right)^2(\delta c)^2 \\ + \left(\frac{\partial x_P}{\partial d}\right)^2(\delta d)^2 + \left(\frac{\partial x_P}{\partial g}\right)^2(\delta g)^2 + \left(\frac{\partial x_P}{\partial h}\right)^2(\delta h)^2\end{array}}, \qquad \text{(A.1)}$$

where:

$$\left(\frac{\partial x_P}{\partial a}\right) = \frac{\partial p}{\partial a}\left[\frac{d\,h}{b}\left(\frac{p\,s}{\sqrt{1-p^2}} - \sqrt{1-s^2}\right) - g\left(1+\frac{h}{b}\right)\frac{p}{\sqrt{1-p^2}}\right], \qquad \text{(A.2)}$$

$$\left(\frac{\partial x_P}{\partial b}\right) = \frac{\frac{\partial s}{\partial b}\left[\frac{d\,h}{b}\left(\frac{p\,s}{\sqrt{1-s^2}} - \sqrt{1-p^2}\right)\right]}{+\frac{h}{b^2}\left[d\left(p\sqrt{1-s^2} + s\sqrt{1-p^2}\right) - g\sqrt{1-p^2}\right]}, \qquad \text{(A.3)}$$

$$\left(\frac{\partial x_P}{\partial c}\right) = \frac{\partial p}{\partial c}\left[\frac{d\,h}{b}\left(\frac{p\,s}{\sqrt{1-p^2}} - \sqrt{1-s^2}\right) - g\left(1+\frac{h}{b}\right)\frac{p}{\sqrt{1-p^2}}\right], \qquad \text{(A.4)}$$

$$\left(\frac{\partial x_P}{\partial d}\right) = \frac{\partial s}{\partial d}\left[\frac{d\,h}{b}\left(\frac{p\,s}{\sqrt{1-s^2}} - \sqrt{1-p^2}\right)\right] - \frac{h}{b}\left(p\sqrt{1-s^2} + s\sqrt{1-p^2}\right), \qquad \text{(A.5)}$$

$$\left(\frac{\partial x_P}{\partial g}\right) = \frac{\frac{\partial p}{\partial g}\left[\frac{d\,h}{b}\left(\frac{p\,s}{\sqrt{1-p^2}} - \sqrt{1-s^2}\right) - g\left(1+\frac{h}{b}\right)\frac{p}{\sqrt{1-p^2}}\right]}{+\frac{\partial s}{\partial g}\left[\frac{d\,h}{b}\left(\frac{p\,s}{\sqrt{1-s^2}} - \sqrt{1-p^2}\right)\right] + \left(1+\frac{h}{b}\right)\sqrt{1-p^2}}, \qquad \text{(A.6)}$$

$$\left(\frac{\partial x_P}{\partial h}\right) = \frac{1}{b}\left[g\sqrt{1-p^2} - d\left(p\sqrt{1-s^2} + s\sqrt{1-p^2}\right)\right]. \tag{A.7}$$

Similarly, with the formula for calculating the y coordinate of point P,

$$y_P(a,b,c,d,g,h) = g\left(1+\frac{h}{b}\right)p - \frac{d\,h}{b}\left(p\,s - \sqrt{1-p^2}\sqrt{1-s^2}\right), \tag{2.22}$$

the uncertainty in the y coordinate of point P is

$$\delta y_P = \sqrt{\begin{array}{l}\left(\frac{\partial y_P}{\partial a}\right)^2(\delta a)^2 + \left(\frac{\partial y_P}{\partial b}\right)^2(\delta b)^2 + \left(\frac{\partial y_P}{\partial c}\right)^2(\delta c)^2 \\ + \left(\frac{\partial y_P}{\partial d}\right)^2(\delta d)^2 + \left(\frac{\partial y_P}{\partial g}\right)^2(\delta g)^2 + \left(\frac{\partial y_P}{\partial h}\right)^2(\delta h)^2\end{array}}, \tag{A.8}$$

where:

$$\left(\frac{\partial y_P}{\partial a}\right) = \frac{\partial p}{\partial a}\left[g\left(1+\frac{h}{b}\right) - \frac{d\,h}{b}\left(s + \frac{p\sqrt{1-s^2}}{\sqrt{1-p^2}}\right)\right], \tag{A.9}$$

$$\left(\frac{\partial y_P}{\partial b}\right) = -\frac{\partial s}{\partial b}\left[\frac{d\,h}{b}\left(p + \frac{s\sqrt{1-p^2}}{\sqrt{1-s^2}}\right)\right] + \frac{h}{b^2}\left[d\left(p\,s - \sqrt{1-p^2}\sqrt{1-s^2}\right) - g\,p\right], \tag{A.10}$$

$$\left(\frac{\partial y_P}{\partial c}\right) = \frac{\partial p}{\partial c}\left[g\left(1+\frac{h}{b}\right) - \frac{d\,h}{b}\left(s + \frac{p\sqrt{1-s^2}}{\sqrt{1-p^2}}\right)\right], \tag{A.11}$$

$$\left(\frac{\partial y_P}{\partial d}\right) = -\frac{\partial s}{\partial d}\left[\frac{d\,h}{b}\left(p + \frac{s\sqrt{1-p^2}}{\sqrt{1-s^2}}\right)\right] - \frac{h}{b}\left(p\,s - \sqrt{1-p^2}\,\sqrt{1-s^2}\right), \tag{A.12}$$

$$\left(\frac{\partial y_P}{\partial g}\right) = \frac{\frac{\partial p}{\partial g}\left[g\left(1+\frac{h}{b}\right) - \frac{d\,h}{b}\left(s + \frac{p\sqrt{1-s^2}}{\sqrt{1-p^2}}\right)\right]}{-\frac{\partial s}{\partial g}\left[\frac{d\,h}{b}\left(p + \frac{s\sqrt{1-p^2}}{\sqrt{1-s^2}}\right)\right] + \left(1+\frac{h}{b}\right)p}, \tag{A.13}$$

$$\left(\frac{\partial y_P}{\partial h}\right) = \frac{1}{b}\left[g\,p - d\left(p\,s - \sqrt{1-p^2}\,\sqrt{1-s^2}\right)\right]. \tag{A.14}$$

As stated in Chapter 2, the maximum uncertainty in any displacement is the sum of the uncertainties of the initial and final positions. Therefore, using the general case of Figure 2.9, where the initial position of P is $(x_P)_1$, $(y_P)_1$ and its final position is $(x_P)_2$, $(y_P)_2$, the uncertainties in x and y displacements are, respectively,

$$\delta(\Delta x_P) = (\delta x_P)_1 + (\delta x_P)_2, \tag{A.15}$$

$$\delta(\Delta y_P) = (\delta y_P)_1 + (\delta y_P)_2. \tag{A.16}$$

A.2 Error Analysis of Rotational Displacements

The orientation of the anterior segment with respect to the posterior segment, α, is calculated for every clinical visit of the patient, and therefore rotational displacements can be determined. Since $\alpha = \sin^{-1} q$, where

$$q(a,b,c,d,g) = \frac{1}{b}\left[d\left(p\sqrt{1-s^2} + s\sqrt{1-p^2}\right) - g\sqrt{1-p^2}\right] \qquad (2.23)$$

and, for example, $\frac{\partial\alpha}{\partial a} = \frac{1}{\sqrt{1-q^2}}\frac{\partial q}{\partial a}$, then the uncertainty in the angle between the anterior and posterior segments is

$$\delta\alpha = \frac{1}{\sqrt{1-q^2}}\sqrt{\begin{array}{c}\left(\frac{\partial q}{\partial a}\right)^2(\delta a)^2 + \left(\frac{\partial q}{\partial b}\right)^2(\delta b)^2 + \left(\frac{\partial q}{\partial c}\right)^2(\delta c)^2 \\ + \left(\frac{\partial q}{\partial d}\right)^2(\delta d)^2 + \left(\frac{\partial q}{\partial g}\right)^2(\delta g)^2\end{array}}, \qquad (A.17)$$

where:

$$\left(\frac{\partial q}{\partial a}\right) = \frac{\partial p}{\partial a}\left[\frac{d}{b}\left(\sqrt{1-s^2} - \frac{ps}{\sqrt{1-p^2}}\right) + \frac{g}{b}\frac{p}{\sqrt{1-p^2}}\right], \qquad (A.18)$$

$$\left(\frac{\partial q}{\partial b}\right) = \frac{\partial s}{\partial b}\left[\frac{d}{b}\left(\sqrt{1-p^2} - \frac{ps}{\sqrt{1-s^2}}\right)\right] - \frac{q}{b}, \qquad (A.19)$$

$$\left(\frac{\partial q}{\partial c}\right) = \frac{\partial p}{\partial c}\left[\frac{d}{b}\left(\sqrt{1-s^2} - \frac{ps}{\sqrt{1-p^2}}\right) + \frac{g}{b}\frac{p}{\sqrt{1-p^2}}\right], \qquad (A.20)$$

$$\left(\frac{\partial q}{\partial d}\right) = \frac{\partial s}{\partial d}\left[\frac{d}{b}\left(\sqrt{1-p^2} - \frac{ps}{\sqrt{1-s^2}}\right)\right] - \frac{1}{b}\left(p\sqrt{1-s^2} + s\sqrt{1-p^2}\right), \qquad (A.21)$$

$$\left(\frac{\partial q}{\partial g}\right) = \begin{array}{l}\frac{\partial p}{\partial g}\left[\frac{d}{b}\left(\sqrt{1-s^2} - \frac{ps}{\sqrt{1-p^2}}\right) + \frac{g}{b}\frac{p}{\sqrt{1-p^2}}\right] \\ + \frac{\partial s}{\partial b}\left[\frac{d}{b}\left(\sqrt{1-p^2} - \frac{ps}{\sqrt{1-s^2}}\right)\right] - \frac{1}{b}\sqrt{1-p^2}\end{array}. \qquad (A.22)$$

With the initial orientation of the anterior segment being α_1 and its final orientation being α_2, the uncertainty in the rotational displacement of the anterior segment is

$$\delta(\Delta\alpha) = \delta\alpha_1 + \delta\alpha_2 . \qquad \text{(A.23)}$$

The angle α also represents the slope of the spring's last node (with respect to its first node), so $\delta\alpha$ indicates the uncertainty in the last node's slope at each clinical visit as well.

A.3 Error Analysis of Last Node Vertical Offset

In addition to the last node's slope, its vertical offset can also be mathematical determined through the same geometric relationships used for the translational and rotational displacements. The last node vertical offset is calculated by

$$y_{last} = y_P - (k\sin\alpha + m) = y_P - (kq + m), \qquad \text{(A.24)}$$

in which k is half the width of the canine tooth bracket (the distance from $\mathbb{P}$ to $\mathbb{Q}$ in Figure 2.13b) and m is the distance from the midpoint on the 1st molar bracket (labelled $\mathbb{S}$ in Figure 2.13b) to the lower posterior point (LP) of the measurement block. The values of k and m are 1.25 mm and 14.21 mm, and their uncertainties, δk and δm, are ±0.25 mm and ±0.12 mm respectively. The uncertainty in the last node vertical offset is therefore

$$\delta y_{last} = \sqrt{\begin{array}{c}\left(\frac{\partial y_{last}}{\partial a}\right)^2(\delta a)^2 + \left(\frac{\partial y_{last}}{\partial b}\right)^2(\delta b)^2 + \left(\frac{\partial y_{last}}{\partial c}\right)^2(\delta c)^2 \\ + \left(\frac{\partial y_{last}}{\partial d}\right)^2(\delta d)^2 + \left(\frac{\partial y_{last}}{\partial g}\right)^2(\delta g)^2 + \left(\frac{\partial y_{last}}{\partial h}\right)^2(\delta h)^2 \\ + \left(\frac{\partial y_{last}}{\partial k}\right)^2(\delta k)^2 + \left(\frac{\partial y_{last}}{\partial m}\right)^2(\delta m)^2\end{array}}, \qquad \text{(A.25)}$$

where:

$$\left(\frac{\partial y_{last}}{\partial a}\right) = \frac{\partial y_P}{\partial a} - k\frac{\partial q}{\partial a}, \qquad \text{(A.26)}$$

$$\left(\frac{\partial y_{last}}{\partial b}\right) = \frac{\partial y_P}{\partial b} - k\frac{\partial q}{\partial b}, \qquad \text{(A.27)}$$

$$\left(\frac{\partial y_{last}}{\partial c}\right) = \frac{\partial y_P}{\partial c} - k\frac{\partial q}{\partial c}, \qquad \text{(A.28)}$$

$$\left(\frac{\partial y_{last}}{\partial d}\right) = \frac{\partial y_P}{\partial d} - k\frac{\partial q}{\partial d}, \qquad \text{(A.29)}$$

$$\left(\frac{\partial y_{last}}{\partial g}\right) = \frac{\partial y_P}{\partial g} - k\frac{\partial q}{\partial g}, \qquad \text{(A.30)}$$

$$\left(\frac{\partial y_{last}}{\partial h}\right) = \frac{\partial y_P}{\partial h}, \qquad \text{(A.31)}$$

$$\left(\frac{\partial y_{last}}{\partial k}\right) = -q, \qquad \left(\frac{\partial y_{last}}{\partial m}\right) = -1. \qquad \text{(A.32 \& A.33)}$$

A.4 Sample Numerical Calculation of Displacements

As an example of the calculation of the translational and rotational displacement of the anterior segment and the uncertainties in these displacements, Table A.1 lists the inter-tooth distances measured on days 0 and 199 (Oct. 16/90 and May 3/91) for the left side of patient RD.

Table A.1: *Sample measurements of inter-tooth distances (in mm)*

	DATE	*c*	*d*	*f*	*g*
1	Oct. 16/90	26.04	26.82	27.18	26.82
2	May 3/91	23.59	26.04	26.04	25.43

By substituting these values into equations (2.3) and (2.5), the values of p and s are determined to be

$$p_1 = 0.2402, \qquad s_1 = 0.9662,$$
$$p_2 = 0.3915, \qquad s_2 = 0.9636.$$

With the values of p and s and the inter-tooth distances, for both days, the cartesian coordinates of point P, (x_P, y_P), the orientation of the anterior segment, α, the last node vertical offset, y_{last}, and all of the corresponding uncertainties can be calculated for each day. For instance, to determine the x coordinate of P on May 3/91 in this example, this requires substituting the values of c_2, d_2, g_2, p_2, and s_2 (as well as the constant quantities

of a, b, h, k, and m; their values can be found in Chapter 2 or Appendix A) into equations (2.21) and (A.1) to (A.7), as described in Section A.1. The results of all of these calculations for the sample measurements are in Table A.2 below.

Table A.2: *Positions, orientations, and last node vertical offsets calculated from sample measurements*

	$x_P \pm \delta x_P$	$y_P \pm \delta y_P$	$\alpha \pm \delta\alpha$	$y_{last} \pm \delta y_{last}$
1	25.22 ± 0.40 mm	13.65 ± 0.81 mm	6.43 ± 2.71°	-0.70 ± 0.82 mm
2	20.89 ± 0.45 mm	16.75 ± 0.75 mm	20.27 ± 2.75°	2.11 ± 0.76 mm

For calculating the translational and rotational displacement which occurs between the two days, the corresponding values in Table A.2 are substituted into equations (2.24), (2.25), (2.26), (A.15), (A.16), and (A.23) and yield the results in Table A.3.

Table A.3: *Translational and rotational displacement calculated from sample measurements*

$\Delta x_P \pm \delta(\Delta x_P)$	$\Delta y_P \pm \delta(\Delta y_P)$	$\Delta\alpha \pm \delta(\Delta\alpha)$
4.33 ± 0.85 mm	3.10 ± 1.56 mm	13.84 ± 5.46°

Appendix B

SENSITIVITY ANALYSIS

The sensitivity analysis described in sub-section 2.4.3 was performed on each parameter of a standard spring individually. This involved varying the value of each parameter to a point of maximum measurement error and observing the effect of this variation on the force systems produced by the spring. The maximum measurement errors for all but two parameters (the exceptions being y_{LAST} and α, which were calculated through the error analysis of Appendix A) are anticipated values, based on reasonable estimates rather than statistical evidence. The purpose of this analysis is to indicate which of the spring's parameters have the most significant effect on the force systems determined by SEGTEC. Subsequently, the dominant parameters help to make fair estimates of the overall error in the axial and shear forces, moment, and moment-to-axial force ratio for all force systems results in this study.

The following three tables show the errors in the force systems calculated by SEGTEC resulting from errors in the measurement of 29 parameters.

Table B.1: *Errors in Force Systems from Measurement Errors in Spring Geometry*

parameter	max. error	F (N)	V (N)	M (N mm)	M/F (mm)
L_1	0.5 mm	±0.36	±0.16	±3.07	±0.20
RoC_2	0.25 mm	±0.12	±0.03	±0.74	
θ_2	5°	±0.04	±0.10	±1.50	±0.30
L_3	0.25 mm	±0.22	±0.03	±0.89	±0.11
RoC_4	0.25 mm	±0.36	±0.04	±0.13	±0.50
θ_4	5°	±0.15	±0.05	±1.25	±0.10
L_5	0.25 mm	±0.13	±0.06	±0.56	±0.32
RoC_6	0.25 mm	±0.04	±0.08	±0.97	±0.28
θ_6	5°		±0.05	±0.45	±0.15
L_7	0.25 mm	±0.09	±0.04	±0.59	
RoC_8	0.25 mm	±0.09	±0.10	±0.96	±0.53
θ_8	5°	±0.20	±0.05	±0.80	±0.50
L_9	0.25 mm	±0.17		±0.27	±0.18
RoC_{10}	0.25 mm	±0.09	±0.10	±1.31	
θ_{10}	5°	±0.20	±0.05	±0.60	±0.15
L_{11}	0.25 mm	±0.09	±0.04	±0.19	±0.17
RoC_{12}	0.25 mm	±0.04	±0.08	±0.80	±0.13
θ_{12}	5°		±0.05		
L_{13}	0.25 mm	±0.13	±0.06	±0.77	
RoC_{14}	0.25 mm	±0.36	±0.04	±1.06	±0.26
θ_{14}	5°	±0.15	±0.05		±0.20
L_{15}	0.25 mm	±0.22	±0.03	±0.20	±0.26
RoC_{16}	0.25 mm	±0.12	±0.03		±0.17
θ_{16}	5°	±0.04	±0.10	±0.35	±0.15
L_{17}	0.5 mm	±0.36	±0.16	±0.43	±0.60

Table B.2: *Errors in Force Systems from Measurement Errors in Bracket Geometry*

parameter	max. error	F (N)	V (N)	M (N mm)	M/F (mm)
IBD	0.5 mm	±0.31		±0.53	±0.33
y_{LAST}	0.8 mm		±0.40	±2.81	±0.66
α	3°	±0.06	±0.42	±3.06	±0.63

Table B.3: *Errors in Force Systems from Error in Accepted Modulus of Elasticity*

parameter	max. error	F (N)	V (N)	M (N mm)	M/F (mm)
E	3 GPa	±0.18		±1.12	

Errors in the cross-sectional dimensions of the spring can also lead to significant errors in the force systems. In the study by El-Rayes [22], the errors in wire cross section height and width were expected to be 3% and 2% respectively. With the estimated error in the modulus of elasticity at about 4% (approximately 3 GPa, as in Table B.3), the error in the axial force was found to be about 10% (±0.40 N for an average of 4 N axial force).

Appendix C

CLINICAL DATA

The clinical data used with the methods described in Chapter 2 and Appendices A and B to determine the results shown in Chapter 3 are displayed in the tables below. Tables C.1 to C.5 list the measurements made of the inter-tooth distances between the four points UA, UP, LA, and LP at each clinical visit on both sides of the maxillary arch of the five patients. The values *c*, *d*, *f*, and *g* in these tables are the distances from points UA to UP, LA to LP, LA to UP, and UA to LP respectively, as shown in Figure 2.6.

Table C.1: *Inter-tooth distances measured in vivo in patient RD (in mm)*

DATE	LEFT SIDE				RIGHT SIDE			
	c	*d*	*f*	*g*	*c*	*d*	*f*	*g*
Oct. 16/90	26.04	26.82	27.18	26.82	23.05	23.35	25.37	25.24
Nov. 23/90	25.82	26.94	27.62	26.94	22.92	24.05	24.31	24.88
Dec. 20/90	24.62	25.98	26.58	25.89	21.97	22.96	24.00	23.81
Jan. 25/91	24.68	26.61	26.76	26.39	21.99	23.66	23.69	24.30
Feb. 22/91	23.93	25.44	25.95	25.28	21.24	23.08	23.20	23.70
Apr. 2/91	24.57	26.88	27.00	26.37	21.11	23.50	23.45	23.75
May 3/91	23.59	26.04	26.04	25.43	20.46	23.32	22.76	23.02
June 6/91	23.66	26.66	26.33	25.61	20.56	23.58	23.18	23.23
July 5/91	21.98	25.16	24.99	24.23	20.85	25.00	23.48	23.35
Aug. 13/91	22.01	24.86	24.84	24.25	20.85	24.98	23.40	23.44

Table C.2: *Inter-tooth distances measured in vivo in patient DK (in mm)*

DATE	LEFT SIDE				RIGHT SIDE			
	c	*d*	*f*	*g*	*c*	*d*	*f*	*g*
Sep. 24/90	27.85	29.45	30.68	29.12	26.71	27.12	27.78	28.00
Oct. 19/90	27.83	29.40	29.96	29.02	26.63	27.13	27.34	27.99
Nov. 22/90	26.52	28.20	28.52	27.85	25.76	26.13	26.72	27.06
Dec. 20/90	26.25	28.13	28.41	27.57	25.59	26.12	26.42	27.06
Jan. 24/91	25.21	26.99	27.24	26.65	25.42	25.86	26.17	26.93
Feb. 22/91	25.10	27.04	27.53	26.51	25.24	26.07	26.16	26.95
Mar 21/91	24.69	26.87	27.04	26.20	24.29	24.98	25.16	25.92
Apr. 17/91	24.06	26.10	26.27	25.72	24.54	25.59	26.58	25.41
May 27/91	23.42	25.74	25.79	25.24	23.83	25.04	24.91	25.73
June 25/91	23.29	25.71	25.81	25.14	24.07	25.38	25.10	26.11

Table C.3: *Inter-tooth distances measured in vivo in patient NM (in mm)*

DATE	LEFT SIDE				RIGHT SIDE			
	c	*d*	*f*	*g*	*c*	*d*	*f*	*g*
Mar 21/91	25.44	26.29	27.21	25.95	24.46	25.00	25.27	25.63
Apr. 18/91	24.29	25.25	26.08	25.27	23.38	23.91	24.37	24.81
May 22/91	23.67	24.89	25.37	24.86	22.67	23.14	23.56	24.24
June 24/91	21.70	22.74	23.39	23.10	20.89	21.06	21.66	22.55
July 29/91	21.48	22.14	23.26	22.97	20.64	21.16	21.62	22.51
Sep. 9/91	20.50	22.06	22.62	22.13	19.25	19.83	20.37	21.12
Oct. 11/91	20.97	23.03	23.39	22.77	19.50	20.68	20.89	21.63

Table C.4: *Inter-tooth distances measured in vivo in patient TT (in mm)*

DATE	LEFT SIDE				RIGHT SIDE			
	c	*d*	*f*	*g*	*c*	*d*	*f*	*g*
Sep. 21/90	21.99	22.99	23.99	23.27	21.83	22.21	22.90	23.45
Oct. 19/90	21.08	22.03	23.14	22.34	20.53	21.29	21.66	22.33
Nov. 15/90	21.31	22.86	23.55	22.93	20.60	21.73	21.77	22.59
Dec. 10/90	20.92	22.46	23.12	22.46	19.97	21.38	21.47	22.10
Jan. 18/91	20.70	22.76	23.16	22.46	19.83	21.77	21.64	22.27
Feb. 19/91	21.00	23.05	23.51	22.74	19.61	21.59	21.77	21.84
Mar 22/91	20.71	23.26	23.53	22.79	19.95	22.28	22.08	22.30

Table C.5: *Inter-tooth distances measured in vivo in patient RZ (in mm)*

DATE	LEFT SIDE				RIGHT SIDE			
	c	*d*	*f*	*g*	*c*	*d*	*f*	*g*
Oct. 26/90	25.30	25.44	26.79	26.02	24.44	23.82	25.11	25.15
Nov. 29/90	25.31	25.86	26.31	27.06	23.24	23.23	23.92	24.96
Jan. 11/91	24.15	25.17	25.61	25.46	23.73	24.62	25.00	25.39
Feb. 6/91	22.86	24.22	24.79	24.35	22.39	23.42	23.90	24.21
Mar. 7/91	22.40	24.04	24.25	23.98	22.35	23.60	23.70	24.25
Apr. 11/91	21.06	22.93	23.23	22.94	21.26	22.89	22.90	23.26
May 17/91	21.23	23.33	23.43	23.20	21.20	22.95	23.41	22.97
June 12/91	20.74	22.68	22.85	22.59	20.54	22.18	22.15	22.56
July 11/91	20.30	22.44	22.46	22.46	19.97	21.88	22.25	21.92
Aug. 15/91	19.86	22.18	22.20	22.13	19.51	21.42	21.59	21.87
Sep. 26/91	20.26	22.81	22.68	22.37	19.49	21.41	21.35	21.83

Tables C.6 to C.10 show the measurements of the inter-bracket distance (I.B.D.) and the lengths of the straight (initially) sections at the ends of the spring (L_1 and L_{17}) taken from the impressions made on both sides of each patient at each visit. These measurements are schematically presented in Figure 2.12. On the left side of the patient, section L_1 is pulled through the tube of the posterior bracket and section L_{17} is pulled through the tube of the anterior bracket. On the right side L_1 is pulled through the anterior bracket tube while L_{17} is pulled through the posterior bracket tube.

Table C.6: *Measurements of spring/brackets geometry taken from impressions of patient RD (in mm)*

DAY	DATE	LEFT SIDE			RIGHT SIDE		
		I.B.D.	L_1	L_{17}	I.B.D.	L_1	L_{17}
0	Oct. 16/90	20.9	5.0	5.2	19.0	4.5	4.2
38	Nov. 23/90	20.2	4.4	4.2	18.1	3.4	3.4
65	Dec. 20/90	19.0	4.4	4.2	17.1	3.4	3.4
101	Jan. 25/91	18.6	3.2	3.6	16.7	2.6	2.4
129	Feb. 22/91	17.7	3.2	3.6	15.8	2.6	2.4
168	Apr. 2/91	17.3	2.7	3.2	15.0	1.6	1.6
199	May 3/91	16.7	2.7	3.2	14.0	1.6	1.6
233	June 6/91	16.3	1.9	2.4	14.0	1.6	1.6
262	July 5/91	14.9	1.9	2.4	14.0	1.6	1.6
301	Aug. 13/91	14.8	1.9	2.4	14.0	1.6	1.6

Table C.7: *Measurements of spring/brackets geometry taken from impressions of patient DK (in mm)*

DAY	DATE	LEFT SIDE			RIGHT SIDE		
		I.B.D.	L_1	L_{17}	I.B.D.	L_1	L_{17}
0	Sep. 24/90	22.4	5.8	6.0	22.7	6.2	6.2
25	Oct. 19/90	22.1	5.2	5.0	22.4	5.4	5.2
59	Nov. 22/90	20.9	5.2	5.0	21.8	5.4	5.2
87	Dec. 20/90	20.3	4.2	4.0	21.7	5.0	4.5
122	Jan. 24/91	19.8	4.2	4.0	21.0	5.0	4.5
151	Feb. 22/91	19.1	3.6	3.4	20.7	4.0	4.0
178	Mar. 21/91	18.3	3.6	3.4	19.9	4.0	4.0
205	Apr. 15/91	18.1	3.0	2.8	19.8	3.4	3.6
245	May 27/91	17.3	3.0	2.8	19.0	3.4	3.6
274	June 25/91	17.2	3.0	2.8	19.0	3.4	3.6

Table C.8: *Measurements of spring/brackets geometry taken from impressions of patient NM (in mm)*

DAY	DATE	LEFT SIDE			RIGHT SIDE		
		I.B.D.	L_1	L_{17}	I.B.D.	L_1	L_{17}
0	Mar. 21/91	20.1	3.8	3.6	20.5	4.2	4.2
28	Apr. 18/91	19.2	3.8	3.6	19.3	4.2	4.2
62	May 22/91	18.0	2.8	2.8	18.4	3.0	3.2
95	June 25/91	16.5	2.8	2.8	17.0	3.0	3.2
130	July 29/91	16.1	2.0	2.0	16.3	2.0	2.2
172	Sep. 9/91	14.8	2.0	2.0	14.9	2.0	2.2
204	Oct. 11/91	14.8	2.0	2.0	14.4	2.0	2.2

Table C.9: *Measurements of spring/brackets geometry taken from impressions of patient TT (in mm)*

DAY	DATE	LEFT SIDE			RIGHT SIDE		
		I.B.D.	L_1	L_{17}	I.B.D.	L_1	L_{17}
0	Sep. 21/90	16.9	2.2	2.0	17.3	2.6	2.6
28	Oct. 19/90	15.8	2.2	2.0	16.0	2.6	2.6
55	Nov. 15/90	15.8	1.5	1.2	15.9	2.0	1.8
80	Dec. 10/90	15.1	1.5	1.2	14.9	2.0	1.8
119	Jan. 18/91	14.5	0.8	0.5	14.0	1.0	1.0
151	Feb. 19/91	14.1	0.8	0.5	13.9	1.0	1.0
182	Mar. 22/91	13.8	0.8	0.5	13.9	1.0	1.0

Table C.10: *Measurements of spring/brackets geometry taken from impressions of patient RZ (in mm)*

DAY	DATE	LEFT SIDE			RIGHT SIDE		
		I.B.D.	L_1	L_{17}	I.B.D.	L_1	L_{17}
0	Oct. 26/90	21.0	4.6	4.4	21.5	4.6	4.8
34	Nov. 29/90	20.6	4.6	4.4	19.9	4.6	4.8
77	Jan. 11/91	18.8	3.6	3.8	19.1	3.6	4.0
103	Feb. 6/91	17.4	3.6	3.8	17.9	3.6	4.0
132	Mar. 7/91	16.9	2.5	2.5	17.5	3.0	3.0
167	Apr. 11/91	15.1	2.5	2.5	16.1	3.0	3.0
203	May 17/91	15.0	1.7	1.7	15.8	1.7	2.3
229	June 12/91	14.2	1.7	1.7	15.0	1.7	2.3
258	July 11/91	14.0	1.0	1.0	14.8	1.2	1.6
293	Aug. 15/91	13.3	1.0	1.0	13.9	1.2	1.6
335	Sep. 26/91	13.2	1.0	1.0	13.8	1.2	1.6

On days in which the spring was reactivated, the measurements shown in Tables C.6 to C.10 were taken *after* reactivation. For determining the force systems *before* activation, the I.B.D. is unchanged for that day but the lengths of L_1 and L_{17} from the one visit prior to that day are used in this case. The ends of the spring have not yet been pulled through the bracket tubes to reactivate it, and therefore the lengths of the ends remain the same up to the time just prior to reactivation.

Tables C.11 to C.16 display the dimensions of the remaining 15 sections (section numbers n = 2 to 16) of each spring used in the treatment of the patients, all of which were determined from the enlarged photocopies of the initial spring geometries. These dimensions, which are shown in Figure 2.12 and are constant throughout treatment, include the lengths of the straight sections (L_n) and for the curved sections, the angles of sweep (θ_n) and radii of curvature (RoC_n). An additional spring was needed for patient DK's right side, as the first spring broke on day 203 (Apr. 15/91) of the treatment, and the second spring's geometry is displayed seperately in Table C.13. These tables also reveal the number of segments each section was divided into. For sections 1 and 17 (not in these tables; from Tables C.6 to C.10), both were split into 500 segments when analyzed. These geometries were input into the computer program SEGTEC for determining the force systems produced at both ends of the spring. In addition to these geometries, the values of the modulus of elasticity and yield strength of the spring's material (which were stated in sub-section 2.4.3), the cross-sectional dimensions of the spring (0.017" × 0.025", or 0.432 mm × 0.635 mm), and the solver tolerance (1×10^{-8} was used in this study) were required for the use of SEGTEC.

Table C.11: *Geometries of springs for both sides of patient RD (in mm, unless noted otherwise)*

section number (n)	number of segments	LEFT SIDE			RIGHT SIDE		
		L_n	θ_n (°)	RoC_n	L_n	θ_n (°)	RoC_n
2	250	-	38	1.7	-	38	1.3
3	150	1.6	-	-	1.7	-	-
4	300	-	101	0.9	-	98	0.8
5	300	3.1	-	-	3.2	-	-
6	200	-	78	1.1	-	81	1.1
7	300	3.0	-	-	3.1	-	-
8	250	-	142	-0.9	-	141	-0.8
9	500	7.6	-	-	7.8	-	-
10	250	-	138	-0.9	-	145	-0.8
11	300	3.0	-	-	3.0	-	-
12	200	-	75	1.1	-	79	1.0
13	300	3.2	-	-	3.2	-	-
14	300	-	107	1.0	-	103	0.8
15	150	1.4	-	-	1.8	-	-
16	250	-	30	2.1	-	38	1.3

Table C.12: *Geometries of springs for both sides of patient DK (in mm, unless noted otherwise)*

section number (n)	number of segments	LEFT SIDE			RIGHT SIDE		
		L_n	θ_n (°)	RoC_n	L_n	θ_n (°)	RoC_n
2	250	-	34	2.4	-	34	2.3
3	150	1.2	-	-	1.2	-	-
4	300	-	107	1.1	-	105	1.3
5	300	2.6	-	-	2.3	-	-
6	200	-	77	1.2	-	80	1.1
7	300	2.9	-	-	2.9	-	-
8	250	-	141	-1.0	-	144	-1.0
9	500	7.4	-	-	7.4	-	-
10	250	-	142	-1.1	-	144	-1.0
11	300	3.0	-	-	2.9	-	-
12	200	-	75	1.1	-	81	1.2
13	300	2.7	-	-	2.5	-	-
14	300	-	104	1.1	-	103	1.2
15	150	1.3	-	-	1.2	-	-
16	250	-	37	1.9	-	37	2.4

Table C.13: *Geometry of replacement spring for right side of patient DK (in mm, unless noted otherwise)*

section number (n)	number of segments	RIGHT SIDE		
		L_n	θ_n (°)	RoC_n
2	250	-	34	1.9
3	150	1.3	-	-
4	300	-	106	1.1
5	300	2.9	-	-
6	200	-	77	1.1
7	300	3.1	-	-
8	250	-	141	-0.9
9	500	7.8	-	-
10	250	-	145	-1.0
11	300	2.9	-	-
12	200	-	82	1.2
13	300	3.0	-	-
14	300	-	99	1.1
15	150	1.1	-	-
16	250	-	37	2.5

Table C.14: *Geometries of springs for both sides of patient NM (in mm, unless noted otherwise)*

section number (n)	number of segments	LEFT SIDE			RIGHT SIDE		
		L_n	θ_n (°)	RoC_n	L_n	θ_n (°)	RoC_n
2	250	-	35	2.3	-	35	1.5
3	150	1.4	-	-	1.6	-	-
4	300	-	101	1.1	-	105	0.8
5	300	3.0	-	-	3.2	-	-
6	200	-	81	0.8	-	77	1.1
7	300	3.2	-	-	2.8	-	-
8	250	-	144	-0.9	-	144	-1.0
9	500	7.6	-	-	7.3	-	-
10	250	-	143	-0.9	-	143	-1.0
11	300	3.1	-	-	3.1	-	-
12	200	-	76	0.9	-	82	0.9
13	300	3.1	-	-	3.0	-	-
14	300	-	105	1.0	-	106	1.0
15	150	1.4	-	-	1.6	-	-
16	250	-	35	2.3	-	38	1.9

Table C.15: *Geometries of springs for both sides of patient TT (in mm, unless noted otherwise)*

section number (n)	number of segments	LEFT SIDE			RIGHT SIDE		
		L_n	θ_n (°)	RoC_n	L_n	θ_n (°)	RoC_n
2	250	-	31	2.3	-	36	1.9
3	150	1.8	-	-	1.8	-	-
4	300	-	103	1.2	-	105	1.0
5	300	2.9	-	-	3.0	-	-
6	200	-	82	1.1	-	76	1.1
7	300	3.0	-	-	2.8	-	-
8	250	-	145	-1.0	-	141	-1.1
9	500	7.4	-	-	7.3	-	-
10	250	-	141	-1.0	-	142	-1.0
11	300	2.8	-	-	2.8	-	-
12	200	-	79	1.2	-	80	1.1
13	300	2.5	-	-	2.9	-	-
14	300	-	103	1.4	-	101	1.0
15	150	1.8	-	-	1.7	-	-
16	250	-	32	1.7	-	34	2.2

Table C.16: *Geometries of springs for both sides of patient RZ (in mm, unless noted otherwise)*

section number (n)	number of segments	LEFT SIDE			RIGHT SIDE		
		L_n	θ_n (°)	RoC_n	L_n	θ_n (°)	RoC_n
2	250	-	51	2.0	-	37	2.1
3	150	1.0	-	-	1.2	-	-
4	300	-	95	1.1	-	103	1.1
5	300	2.8	-	-	3.0	-	-
6	200	-	84	1.0	-	80	1.1
7	300	3.1	-	-	2.8	-	-
8	250	-	145	-1.0	-	144	-1.0
9	500	7.6	-	-	7.4	-	-
10	250	-	144	-0.9	-	145	-1.0
11	300	2.8	-	-	2.8	-	-
12	200	-	83	1.2	-	80	1.2
13	300	2.4	-	-	2.6	-	-
14	300	-	100	1.2	-	106	1.1
15	150	1.4	-	-	1.1	-	-
16	250	-	36	1.8	-	34	2.1